UNIVERSITY OF MODENA AND REGGIO EMILIA

PhD Program in Molecular and Regenerative Medicine

XXXIV Cycle

EFFICACY AND SAFETY OF CHEMO AND GENE THERAPY COMBINATORY PRE-CLINICAL MODELS TARGETING PANCREATIC CANCER AND ITS MICROENVIRONMENT

PhD Candidate: Dr. Giulia Casari

Tutor: Prof. Massimo Dominici

PhD Program Coordinator: Prof. Michele De Luca

Academic Year 2020/2021

ABSTRACT

Introduction. Pancreatic ductal adenocarcinoma (PDAC) has still a poor response to available therapies. A hallmark of this malignancy is the pronounced fibrotic stroma, composed by tumor-associated fibroblasts (TAF), immune cells, cytokines and growth factors stored in the extracellular matrix (ECM), with a key role in PDAC progression and drug resistance [1]. For these reasons, efforts have been focused on the development of novel therapies able to target both malignant cells and TAF [2]. Since years, we have developed an anticancer gene therapy based on human adipose mesenchymal stromal/stem cells (AD-MSC) secreting the proapoptotic soluble (s)-TRAIL to mostly target PDAC malignant cells [3,4]. Here, by in vitro and in vivo models, we investigated the potential synergistic impact of a novel combinatory approach between the chemotherapy agent Gemcitabine (GEM) and AD-MSC sTRAIL on both PDAC tumor and TAF. Moreover, to initially verify the safety of this strategy, we assessed the impact of AD-MSC sTRAIL on normal tissues and in particular against white blood cells.

Materials and methods. *In vitro assay on PDAC cell lines:* sensitivity of PDAC cell lines (WT BxPC-3, MIA PaCa-2 and sTRAIL-resistant BxPC-3) to sTRAIL, alone or in combination with GEM, was evaluated by CellTiter-Glo assay and Propidium Iodide staining in 2D. PDAC in vivo-like microenvironment was reproduced loading PDAC cell lines in 3D bioreactor and cell death was quantified after GEM & AD-MSC sTRAIL combinatory treatment. *In vivo animal model:* PDAC orthotopic xenotransplant murine model was developed by implantation of WT BxPC-3 in the pancreas of NOD/SCID mice. Synergistic effect of the combinatory approach on tumor growth was verified by Ultrasound imaging. Paraffin embedded tumor sections were evaluated by H&E staining and Cytokeratin 7 IHC. *Cytotoxicity study on human PDAC TAF:* primary TAF isolated by mechanical and enzymatic digestion were tested for sensitivity to sTRAIL, alone or in combination with GEM, by CellTiter-Glo. *Immunotoxicity study:* viability of immune cells (monocytes, polymorphonuclear cells and T lymphocytes) isolated from peripheral blood of healthy donors and treated with sTRAIL or co-cultured with AD-MSC sTRAIL was evaluated by metabolic assays and FACS.

Results. PDAC cell lines showed different sensitivity levels to GEM or sTRAIL alone. GEM & sTRAIL combinatory approach revealed a synergistic cytotoxic effect on PDAC cells both

in 2D and 3D systems. Synergy between GEM and AD-MSC sTRAIL was confirmed in the orthotopic PDAC murine model, showing a relevant tumor tissue degeneration compared to control and GEM alone. Human primary PDAC TAF were refractory to the sTRAIL cytotoxic effect as single agent, however pre-treatment with GEM was able to restore sTRAIL sensitivity. Finally, immunological safety study confirmed that white blood cells were refractory to the proapoptotic effect displayed by sTRAIL and the direct cell-to-cell contact with AD-MSC sTRAIL had negligible impact on monocyte and T cell viability.

Conclusions. These data demonstrated the safety and therapeutic potential of combining a gene therapy approach with chemotherapy to target both the tumor and stromal compartment in PDAC.

Keywords: pancreatic cancer, TAF, synergy, TRAIL, gemcitabine

SINTESI

Introduzione. Il tumore del pancreas, ed in particolare l'adenocarcinoma duttale (PDAC), mostra ancora una scarsa risposta alle terapie disponibili. Un elemento peculiare è l'abbondante stroma fibrotico, composto da fibroblasti associati al tumore (TAF), cellule immunitarie, citochine e fattori di crescita immersi nella matrice extracellulare (ECM), con un ruolo chiave nella progressione e farmacoresistenza del PDAC [1]. Sforzi significativi si sono così focalizzati sullo sviluppo di terapie capaci di bersagliare sia cellule tumorali che TAF [2]. Da anni, stiamo sviluppando una terapia genica antitumorale a base di cellule stromali/staminali mesenchimali da tessuto adiposo (AD-MSC) secernenti la molecola pro-apoptotica solubile TRAIL (sTRAIL) per bersagliare cellule tumorali di PDAC [3,4]. Qui, abbiamo investigato in vitro ed in vivo l'impatto sinergico di un approccio combinatorio tra il chemioterapico Gemcitabina (GEM) e le AD-MSC sTRAIL sia su cellule tumorali che su TAF di PDAC. Inoltre, per verificare la sicurezza di tale terapia, abbiamo valutato l'impatto citotossico delle AD-MSC sTRAIL su tessuti sani ed in particolare sui leucociti.

Materiali e metodi. *Saggi in vitro su linee di PDAC:* la sensibilità di linee cellulari di PDAC (WT BxPC-3, MIA PaCa-2 e BxPC-3 resistenti a sTRAIL) a sTRAIL, da solo o in combinazione con GEM, è stata valutata con CellTiter-Glo e ioduro di propidio in 2D. Un microambiente di PDAC in vivo-like è stato riprodotto caricando linee di PDAC in un bioreattore 3D e la mortalità cellulare è stata quantificata dopo trattamento con GEM & AD-MSC sTRAIL. *Modello animale in vivo:* un modello murino ortotopico di PDAC è stato sviluppato mediante impianto di WT BxPC-3 nel pancreas di topi NOD/SCID. L'effetto sinergico dell'approccio combinatorio sulla crescita tumorale è stato verificato mediante ecografia. Sezioni di tumore in paraffina sono state valutate con H&E e IHC per citocheratina 7. *Citotossicità su TAF umani di PDAC:* TAF primari sono stati isolati e testati per la sensibilità a sTRAIL, da solo o in combinazione con GEM, tramite CellTiter-Glo. *Immunotossicità:* la vitalità di cellule immunitarie (monociti, granulociti e linfociti T) da sangue periferico di donatori sani trattate con sTRAIL o co-coltivate con AD-MSC sTRAIL è stata valutata con saggi metabolici e FACS.

Risultati. Le linee cellulari di PDAC mostrano differenti livelli di sensibilità a GEM o sTRAIL da soli e la combinazione GEM & sTRAIL ha rivelato un effetto sinergico sulle cellule di PDAC in 2D ed in 3D. La sinergia tra GEM e AD-MSC sTRAIL è stata confermata

nel modello murino ortotopico di PDAC con una significativa degenerazione del tessuto tumorale rispetto al controllo e alla sola GEM. I TAF umani primari di PDAC sono resistenti all'effetto citotossico di sTRAIL da solo, mentre il pre-trattamento con GEM ne ripristina la sensibilità. Infine, studi sulla sicurezza immunologica hanno confermato che i leucociti sono refrattari all'effetto di sTRAIL e il contatto diretto con le AD-MSC sTRAIL ha un impatto trascurabile sulla vitalità di monociti e cellule T.

Conclusioni. Questi dati hanno dimostrato la sicurezza ed il potenziale terapeutico di combinare terapia genica e chemioterapia per bersagliare sia la componente tumorale che stromale del PDAC.

Parole chiave: tumore pancreatico; TAF; sinergia; TRAIL; gemcitabina

INDEX

1. ABBREVIATIONS

7-AAD	7-aminoactinomycin D
ACT	adoptive cell therapy/transfer
AD-MSC	adipose mesenchymal stromal/stem cell
AD-MSC EMPTY	AD-MSC transduced with lentiviral empty vector
AD-MSC sTRAIL	AD-MSC transduced with a lentiviral vector coding for soluble TRAIL gene
APC	allophycocyanin
ATRA	all-trans retinoic acid
Bak	Bcl-2 homologous antagonist/killer
Bax	Bcl-2 associated X protein
Bcl-2	B-cell lymphoma 2
Bcl-xL	Bcl-extra large
BID	BH3-interacting domain death agonist
BM-MSC	bone marrow-derived mesenchymal stromal/stem cell
CA 19-9	carbohydrate antigen 19-9
CCL5	C-C motif chemokine ligand 5
CDKN2A	cyclin dependent kinase inhibitor 2A
cFLIP	cellular FLICE inhibitory protein
CK-7	cytokeratin 7
CM	conditioned medium
c-Myc	c-myelocytomatosis oncogene product
CT	computed tomography
CTLA-4	cytotoxic T-lymphocyte-associated antigen 4
CXCL8	C-X-C motif chemokine ligand 8
DAMP	damage-associated molecular pattern
DC	dendritic cell
DcR1 and -2	TRAIL decoy receptors
DISC	death-inducing signaling complex
DR4 and -5	TRAIL death receptors
E : T	effector : target ratio
ECM	extracellular matrix
EGF	epidermal growth factor
EGFR	EGF receptor
EMT	epithelial-to-mesenchymal transition
Erk	extracellular signal-regulated kinase

EUS	endoscopic ultrasound
EV	extracellular vesicle
FACS	fluorescent-activated cell sorter
FADD	Fas-associated death domain
FAP	fibroblast-activation protein α
FBS	fetal bovine serum
FDA	Food and Drug Administration
FFPE	formalin-fixed and paraffin-embedded
FGF2	fibroblast growth factor 2
FITC	fluorescein isothiocyanate
Foxp3	forkhead box P3
GAL1	galectin-1
GEM	gemcitabine
GFAP	glial fibrillary acidic protein
GM-CSF	granulocyte macrophage colony-stimulating factor
H&E	hematoxylin-and-eosin staining
HA	hyaluronic acid
HGF	hepatocyte growth factor
HGFR	HGF receptor
HRAS	harvey rat sarcoma viral oncogene homolog
i.p.	intraperitoneally
i.t.	intratumor
IFN	interferon
IGF-1	insulin-like growth factor 1
IHC	immunohistochemistry
IL	interleukin
IPMN	intraductal papillary mucinous neoplasm
ISCT	International Society for Cellular Therapy
iTAF	secretory/inflammatory TAF
JNK	c-jun N-terminal kinase
KRAS	kirsten rat sarcoma 2 viral oncogene homolog
Luc	luciferase
MAPK	mitogen-activated protein kinase
MC	mast cell
Mcl-1	myeloid cell leukemia 1
M-CSF	macrophage colony-stimulating factor
MDSC	myeloid-derived suppressor cell
MHC	major histocompatibility complex

miRNA	microRNA
MMP	matrix metallopeptidase
MRI	magnetic resonance imaging
MUC	mucin
myTAF	myofibroblast
Nab-Paclitaxel	paclitaxel administered in a nanoparticle albumin bound formulation
NEMO/IKK	NF-kB essential modulator
NF-kB	factor nuclear kappa B
NK	natural killer cell
NO	nitric oxide
NP	nanoparticle
OAd	adenovirus
OPG	osteoprotegerin
PanIN	pancreatic intraepithelial neoplasia
PanNET	pancreatic neuroendocrine tumor
PBMC	peripheral blood mononuclear cell
PC	pancreatic cancer
PD-1	programmed cell death protein-1
PDAC	pancreatic ductal adenocarcinoma
PDGF	platelet-derived growth factor
PE	phycoerythrin
PEG	polyethylene glycol
PEGPH20	pegylated recombinant human hyaluronidase 20
PerCP	peridinin-chlorophyll-protein
PHA-M	phytohemagglutinin
PI	propidium iodide
PI3K-PKB/AKT	phosphoinositide 3-kinase - protein kinase B
PMN	polymorphonuclear cell
POSTN	periostin
PSC	pancreatic stellate cell
PTEN	phosphatase and tensin homolog
rhTRAIL	recombinant human TRAIL
RIPK1	receptor-interacting serine/threonine-protein kinase 1
SCF	stem cell factor
SEM	standard error of the mean
SHH	sonic hedgehog
siRNA	short interfering RNA

Smac/DIABLO	second mitochondria-derived activator of caspase
SMAD4	mothers against decapentaplegic homolog 4
sTRAIL	soluble TRAIL
sT-resistant BxPC-3	sTRAIL resistant BxPC-3
T reg	T-regulatory cell
TAF	tumor-associated fibroblast
TAM	tumor-associated macrophage
TAN	tumor-associated neutrophil
TGF-β	transforming growth factor β
Th1	T helper 1
TNFα	tumor necrosis factor α
TRAF2	TNF receptor-associated factor 2
TRAIL	TNF-related apoptosis-inducing ligand
VEGF	vascular endothelial growth factor
VEGFR	VEGF receptor
WT BxPC-3	wild-type BxPC-3
XIAP	X-linked inhibitor of apoptosis protein
αSMA	α-smooth muscle actin

2. INTRODUCTION

2.1 Pancreatic ductal adenocarcinoma

2.1.1 Pathology and epidemiology of Pancreatic Ductal Adenocarcinoma

Pancreatic cancer (PC) is one of the most challenging malignancies, which includes both endocrine and exocrine tumors of the pancreas. However, pancreatic neuroendocrine tumors (PanNET) account only for the 5% of all PC, whereas the majority of PC derives from the exocrine portion of the organ including connective and lymphatic tissues, ductal epithelium and acinar cells [5]. Among all, almost 90% of exocrine PC originate from ductal epithelium (known as pancreatic ductal adenocarcinoma, PDAC), thus representing the most common type of pancreatic neoplasm [6].

Focusing on PDAC, it is the seventh leading cause of cancer death in industrialized countries, the third most frequent tumor in the USA and the eleventh in the world. PDAC incidence is positively related to increasing age, slightly higher in men compared to women, and is expected to increase up to 355,317 new cases in 2040 [7]. PDAC etiology is intricate and multifactorial, with a crucial role played by smoking, obesity, family history and genetic predisposition [8]. Despite the progress in diagnostic procedures and the development of innovative approaches, 1-year survival rate is around 24%, and decreases up to 9% at 5 years after diagnosis with an almost complete overlap between death and incidence rates [9]. The worst prognosis detected in PDAC compared to PanNET is related to the late-stage diagnosis typical of PDAC, due to the unspecific symptoms during tumor progression, together with the presence of a pronounced fibrotic stroma that promotes PDAC drug resistance and tumor progression [10].

2.1.2 Molecular pathogenesis of PDAC from precursor lesions

PDAC is preceded by the development of precursor lesions known as pancreatic intraepithelial neoplasia (PanIN) and intraductal papillary mucinous neoplasm (IPMN), that represent preneoplastic conditions with a propensity to develop into cancer [11]. PDAC mainly originates from PanINs, microscopic lesions in pancreatic ducts, that are classified into PanIN-1A, PanIN-1B, PanIN-2 and PanIN-3 based on their histological atypia [12].

Instead, IPMN is defined by a ductal epithelium papillary proliferation and is categorized in gastric, intestinal, pancreatobiliary and oncocytic subtypes [13]. Distinctive mucin (MUC) expression profiles characterize the different PDAC precursor lesions, as well as their grade. MUC1 expression, that is associated with tumor cell invasion and poor prognosis, progressively increases with the PanIN and PDAC stage. Instead, MUC2, related to a non-invasive tumor phenotype and favourable prognosis, is differentially expressed by the several IPMN subtypes and is suitable for differentiating the two precursor lesions due to its lack of expression in PanIN. Lastly, all PanIN, IPMN and PDAC express MUC5AC [11].

Through different stages of PDAC pathogenesis, gene abnormalities progressively arise within PDAC precursor lesions, leading to the high molecular heterogeneity of this disease with an average of 63 genetic alterations per pancreatic cancer cells [14]. In particular, PDAC development and progression from both PanIN and IPMN begin with activating mutation in Kirsten rat sarcoma 2 viral oncogene homolog (KRAS), that is a potent driver of cancer initiation, and inactivation of the tumor suppressor gene p16/cyclin dependent kinase inhibitor 2A (CDKN2A). Subsequently, later events include further somatic inactivating mutations in TP53 and mothers against decapentaplegic homolog 4 (SMAD4), which ultimately lead to the PDAC invasive malignancy [15].

2.1.3 Symptoms and diagnosis of PDAC

PDAC clinical signs are affected by tumor size, location and metastases. Early stages of the disease are characterized by a lack of symptoms, whereas non-specific symptoms such as weight loss, jaundice, fatigue and abdominal pain with an intermittent nature occur during tumor progression, resulting into a late-stage diagnosis [16]. In particular, patients with tumor in the head of the pancreas present with obstructive jaundice due to the bile duct compression, dark urine and acute pruritus caused by conjugated bilirubin, and anorexia, fatigue and hematomas because of impaired liver function. Instead, weight loss and back or epigastric pain occur in patients with tumor in the body and tail of the pancreas, which does not typically induce biliary duct obstruction [17].

Several diagnostic tests are considered effective for the early diagnosis of PDAC, crucial to achieve the best clinical outcomes for patients, including imaging-based approaches and tumor biomarker detection. Traditional imaging techniques for PDAC detection are the endoscopic ultrasound (EUS), multi-detector computed tomography (CT) and magnetic

resonance imaging (MRI) [18]. EUS is the most sensitive method to visualize signs of PDAC presence, such as expansion of both pancreatic and bile ducts and a low echoic mass. However, since its performance is highly related to operator expertise, it is usually used as complementary diagnostic imaging to CT for the histological characterization of tumor tissues through fine-needle biopsies [19]. Hence, multi-detector CT is the gold standard method for PDAC diagnosis with an excellent spatial and temporal resolution and sensitivity of 76-92%, which is also useful for detecting tumor metastasis to the nearby organs and lymph nodes and determining eligibility for surgery. Another imaging approach used for staging PDAC patients without ionizing radiations is MRI, that allow a superior soft tissue resolution compared to CT but the parameters used can not be standardized [20]. In addition to imaging-based techniques, different serum biomarkers such as the most validated serum carbohydrate antigen (CA 19-9) may help in confirming PDAC symptomatic patient diagnosis, determining tumor stage and predicting overall survival. Nevertheless, the evaluation of CA 19-9 serum levels in PDAC is limited by its poor sensitivity and specificity, thus preventing its applicability in asymptomatic patient screening [21].

2.1.4 Current therapeutic options for PDAC

Among the current therapies used for PDAC treatment, tumor surgical resection, alone or followed by adjuvant radio- or chemotherapy, remains the only therapeutic option able to provide a potential cure for patients affected by this malignancy [22]. Surgical options for eligible patients, that represent only about 20% of patients affected by PDAC, include the pancreatico-duodenectomy, known as Whipple's procedure, and the distal or total pancreatectomy to obtain a R0 resection [23]. Innovations in these surgical approaches, such as a pre-operative biliary decompression in patients with jaundice, minimally invasive surgery using laparoscopic or robotic techniques, vascular resection and post-operative anastomosis to recreate the alimentary tract, may help to provide a more aggressive resection further improving microscopic clearance and patient survival rate [22]. However, despite the progress achieved in surgical techniques, surgery shows a potential curative intent mainly in early tumor stages, which is a huge limitation due to the late-stage diagnosis typical of PDAC, and about 80% of patients undergoing surgery exhibit cancer relapse as early as two months after surgical approach.

Therefore, adjuvant treatment is often scheduled post-surgical resection with the aim of improving patient survival [24]. Since 1997 Gemcitabine (2', 2'-difluorodeoxycytidine; GEM), a difluoro analog of deoxycytidine, has been the standard of care for resectable PDAC for more than two decades. Its mechanism of action relies on DNA synthesis inhibition, hampering the activity of ribonucleotide reductase or DNA polymerase or through a mis-insertion within the DNA that blocks chain extension [25]. It has been demonstrated that adjuvant GEM administered after surgical approach results into a statistically significant improvement in terms of both median disease-free survival (13.4 vs 6.7 months) and five- and ten-year overall survival (20.7% vs 10.4% and 12.2% vs 7.7%, respectively) compared to surgery alone. However, efficacy of this chemotherapeutic drug is limited by the development of both innate and acquired chemoresistance in PDAC cells, which can occur through different mechanisms including the absence of nucleotide transporters crucial for GEM transfer in the target cells and the reduced expression of the enzyme deoxycytidine kinase responsible for GEM cytotoxic effect [26].

Hence, other chemotherapy regimens have been further investigated to identify the best one. Among the antimetabolite drugs, 5-fluorouracil has been the first chemotherapeutic agent approved for PDAC treatment and acts as an inhibitor of the enzyme thymidylate synthetase involved in DNA synthesis [17]. Its effectiveness as monotherapy is lower than GEM, but it has been combined with oxaliplatin, irinotecan and leucovorin to obtain the chemotherapy regimen FOLFIRINOX, approved for both resectable and metastatic PDAC treatment in 2011 by Food and Drug Administration (FDA). Both overall survival and disease-free survival of PDAC patients improve in response to FOLFIRINOX treatment compared to GEM, but this combinatory regimen is associated with a severe toxicity and complications, thus limiting its administration. Similar to GEM, FOLFIRINOX therapeutic potential is further limited by the development of 5-fluorouracil resistance [27]. Subsequently, in 2013 it has been approved a combinatory approach between GEM and Paclitaxel administered in a Nanoparticle Albumin Bound formulation (Nab-Paclitaxel) as a first-line treatment for PDAC, showing an improved median survival of approximately 8.5 months and becoming the current standard of care for advanced PDAC. Indeed, Nab-Paclitaxel belongs to the Taxane family and is a microtubule stabilizing agent characterized by a high perfusion through endothelial gaps in vascular system and accumulation within stromal compartments, that displays a potent synergistic impact when combined with GEM for PDAC treatment [28]. Instead, for resectable PDAC,

combination of GEM with capecitabine, that belongs to the antimetabolite drugs, has been approved with an improved media overall survival of 28 months compared to 25.5 months of GEM alone [29].

However, despite the survival benefits achieved using adjuvant chemotherapy, about 74% of patients experience a tumor recurrence within two years due to the PDAC nature and development of resistance mechanisms against conventional treatments. Therefore, due to the several limitations displayed by the current standard of care therapeutic options, novel promising opportunities have been further investigated in both pre-clinical and early clinical practice for improved PDAC therapy [30].

2.1.5 Future directions for PDAC treatment

Potential promising approaches for PDAC treatment comprise targeted therapies, immunotherapy and gene therapies.

2.1.5.1 Targeted therapies

In view of the several genetic mutations within PDAC tumor cells, different targeted therapies including the antiangiogenic treatments, DNA repair inhibitors and KRAS pathway inhibitors have been tested as single agents or combined with other approaches against PDAC [30]. Inhibition of angiogenesis has been performed using monoclonal antibodies, targeting vascular endothelial growth factor (VEGF) signaling, and small-molecule tyrosine kinase inhibitors such as sorafenib in combination with GEM, with promising pre-clinical results due to the crucial role played by pro-angiogenic mechanisms into PDAC progression. However, their efficacy is limited in clinical setting because of drug resistance or alternative angiogenic processes [31]. Instead, DNA repair targeted therapy blocks repair mechanisms of DNA damage induced by chemotherapeutic agents within tumor cells, inhibiting cell cycle regulators or directly the DNA repair mechanism, thus leading to cell death. DNA repair inhibitors are often used combined with GEM or radiotherapy and evaluation of their efficacy in clinical practice is still ongoing [30]. Lastly, given that activating KRAS alteration is the most common genetic mutation in PDAC cells (> 90%), KRAS pathway inhibitors directly targeting KRAS or upstream activators, such as the transmembrane tyrosine kinase epidermal growth factor receptor (EGFR), or downstream effector pathways, like mitogen-activated protein kinase (MAPK) and phosphoinositide 3-kinase - protein kinase B (PI3K-PKB/AKT)

signaling, have been investigated. Thus far, the most promising outcomes are obtained with an EGFR inhibitor, known as erlotinib, combined with GEM chemotherapy, resulting in a statistically significant improvement of patient overall survival, but further studies are needed [26].

2.1.5.2 Immunotherapy

Among immunotherapy strategies, immune-checkpoint inhibitors, monoclonal antibodies, targeting of immunosuppressive cells, adoptive cell therapy/transfer (ACT) and vaccines have been evaluated as potential approaches for this malignancy, despite the PDAC dense fibrotic stroma that interferes with immunotherapies. Immune-checkpoint proteins, like programmed cell death protein-1 (PD-1) and cytotoxic T-lymphocyte-associated antigen 4 (CTLA-4), can be targeted by immune-checkpoint inhibitors in PDAC, showing discouraging results as single agents and patient improved outcomes when combined with radio- or chemotherapy [32]. A promising target of monoclonal antibodies in PDAC is mesothelin, that is up-regulated in this malignancy and directly correlated with unfavourable clinical outcomes. Its targeting with the monoclonal antibody amatuximab is a safe strategy but no enhancements in survival rates of PDAC patients has been reported [33]. Similar to monoclonal antibodies, targeting of immunosuppressive cells, including T-regulatory cells (T reg) and tumor-associated macrophages (TAM), using chemotherapy does not show promising results [34]. Instead, more encouraging data emerged from the ACT strategy, based on the transfer of genetically engineered T lymphocytes in PDAC patients, thus increasing the cytotoxic impact of both CD4 + and CD8+ T cells against tumor compartment. However, development of resistance mechanisms together with the significant time necessary to genetically modified cells are the major limitations of this innovative technology [35]. Lastly, studies investigating the therapeutic efficacy of the cancer vaccines CRS 207, developed by the recombinant *Listeria* bacterium, and GVAX, based on genetically engineered PDAC tumor cells, are still ongoing. Their use shows an evident safety along with an effectiveness in improving patient outcomes but only if used together [35].

2.1.5.3 Gene therapies

Recent breakthroughs in gene therapy approaches, including virotherapy, therapeutic transgene-expressing vectors and gene-editing strategy, provide innovative opportunities for

PDAC treatment. Among virotherapies, oncolytic viruses, used alone or combined with multiple chemotherapies and radiation, have been investigated due to their amplification within tumor cells and severe oncolytic impact [36]. Their anticancer effect can be further enhanced through the expression of an antitumor transgene from oncolytic viruses such as adenoviruses (OAd) and vaccinia. Indeed, OAd expressing interferon α (IFNα) efficiently replicates into PDAC cancer cells and shows promising benefits, even if several adverse events related to IFNα, such as systemic toxicity and its poor pharmacokinetics and biodistribution, were reported limiting the potential clinical use of this approach [37]. An increased antitumor effect has been also detected with OAd expressing immunomodulatory genes, like granulocyte macrophage colony-stimulating factor (GM-CSF) and interleukin-12 (IL-12), resulting in both CD4+ and CD8+ T lymphocyte activation [38]. Moreover, an appealing novel strategy could be the combination of oncolytic viruses with immune-checkpoint inhibitors [36]. Besides virotherapies, non-viral strategies progress thanks to the development of innovative RNA interference, plasmid DNA and gene-editing technologies for PDAC treatment. RNA interference mechanisms, tested in ongoing clinical trials, comprise antisense oligonucleotides targeting harvey rat sarcoma viral oncogene homolog (HRAS) and X-linked inhibitor of apoptosis protein (XIAP) with discouraging results, and short interfering RNA (siRNA) targeting mutant KRAS [36]. A systematically delivered plasmid DNA encoded for the wild-type p53 has been also developed, together with gene-editing techniques studying genetic aberration mechanisms for future PDAC targeted therapies [39].

In conclusion, in view of the modest results obtained thus far despite serious efforts, PDAC treatment remains a major challenge that needs innovative, safer and more effective targeted and gene therapies, able to overcome the development of drug resistance mechanisms mainly related to the fibrotic desmoplastic reaction typical of PDAC microenvironment.

2.2 Stromal compartment in PDAC

A hallmark of this malignancy is the pronounced fibrotic stroma, which represents up to 75% of the tumor volume, thus making PDAC one of the most desmoplastic cancers. Besides malignant component, the heterogeneous PDAC microenvironment includes tumor-associated fibroblasts (TAF), immune and inflammatory cells, that constantly interact with the nearby

tumor cells, and collagen, fibronectin and soluble factors stored in the extracellular matrix (ECM) (**Fig. 1**). Due to its key role in PDAC progression, metastasis and drug resistance, investigation of PDAC stromal component offers innovative therapeutic targets against PDAC and its microenvironment [1,40].

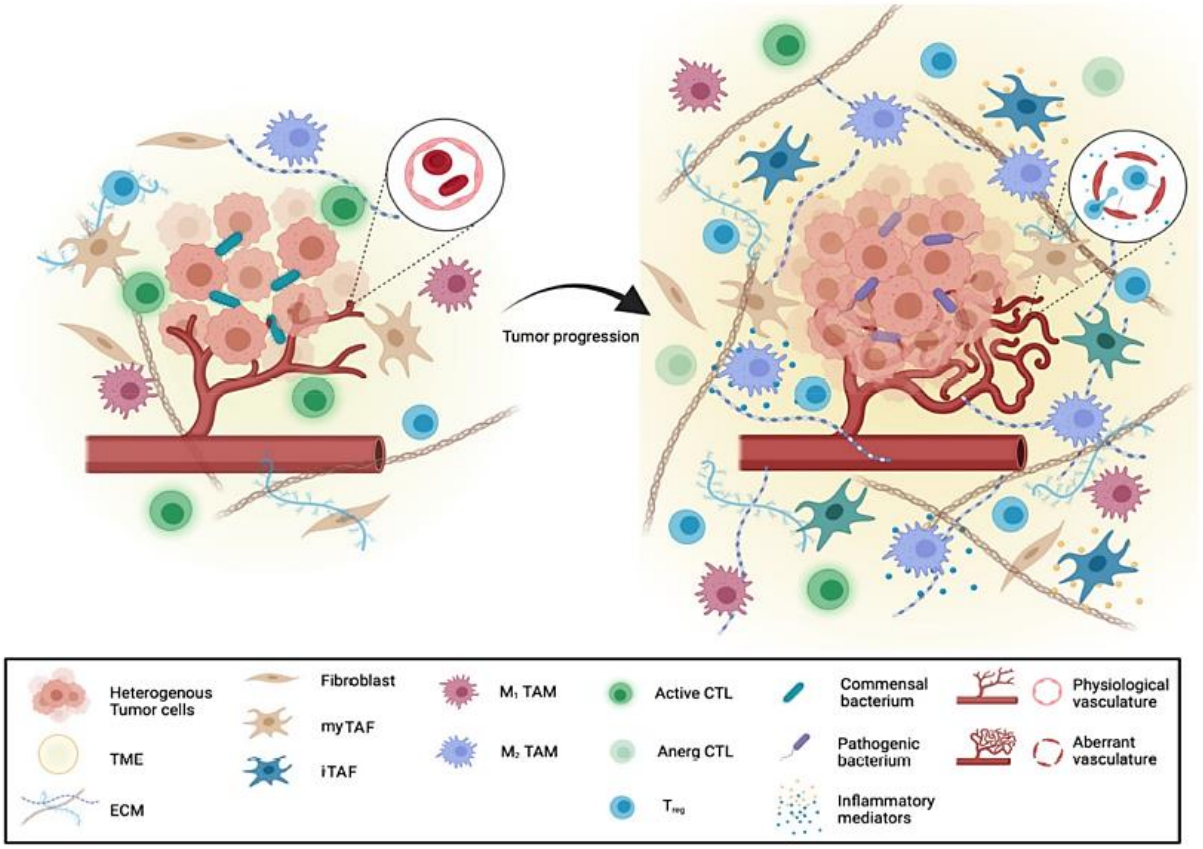

Figure 1. Heterogeneity in stromal component of PDAC

During pancreatic ductal adenocarcinoma (PDAC) oncogenesis, along with the multiple mutations progressively acquired by tumor cells, tumor microenvironment (TME) is subjected to crucial modifications, including (i) activation of tumor-associated fibroblasts (TAF) with distinctive functional phenotypes (myofibroblasts_myTAF and secretory/inflammatory TAF_iTAF), (ii) recruitment of immunosuppressive immune cells, such as tumor-associated macrophages (M1 and M2 TAM) and neutrophils (N1 and N2 TAN) and T regulatory cells (T reg), and anergy induction of cytotoxic T cells (CTL), (iii) alteration of tumor extracellular matrix (ECM) architecture and composition, and (iv) development of novel aberrant blood vessels. Figure is modified from Group Young Researchers in Inflammatory Carcinogenesis et al. (2021) and adapted [41].

2.2.1 TAF and their impact on PDAC progression

TAF represent the major contributor to the PDAC desmoplastic reaction through both the ECM deposition and remodeling and the secretion of cytokines, chemokines and growth factors within the ECM (**Fig. 1**). Pancreatic TAF are characterized by heterogeneous mesodermal origins, such as the activation of quiescent pancreatic stellate cells (PSC) and resident fibroblasts, differentiation of bone marrow-derived mesenchymal stromal/stem cell (BM-MSC) recruited in the pancreas, and transdifferentiation by epithelial-to-mesenchymal transition (EMT), even if the first one is the most remarkable [2]. In healthy conditions PSC show a quiescent phenotype, characterized by vitamin-A storing fat droplets together with desmin and glial fibrillary acidic protein (GFAP) and involved into connective tissue architecture maintenance. Instead, during carcinogenesis the altered ECM composition in terms of inflammatory cytokines, including tumor necrosis factor α (TNFα) and IL-8, and growth factors, such as transforming growth factor β (TGF-β) and platelet-derived growth factor (PDGF), activates PSC, also increasing their proliferation [42]. Once activated, PSC acquire a myofibroblast-like phenotype through the loss of vitamin-A storing droplets and the overexpression of α-smooth muscle actin (αSMA), collagen I and fibroblast-activation protein α (FAP), along with significant ECM synthesis and deposition [43]. In addition to PSC, TAF population can arise from tissue-resident fibroblasts in response to TGF-β or genetic inactivating mutations of the phosphatase and tensin homolog (PTEN) and p53. Moreover, BM-MSC, adipose-derived MSC (AD-MSC) and transdifferentiation through both EMT and endothelial-to-mesenchymal transition also contribute to TAF. However, it is unclear whether their different origins influence their functional polarization [44].

Based on their fibrogenic or secretory/inflammatory functions and distinct levels of α-SMA, two TAF subpopulations known as myofibroblasts TAF and secretory TAF have been identified [44]. Myofibroblasts-phenotype in TAF is induced by the secreted mediators TGF-β, through extracellular signal-regulated kinases (Erk)/MAPK, and PDGF, along with sonic hedgehog (SHH) signaling. Myofibroblasts, expressing high levels of α-SMA and located closely nearby to tumor cells, play a crucial role in promoting fibrosis by ECM production and deposition, EMT processes and tumor metastasis [42]. Instead, secretory TAF, also known as inflammatory TAF, develop because of inflammatory mediators, such as IL-8 and damage-associated molecular patterns (DAMP), and are found distant from cancer cells. They express low levels of α-SMA but secrete high amount of inflammatory soluble factors,

including IL-6, C-X-C motif chemokine ligand 8 (CXCL8) and VEGF, thus resulting in tumor growth through inflammatory mechanisms, immunosuppression, cancer cell proliferation, angiogenesis and drug resistance [43]. Hence, the different markers expressed by the distinct subsets of TAF account for the lack of consensus about TAF molecular definition.

Both myofibroblasts and secretory TAF impact PDAC progression, affecting the multiple hallmarks of this malignancy including proliferation, metastasis, angiogenesis, tumor immunity and drug resistance [2]. TAF, in particular the secretory ones, increase PDAC proliferation and growth thanks to proteins involved in stroma-tumor crosstalk, like FAP, and the secreted growth and inflammatory factors, thus establishing an inflammatory environment which sustains tumorigenesis [45]. TAF are also tied to the invasion and metastasis of PDAC enhancing both malignant cell contractility and persistent remodelling of tumor stroma, along with the upregulation of EMT process [46]. In view of their constitutive expression of VEGF and additional neovascularization regulatory proteins such as VEGF receptors (VEGFR), TAF regulate cancer angiogenesis, also showing the ability to pass through blood vessels supporting tumor cell migration [47]. TAF contribution in PDAC also extends to the regulation of the tumor immunity through the secretion of immunosuppressive cytokines, such as IL-6, TGF-β and CXCL12, which inhibit natural killer (NK) cell and cytotoxic T cell activation whereas promote T reg differentiation, thus allowing the maintenance of an immunosuppressive microenvironment [48]. Lastly, PDAC chemoresistance is significantly promoted by TAF, acting as a both physical and biochemical barrier that interferes with the delivery of chemotherapeutics into neoplastic tissues. Indeed, the pronounced fibrotic stroma produces a high interstitial fluid pressure which compromises the drug transportation from blood vessels to the extracellular target sites. Moreover, in response to the low TAF expression of drug-metabolising enzymes, chemotherapeutic agents including GEM get trapped within TAF, making them not available to tumor cells [2]. Therefore, TAF accelerate cancer proliferation and metastasis, promote angiogenesis, inflammation, immunosuppression, and contribute to chemoresistance, acting as critical players within PDAC microenvironment.

2.2.2 Immune and inflammatory components

Multiple immune cell populations infiltrate PDAC microenvironment (**Fig. 1**). During early phases of carcinogenesis, effector immune cells, including both CD8+ and CD4+ T lymphocytes and NK cells, can be present into the precursor lesions, even if the most of these cells are entrapped within the dense fibrotic stroma and do not reach the malignant component. Subsequently, at later stages, monocytes and neutrophils with an anti-inflammatory phenotype, myeloid-derived suppressor cells (MDSC) and T reg are recruited into the tumor microenvironment, whereas activation of NK cells, CD8+ T lymphocytes and dendritic cells is inhibited, thus accelerating tumor progression and angiogenesis [49].

2.2.2.1 Effector immune cells

Peripheral blood levels of CD8+ cytotoxic and CD4+ helper T lymphocytes, along with NK cells, are significantly reduced in PDAC patients compared to healthy controls [50]. In particular, tumor infiltrating CD8+ T cells are able to induce cancer cell death though perforin- and granzyme-based mechanisms and their levels positively correlate with improved clinical outcomes. However, once activated, within tumor microenvironment CD8+ T lymphocytes activity is inhibited by the translocation of the co-receptor protein CTLA-4 to the cell membrane and its binding to B7 ligand. Moreover, PD1 on activated T cells binds to PD-L1 expressed on PDAC tumor cells, thus leading to T lymphocyte anergy or death [51]. Instead, CD4+ T cells regulate the functions of CD8+ T and B lymphocytes by secreting cytokines and growth factors. Indeed, CD4+ T lymphocytes can differentiate in T helper 1 (Th1) or Th2 cells according to the cytokine released. The first ones promote macrophage activation and CD8+ T cell proliferation through IL-2 and IFNγ, while the latter ones support B cell proliferation by IL-4, IL-6 and IL-10. Adverse outcomes are associated with a phenotype shift, mediated by TAF, from Th1 to Th2 pro-tumorigenic lymphocytes [52]. Lastly, NK cells, belonging to the innate immune system, express low levels of their activating receptors CD226 and CD96 in PDAC patients, thus resulting in NK dysfunction and subsequent PDAC progression [53].

2.2.2.2 Anti-inflammatory myeloid cells

Among the anti-inflammatory myeloid cells infiltrating PDAC, there are tumor-associated macrophages (TAM) and neutrophils (TAN), MDSC and mast cells (MC), which are

significantly increased in PDAC compared to normal controls and correlate with poor patient prognosis [50]. TAM arise from the differentiation of monocytes, recruited by TAF to the tumor tissue, through IL-10, macrophage colony-stimulating factor (M-CSF) and GM-CSF, and represent the most plentiful immune cell population within PDAC microenvironment. During the early tumor phases, both pro- and anti-inflammatory TAM phenotypes (M1 and M2, respectively) can be present, whereas at later stages pro-tumorigenic M2 subpopulation characterized by CD163 and CD204 is prevalent [54]. TAM play a crucial role by supporting the creation of immunosuppressive environment through the secretion of both immunosuppressive and angiogenic factors, such as IL-6, IL-10, TGF-β and VEGF, along with chemokines and cytokines [55]. Like TAM, TAN can be polarized into the N1 or N2 phenotype, and the latter one shows a pro-tumorigenic function mediated by GM-CSF, TNFα and VEGF secretion and matrix metallopeptidase 8 and 9 (MMP-8 and -9) production [56]. Moreover, the same phenotypic features of TAM and TAN can be acquired by MDSC, which are immature immune-suppressive myeloid cells characterized by a myeloid source and the capability to inhibit immune system response. Indeed, MDSC suppress T lymphocyte activation and proliferation, promote T reg polarization and sustain tumor progression through MMP9 and VEGF [57]. PDAC microenvironment also includes MC, recruited by TAF and able to support the attraction of other immune populations within tumor site, thus promoting tumor progression and angiogenesis [58].

2.2.2.3 Anti-inflammatory lymphoid cells

Immunosuppressive lymphoid cells within PDAC microenvironment comprise T reg, Th17 lymphocytes and γδ T cells [50]. T reg, expressing CD4, CD25, forkhead box P3 (Foxp3) and CTLA-4, secrete IL-10 and TGF-β, thereby reducing effector T cell activation and promoting macrophage and neutrophil polarization toward M2 and N2 phenotypes, respectively [59]. Instead, Th17 lymphocytes, characterized by a high plasticity, display both pro- and anti-inflammatory functions in response to different cytokines and growth factors, and can also shift to T reg cells [60]. Finally, γδ T cells expressing T lymphocyte exhaustion markers have pro-tumorigenic impact on PDAC by inhibiting immune checkpoint [61].

2.2.3 Acellular component of PDAC microenvironment

ECM is the acellular component of stromal compartment in PDAC, that provides both the physical structure and biochemical signaling to the nearby cell populations, thus sustaining cancer tissue stiffness and growth. Compared to healthy conditions, tumor ECM architecture exhibits a higher density and different protein composition which changes in response to the requirements of surrounding cells (**Fig. 1**). It consists of collagens, integrins, proteoglycans and glycoproteins, along with growth factors, cytokines and chemokines stored within ECM [1]. Collagens, including type I, III, IV, V and XV, represent the most prevalent ECM component and contribute to tumor progression and chemoresistance through their interaction with signaling integrins expressed on PDAC tumor cells. Moreover, collagen-derived prolines are the major alternative power supply for proliferating cancer cells in absence of glucose, further supporting tumor growth [62]. In particular, collagens I and III are crucial contributors to PDAC desmoplasia and their levels are directly correlated with disappointing patient outcomes. However, when cleaved by proteinases, their involvement can shift toward the inhibition of tumor progression. Even the less abundant collagens IV and V promote tumor cell proliferation, invasion and metastasis [63]. In addition to collagen, ECM also includes integrins, proteoglycans and glycoproteins. Integrins are transmembrane cell-surface receptors, which regulate the interactions between cellular components of PDAC microenvironment and ECM proteins such as glycoproteins and proteoglycans. Moreover, integrins contribute to the migration of cancer cells from dense fibrotic stroma to blood vessels and their extravasation through the induction of MMP expression, thus promoting the metastatic process. Compared to healthy controls, integrins such as β1, β3 and β6 are significantly up-regulated within PDAC microenvironment [64]. Instead, both glycoproteins and proteoglycans within PDAC ECM are characterized by aberrant post-transcriptional glycosylation which alters their role compared to physiological conditions. Glycoprotein galectin-1 (GAL1) together with periostin (POSTN), fibulin and fibronectin 1 are overexpressed in PDAC microenvironment. In particular, fibronectin 1 plays several roles within PDAC ECM, acting as a scaffolding protein, supporting the interactions among integrins and collagens and inducing stromal cell activation through TGF-β release [65]. Proteoglycans are the major contributor to the increased interstitial pressure in PDAC by interacting with hyaluronic acid (HA), whose synthesis begins at precursor lesion stage [66]. Moreover, among the several cytokines, chemokines and growth factors secreted within the

PDAC ECM, SHH signaling regulator, TGF-β and fibroblast growth factor 2 (FGF2), responsible to the TAF generation from PSC, are the most abundant components [67]. Therefore, ECM orchestrates the strong signaling interplay between stromal and malignant components, thus leading to a more aggressive behaviour of PDAC tumor cells.

2.2.4 Anti-stroma therapeutic options

Since the stromal compartment in PDAC plays a key role in promoting PDAC progression and resistance mechanisms toward the traditional chemotherapy along with the more innovative immunotherapy, gene and targeted approaches, significant efforts have been recently focused on the development of novel strategies able to target stromal cellular elements. In this sense, anti-stroma therapeutic options targeting TAF and ECM components or reducing the increased interstitial fluid pressure within PDAC ECM and normalizing tumor blood vessels have been developed and tested both pre-clinically and clinically [68].

2.2.4.1 Targeting TAF

Due to their pro-tumorigenic impact and association with adverse clinical outcomes in cancer patients, inhibition or inactivation of TAF toward quiescent PSC may be a promising strategy for PDAC treatment. In particular targeting SHH pathway, that is the major responsible for the TAF activation, showed promising results in pre-clinical studies using SHH inhibitors, such as the natural alkaloid cyclopamine, IPI-926 or vismodegin, alone or combined with GEM. However, no clinical benefit with a reduction of patient overall survival has been reported in clinical trials. Moreover, the use of diphtheria toxin targeting TAF expressing FAP has been tested, obtaining an increased CD8+ T cell activation and reduced cancer progression in pre-clinical models, in contrast to its disappointing results in clinical studies [68]. Therefore, in view of discouraging data obtained in clinical practice, one possible explanation could be that a complete depletion of stromal microenvironment in PDAC can be related to a more aggressive tumor phenotype with a worst clinical outcome, due to the TAF heterogeneous functions. TAF, especially secretory TAF or those expressing FAP or CD271, may to some extent inhibit PDAC progression rather than promote it. In addition, the interplay between stromal and malignant components within tumor environment may be accountable for a dynamic functional shift toward a pro- or anti-tumorigenic role of TAF [2]. Hence, stroma remodeling with selective blocking of specific stromal subpopulations, instead

of its simple depletion, may be a more effective strategy against PDAC. In this view, analogues of vitamin D such as calcipotriol and paricalcitol are able to reprogram TAF into a quiescent phenotype, thus decreasing tumor fibrosis. Several clinical trials testing vitamin D analogues, in combination with chemotherapy, in resectable and metastatic PDAC patients are ongoing with promising results [69]. Moreover, treatment with vitamin A derivatives like all-trans retinoic acid (ATRA) results into a TAF quiescence induction through Wnt signaling inhibition, leading to a decreased tumor cell proliferation. Evaluation of its clinical efficacy when combined with GEM/Nab-Paclitaxel in PDAC patients is underway [68,70].

2.2.4.2 Targeting ECM components

Among ECM protein-targeting strategies, collagenases were tested in order to decrease ECM stiffness and support chemotherapy delivery to the target sites, even if their effectiveness is limited by growth factor and cytokine release during collagen degradation promoting tumor growth [71]. Another therapeutic target against PDAC ECM is the TGF-β signaling. Indeed, blocking TGF-β using the anticoccidial halofuginone or monoclonal antibody fresolimumab inhibits collagen synthesis and deposition. Pre-clinical studies have achieved promising results, and clinical trials are ongoing [72]. Additionally, the anti-angiotensin vasodilator nitric oxide (NO) combined with GEM, as well as monoclonal antibodies targeting integrins, has been investigated, showing a therapeutic efficacy in PDAC in vivo models with a fibrosis and ECM stiffness reduction [68]. Lastly, MMP inhibitors, such as marimastat and anti-MMP9 antibody, have been also developed with encouraging results due to their ability to remodel ECM proteins; however, no clinical benefit compared to GEM has been reported yet in clinical trials [73].

2.2.4.3 Decreasing interstitial fluid pressure within PDAC microenvironment

Reducing the interstitial fluid pressure in PDAC ECM can be promising to bypass the stromal physical and biochemical barrier that interferes with drug delivery [68]. With the aim of degrading HA, pegylated recombinant human hyaluronidase 20 (PEGPH20) was developed, resulting into an increase of tumor blood vessel diameter and significant reduction of tumor volume in pre-clinical setting when associated with GEM [74]. Instead, PEGPH20 combined with mFOLFIRINOX did not improve the median survival rate of metastatic PDAC patients

compared to chemotherapy alone, even if four patients treated with combinatory strategy (out of the total 138) show a complete response [75].

2.2.4.4 Normalizing tumor blood vessels

Strategies able to normalize tumor blood vessels recovering both their structure and functions were proposed to overcome drug resistance mechanisms [68]. The synthetic antagonist N6L, targeting the angiogenic vessel marker nucleolin that is overexpressed in PDAC patients, enhances perivascular cell recruitment, thus leading to blood vessel normalization [76]. Like nucleolin, nestin is an intermediate filament protein involved in vascular endothelial cell proliferation; its targeting using siRNA has an anti-tumorigenic impact on PDAC in vivo models by inhibiting cancer angiogenesis [77]. Therefore, both nucleolin and nestin targeting could be promising therapeutic approaches to be further investigated in clinical practice.

In conclusion, due to the disappointing results obtained in several clinical trials testing anti-stroma strategies, emerging evidence suggests that the selective inhibition or adjustment of specific PDAC stromal components could result into improved clinical outcomes compared to the complete depletion of tumor stroma [2]. In view of these recent highlights, further studies aimed at designing novel anti-stroma therapies able to selectively target both PDAC stromal and malignant components, in combination with chemo- or immunotherapy, are required. To do this, a deeper understanding of PDAC microenvironment composition and organization is worthwhile.

2.3 MSC

2.3.1 Biology of MSC

MSC have been first identified by Friedenstein et al. in 1968 within bone marrow of adult organisms, thanks to their ability to support hematopoiesis, differentiate into osteoblasts and ex vivo expand forming clonogenic colonies. Along with bone formation, MSC can also spontaneously differentiate toward other mesenchymal tissue cells, such as adipocytes and chondrocytes, in vitro and reconstitute the hematopoietic microenvironment in vivo. Hence, in 1991 Caplan proposed the term MSC [78,79].

In addition to bone marrow, MSC populations can be obtained from other adult tissues, including adipose tissue (AD-MSC), dental pulp, menstrual blood and endometrium, together

with fetal tissues, such as umbilical cord, placenta, Wharton jelly and amniotic fluid [80]. In particular, adipose tissue represents one of the most suitable sources of MSC since it can be easily obtained in large quantity and with negligible patient discomfort under local anaesthesia by all, or most of patients, thus allowing MSC-based autologous treatments. Moreover, adipose tissue is easily processed by enzymatic digestion to isolate AD-MSC with a 500-fold greater yield compared to BM-MSC [81]. However, different MSC origins and developmental stages of the donor may be related to slightly distinct MSC properties in terms of clonogenic colonies, surface antigen expression and propensity to differentiate toward specific cell types. Indeed, compared to the other anatomical sources, both BM-MSC and AD-MSC display a higher capability to form clonogenic colonies and propensity to differentiate into osteoblasts [82].

In order to define MSC population using globally accepted criteria, guidelines have been provided in 2006 by the International Society for Cellular Therapy (ISCT). Characteristic features of in vitro expanded MSC are their plastic-adherence capability in vitro and lack of hematopoietic (CD11b, CD14 and CD45) and endothelial (CD31) cell markers as well as major histocompatibility complex II (MHC II). Contrariwise, MSC express the surface antigens CD73 (ecto-5'-nucleotidase), CD90 (thymocyte differentiation antigen 1, Thy-1) and CD105 (TGF-β receptor III or endoglin), and show a low expression of MHC I. Lastly, their differentiation potential must include bone, fat and cartilage [83]. Indeed, MSC can be in vitro differentiated into these three cell types using cell culture medium added to specific supplements. Additionally, it has been reported that MSC might also differentiate in fibroblasts, ligaments, tendon and myoblasts, or transdifferentiate in pancreatic β cells, hepatocytes and nerve cells [80].

The major contributor to the effects exerted by MSC is their secretoma, composed of cytokines, chemokines and growth factors released by MSC and involved in the modulation of several processes, such as angiogenesis, cell chemotaxis, apoptosis, proliferation, fibrosis and immune response. Firstly, MSC can promote angiogenesis by VEGF, or suppress angiogenetic process through metalloproteinase inhibitors [84], as well as induce or inhibit cellular chemotaxis through CXCL12 and C-C motif chemokine ligand 5 (CCL5) secretion. Moreover, during tissue regeneration MSC release osteopontin, growth hormone and insulin-like growth factor 1 (IGF-1) suppressing apoptosis, TGF-α, bFGF and M-CSF promoting cell proliferation, and angiopoietin-1, VEGF and epidermal growth factor (EGF) reducing fibrotic

process [84]. Paracrine factors secreted by MSC are also the major responsible for their immunomodulatory properties by regulating both primary and acquired immune response, thereby aiding tissue repair. MSC exert their immunoregulatory impact by promoting mobilization of macrophages to damaged tissues and their phenotype conversion from M1 to M2 macrophages [85]. Co-culture with MSC inhibits apoptosis of both resting and activated neutrophils, as well as their mobilization to the injury area [86], and promotes pro-inflammatory chemokine secretion by neutrophils [87]. Moreover, under MSC influence, a direct inhibition of both CD4+ and CD8+ T lymphocyte proliferation is observed especially at high MSC concentrations, while the percentage of FoxP3+ T reg lymphocytes increases [88,89]. Reduction of the levels of pro-inflammatory cytokines secreted by T lymphocytes, like IFNγ and TNFα, and increase of anti-inflammatory cytokine synthesis, such as IL-4, have been detected after co-culture with MSC. MSC exert their modulatory functions also on B lymphocytes, reducing the secretion of immunoglobulins by activated B cells and preventing their differentiation into plasma cells [90].

Therefore, their availability from several tissues, multipotent differentiation, paracrine factor secretion and immunomodulatory properties make MSC-based strategies a promising therapeutic opportunity in the field of regenerative medicine, in particular for musculo-skeletal regeneration, and immunological disorders, currently reaching nearly 1,000 registered clinical trials using MSC [80].

2.3.2 MSC and cancer

In addition to the aforementioned MSC peculiar properties, their natural capacity to selectively migrate and engraft into inflammatory sites, including tumor tissues, along with their immune privileged status make MSC an efficient tool for cell-based anticancer approaches too [91]. Indeed, tissue damage, inflammation and hypoxia, that characterize tumor microenvironment, drive inflammatory cells to secrete chemoattractant factors, including growth factors, cytokines and cancer proteases, which promote the recruitment of MSC also from distant organs such as adipose tissue and bone marrow [92]. The major inflammatory signals responsible for MSC chemotaxis into tumor area include IL-6, IL-8 and TGF-β1, along with several cytokine-receptor pairs, such as VEGF/VEGFR, stem cell factor (SCF)/SCF receptor (c-Kit) and hepatocyte growth factor (HGF)/HGF receptor (HGFR) [68]. MSC capacity for tumor tropism has been reported in nearly all human tumor cell lines,

including pancreatic cancer, ovarian cancer, melanoma, breast cancer, malignant glioma and lung cancer [93]. Once recruited in damaged sites, MSC engraft into tumor microenvironment.

Although MSC display natural abilities for tumor tropism and engraftment, clinical trials evaluating their safety and efficacy reveal that both locally and systemically administered MSC can experience difficulties into their migration toward target tissues and survival [94]. Indeed, for locally delivery, MSC can be eliminated by immune system, apoptotic process or washout. During systemic delivery, instead, most of injected MSC are entrapped into the lung, spleen and liver, and are lost, thus resulting in a limited engraftment into target tissues. Hence, with the aim of improving MSC tumor targeting and thereby their therapeutic effectiveness, several targeting strategies such as physical, physiological and biological mechanisms have been investigated [91]. Physical targeting is based on the MSC placement directly within the target area through surgery or the use of catheters and external magnets or incorporating MSC in biodegradable matrices [95]. Instead, among the physiological mechanisms for MSC tumor targeting, the systemic circulation is exploited for the treatment of lung cancers, since lung capillaries are characterized by a narrow diameter and represent a physical barrier to MSC transition. Therefore, physiological targeting relies on natural forces which drive injected MSC to specific tissues [96]. Several biological targeting approaches have been also developed to increase the efficacy of the systemic delivery against widespread diseases, including metastases. Biological methods comprise strategies able to improve MSC homing potential, such as the use of culture media supplemented with soluble factors and radiation against damaged tissues to increase inflammatory signaling, and augment MSC affinity for tumor sites by specific interactions between highly expressed proteins on target cells and their artificial receptors on MSC [97]. Moreover, despite the promising results obtained with each of the aforementioned approaches, MSC tumor homing may be further improved by a combination of physical, physiological and biological targeting strategies, thus overcoming the major limitations related to post-implantation MSC localization and engraftment in clinical practice.

Once engrafted into tumor microenvironment, MSC are able to support tissue regeneration and restoration of physiological functions through their secretome [92]. Intrinsic anti-tumorigenic effects mediated by recruited MSC comprise the promotion of effector immune cell activation and proliferation, inhibition of AKT, Wnt/β-catenin, B-cell lymphoma 2 (Bcl-

2) and c-myelocytomatosis oncogene product (c-Myc) signaling pathways, and suppression of angiogenesis, thus leading to reduced tumor cell proliferation, arrest in G1 phase and increased cancer cell death both in vitro and in vivo models of tumors, including PDAC [98,99]. However, MSC can to some extent also promote tumor progression through their differentiation toward TAF, thus supporting ECM remodeling, inhibition of both primary and acquired immune response, and induction of EMT and angiogenesis, thus enhancing cancer cell survival, proliferation and metastasis [100]. The dual role played by MSC within tumor microenvironment could be related to MSC anatomical source and degree of differentiation, cancer type, in vitro or in vivo models, interplay of MSC with stromal, malignant and immune cells, and, especially, the large variety of paracrine factors secreted by MSC. Moreover, it may depend on potential reprogramming of naive MSC with anticancer functions toward pro-tumorigenic MSC by tumor cells [101]. Further studies are needed to highlight the intricate interactions between recruited MSC and tumor microenvironment, thus deepening MSC effects on tumor development, progression and migration.

2.3.3 Arming MSC against cancer

Potential limitations of MSC, related to their controversial impact on tumorigenesis, can be successfully overcome using MSC as cellular vehicles for the delivery of antitumor agents, thus enhancing their bioavailability in tumor sites in both pre-clinical and clinical setting. In particular, to achieve this, MSC can be exposed to nongenetic modifications, including the MSC loading with drugs or drug-loaded nanoparticles (NP), or can be genetically manipulated using viral vectors to express suicide genes and antitumor bioactive molecules or incorporate oncolytic viruses (**Fig. 2**) [91].

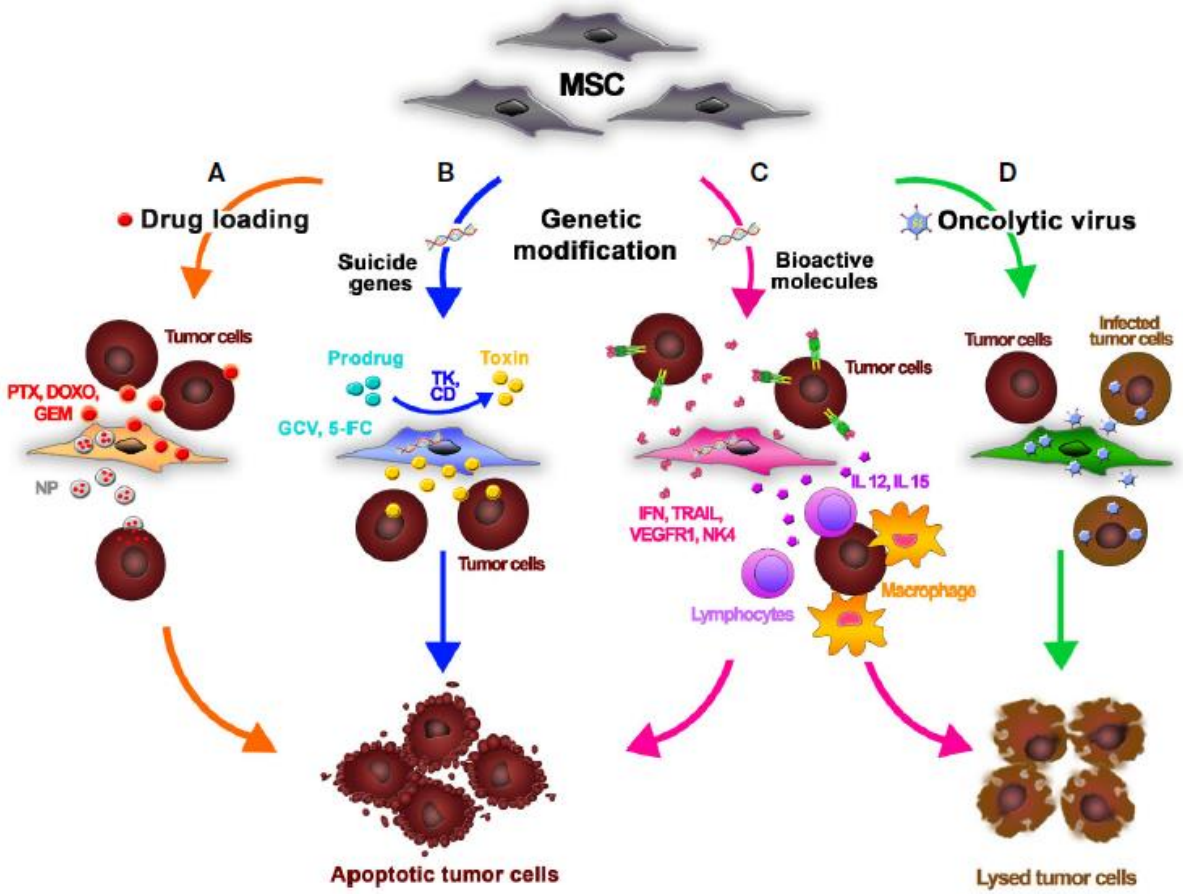

Figure 2. MSC as cellular vehicles for the delivery of antitumor agents by genetic and nongenetic modifications

(**A**) Mesenchymal stromal/stem cells (MSC) can incorporate into their cytoplasm antitumor drugs dissolved into culture medium, such as paclitaxel (PTX), doxorubicin (DOXO) and gemcitabine (GEM), and next release them within tumor sites. MSC can also deliver drug-loaded nanoparticles (NP), improving drug pharmacokinetics and pharmacodynamics. (**B**) MSC can be genetically engineered to produce specific enzymes (e.g., thymidine kinase_TK and cytosine deaminase_CD) which convert prodrugs (e.g., ganciclovir_GCV and 5-fluorocytosine_5-FC), systematically administered before MSC injection, into active cytotoxic derivatives inside the tumor tissue. (**C**) Genetic manipulation of MSC can be also carried out to express antitumor bioactive proteins, such as interferons (IFN), interleukins (e.g., interleukin 12_IL-12 and IL-15), antiangiogenic molecules (e.g., vascular endothelial growth factor receptor 1_VEGFR1 and NK4) and proapoptotic proteins (e.g., tumor necrosis factor-related apoptosis-inducing ligand_TRAIL), inducing a direct action against tumor cells and indirect response by immune cells. (**D**) MSC can be used as carriers and amplifiers of oncolytic viruses into tumor tissues, promoting selectively cancer cell death by oncolysis. Figure is modified from Golinelli et al. (2020) [91].

2.3.3.1 Nongenetic modifications of MSC

Due to their resistance to the cytotoxic effects mediated by chemotherapy, MSC represent the ideal cellular vehicle for the incorporation and subsequent release of anticancer drugs, such as GEM, paclitaxel, doxorubicin and sorafenib, within tumor sites (**Fig. 2A**). In particular, paclitaxel-loaded BM-MSC and AD-MSC significantly decrease tumor cell proliferation and angiogenesis in both in vitro and in vivo models of several cancers, such as myeloma, leukemia and melanoma [102–104].

MSC can also be charged with antitumor drug-loaded NP in order to ameliorate drug stability and pharmacokinetics (**Fig. 2A**). Moreover, the use of MSC as cellular carrier for NP delivery is able to overcome the several limitations associated with NP distribution and immunogenicity. Indeed, due to their immune privileged status along with their tumor homing capacity, MSC avoid immune response activation toward NP and allow the release of chemotherapeutic agents directly into the tumor site [105]. Loading of MSC can be further improved by covalent binding or electrostatic and hydrophobic interactions between MSC and NP. Similar to the paclitaxel-loaded MSC, treatment with MSC delivering paclitaxel-loaded NP decreases tumor proliferation in a lung cancer in vivo model, showing a reduced toxicity than systemically administered paclitaxel or free paclitaxel-loaded NP [106].

Additionally, in contrast to the synthetic NP, MSC can also secrete proteins, lipids, nucleic acids and microRNA (miRNA) associated with extracellular vesicles (EV) acting as “natural NP” against cancer progression [107]. Indeed, EV, classified into exosomes, microvesicles and apoptotic bodies according to their size, are membrane-bound nanomolecules secreted by cells and characterized by an immune privileged status along with a higher stability and slower clearance compared to NP [91]. Since EV content is highly dependent on the EV secreting cellular type, to overcome their heterogeneity, engineered EV may be a promising natural strategy for anticancer drug delivery [108]. For example, it has been reported that BM-MSC can incorporate paclitaxel into their exosomes by diffusion and deliver the chemotherapeutic drug toward PDAC microenvironment, thus resulting into a reduced tumor growth [103]. However, some limitations on EV-based approaches, such as EV large-scale production for clinical practice, need to be further investigated.

2.3.3.2 Genetic manipulation of MSC

Among MSC genetic modifications targeting cancer, MSC can incorporate oncolytic viruses and deliver their cargo toward tumor tissues, thus inducing selectively cancer cell death by oncolysis (**Fig. 2D**) [91]. In view of the MSC nonimmunogenic properties, oncolytic viruses delivered by MSC do not activate immune cell response and can reach the tumor area without being classified as "non self". Hence, the anticancer impact of MSC as carriers of oncolytic viruses is higher compared to the free oncolytic viruses in mouse models of glioma, lung and ovarian cancers [109,110]. A Phase I clinical trial investigating both the best dose and off-target effects of BM-MSC delivering the oncolytic adenovirus DNX-2401 for recurrent glioblastoma, astrocytoma and gliosarcoma is currently ongoing (ClinicalTrials.gov, NCT03896568).

Another genetic approach to target cancer is the MSC engineering, using viral vectors, to produce enzymes able to transform prodrugs, systematically injected before MSC treatment, into active cytotoxic drugs (**Fig. 2B**) [111]. Since conversion occurs only in tumor sites with minimal off-target effects, the ideal drugs for this gene-therapy strategy could be characterized by a poor stability or relevant toxicity, like 5-fluorouracil. The most used enzyme-prodrug approach combined with MSC is based on MSC engineering by herpes simplex virus to secrete the yeast cytosine deaminase, able to convert 5-fluorocytosine in 5-fluorouracil. Indeed, it has been reported that combined treatment between genetically modified AD-MSC expressing the cytosine deaminase and 5-fluorocytosine results into colon cancer inhibition in mouse model [112].

Lastly, MSC can be genetically engineered by viral vectors to express antitumor bioactive proteins, thus resulting into a direct action against cancer cells (**Fig. 2C**) [91]. Among the bioactive molecules delivered by MSC, interleukins (e.g., IL-2, IL-15, IL-18), interferons (e.g., IFNα, -β, -γ) and chemokines, along with molecules involved into antiangiogenetic processes (e.g., VEGFR) and with proapoptotic roles (e.g., tumor necrosis factor-related apoptosis-inducing ligand, TRAIL) have been tested in pre-clinical models of several cancers (e.g., melanoma, lung cancer, glioma, pancreatic cancer) with encouraging results [110]. Furthermore, thanks to the immunoregulatory and immune-effector functions of these therapeutic genes, engineered MSC also promote the activation of immune cells, like NK cells and cytotoxic T lymphocytes, against tumor, thus increasing the anticancer role of MSC [113]. In particular, TRAIL, physiologically expressed by various cells of both innate and

adaptive immune system, represents one of the most promising anticancer molecules used in MSC-based approaches, whose effectiveness has been proved against pancreatic cancer, glioblastoma, lung cancer, hepatocarcinoma and sarcoma both in vitro and in vivo [91]. Instead, in clinical setting, a Phase I trial testing the safety and the best calibrated dose of engineered BM-MSC delivering IFNβ is underway in patients affected by ovarian cancer (ClinicalTrials.gov, NCT02530047).

2.3.4 MSC-based therapeutic approaches for PDAC treatment

Several pre-clinical evidences support the use of both drug-loaded and genetically engineered MSC, isolated from different sources including adipose tissue, for PDAC targeting in vitro or in vivo models. Among the nongenetically modified MSC, loading of BM-MSC with the chemotherapeutic agent GEM allows to reach higher GEM concentrations within tumor sites compared to the GEM intravenous injection, thus leading to a reduction in PDAC tumor cell proliferation [114]. As well as BM-MSC, AD-MSC have been loaded with NP carrying the antineoplastic pirarubicin, thus inhibiting tumor growth, angiogenesis and promoting cancer cell death in a PDAC mouse model. Moreover, it has been demonstrated that BM-MSC can incorporate paclitaxel into their exosomes by diffusion and subsequently deliver the chemotherapeutic agent to PDAC cells with promising results [103]. Pancreatic tumor cell proliferation, migration and invasion are also inhibited by BM-MSC-derived exosomes delivering either miR-124 or miR-126-3p in PDAC in vitro models [115,116]. Instead, among the genetic manipulations of MSC to target PDAC, the delivery of an engineered oncolytic adenovirus, expressing the antitumor molecule TRAIL, by AD-MSC displays a severe oncolytic impact on infected cancer cells, along with a proapoptotic effect mediated by TRAIL on noninfected malignant cells in a mouse model of PDAC [117]. Additionally, umbilical cord-derived MSC engineered to express IL-15 strongly activate both CD8+ T lymphocytes and NK cells in PDAC microenvironment, thus inhibiting tumor growth in vivo [118]. Several efforts have been also focused on genetically modified MSC to express the proapoptotic molecule TRAIL for PDAC targeting, which will be discussed into the 2.4.4 paragraph of this introduction [91].

In the clinical scenario, a single clinical trial using MSC against PDAC is currently underway. It is a Phase I study investigating the best dose and potential side effects of MSC-derived exosomes carrying KRAS G12D siRNA, for metastatic PDAC patients harboring KRAS

G12D mutation. Clinical protocol includes infusions of MSC-derived exosomes on days 1, 4, and 10, followed by three additional courses every 14 days in patients without evidence of toxicity or cancer progression (ClinicalTrials.gov, NCT03608631). Moreover, the Phase I/II clinical trial TREAT-ME1 based on autologous BM-MSC, genetically modified by herpes simplex virus to deliver thymidine kinase, has been designed and conducted in advanced gastrointestinal or hepatopancreatobiliary adenocarcinoma, since their promising results obtained in pre-clinical studies. Clinical protocol is based on systematically administration of engineered MSC and subsequent repeated treatments with ganciclovir. A suitable safety and tolerability of this chemo and gene therapy combinatory approach have been demonstrated [119,120].

In conclusion, MSC-based strategies, as single agents or combined with chemotherapy, represent promising therapeutic options for PDAC treatment in clinical practice, thanks to MSC ability to be armed with drugs, oncolytic viruses, suicide genes and, especially, anticancer bioactive molecules.

2.4 TRAIL

TRAIL is a type II transmembrane protein belonging to the TNF superfamily, whose extracellular domain can be proteolytically cleaved by cysteine protease to obtain a soluble ligand [121]. It is physiologically expressed by various cells of immune system and mediates immunoregulatory and immune-effector functions by binding to its functional death receptors, TRAIL-R1/DR4 and TRAIL-R2/DR5, expressed on the target cell surface, with the consequent activation of apoptotic signaling pathways [122,123]. Additionally, TRAIL expressed by immune cells plays a fundamental role in immunosurveillance against tumors, acting as a tumor suppressor [124]. Based on its anticancer activity, TRAIL-based strategies, including MSC genetically engineered to express this proapoptotic protein, have attracted significant attention for treating tumors, including PDAC.

2.4.1 Molecular basis of TRAIL/TRAIL receptor signaling

Human TRAIL, also known as Apo2L, can bind to five distinct receptors on target cell surface (**Fig. 3**). DR4 and DR5 are the transmembrane functional receptors, characterized by a cytoplasmic death domain able to activate the downstream apoptotic signaling. Instead,

TRAIL-R3/DcR1 and TRAIL-R4/DcR2 are membrane-bound receptors referred to as decoy receptors due to their lack of an integral death domain and their consequent incapacity to trigger apoptotic cascade. Lastly, TRAIL binds to the soluble antagonistic receptor osteoprotegerin (OPG), even if with a reduced affinity compared to DcR1 and DcR2. In contrast to humans, only one functional TRAIL receptor is expressed by murine cells, that is structurally different from either of human agonistic TRAIL receptors [125].

Activation of apoptotic signaling pathways mediated by TRAIL occurs through TRAIL interaction as a homotrimer with DR4 and DR5, resulting in receptor trimerization. Subsequently, thanks to their conserved intracellular death domain, DR4 and DR5 recruit the adaptor protein Fas-associated death domain (FADD), allowing the assembly of the death-inducing signaling complex (DISC) [126]. Initiator procaspase-8 and -10, recruited by DISC, are activated by proteolysis, thus leading to the consequent activation of downstream effector caspases, such as caspase-3, -6 and -7, that mediate apoptotic process. This TRAIL-mediated apoptotic pathway is referred to as the "extrinsic apoptosis pathway" and is sufficient to trigger apoptosis in some cell types (**Fig. 3**) [127]. However, in other cellular types the activation of the "intrinsic or mitochondria-initiated apoptosis pathway" is also required to trigger apoptotic signaling (**Fig. 3**) [125]. Interplay between extrinsic and intrinsic apoptosis pathways occurs through the BH3-interacting domain death agonist (BID), belonging to the Bcl-2 superfamily. Indeed, mature caspase-8 is capable of activating BID by cleavage, which, once migrated to the mitochondria along with Bcl-2 associated X protein (Bax) and Bcl-2 homologous antagonist/killer (Bak), promotes cytochrome c and second mitochondria-derived activator of caspase (Smac/DIABLO) release in cell cytoplasm. Thereafter, the establishment of the apoptosome signaling complex between cytochrome c, the adaptor protein Apaf-1 and procaspase-9 induces the formation of mature caspase-9, that in turn activates the effector caspase-3, -6 and -7, thus resulting into apoptosis promotion [128]. Chemo- and radiotherapy also induce apoptosis through the intrinsic pathway, even if, as opposed to TRAIL, they require p53 activation. Therefore, compared to conventional drugs, TRAIL is able to trigger apoptotic cascade in tumors harboring p53 mutations or deletions too [129].

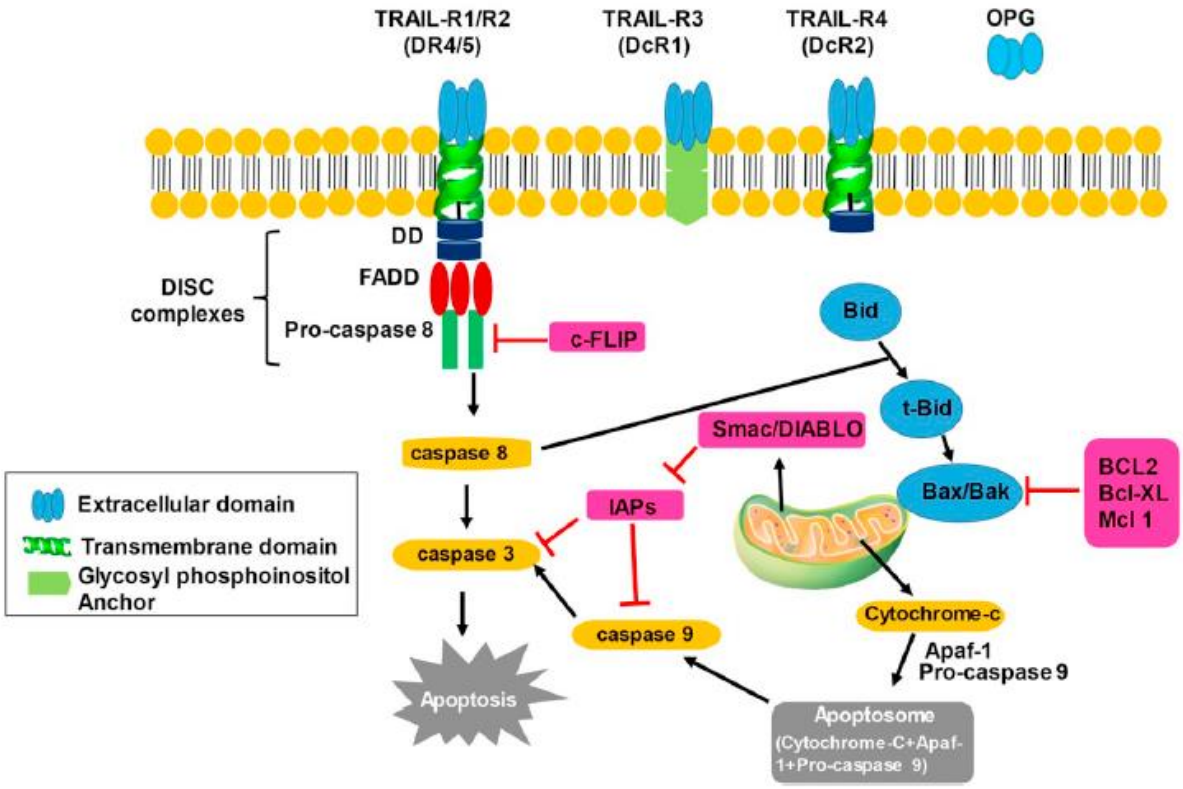

Figure 3. Extrinsic and intrinsic apoptosis pathways activated by TRAIL/TRAIL receptor signaling

TRAIL induces apoptosis through its binding to the functional death receptors TRAIL-R1/DR4 and TRAIL-R2/DR5 thanks to their cytoplasmic death domain (DD). Instead, the TRAIL interaction with decoy receptors TRAIL-R3/DcR1 and TRAIL-R4/DcR2 and the soluble receptor osteoprotegerin (OPG) is unable to trigger apoptotic cascade due to the lack of an integral DD. Extrinsic apoptosis pathway is activated by TRAIL binding as a homotrimer to its functional receptors, which induces the formation of the death-inducing signaling complex (DISC) and the consequent activation of caspase-8. In turn, mature caspase-8 activates the downstream effector caspase-3, resulting into cell apoptosis. Additionally, mature caspase-8 is also able to cleave the BH3-interacting domain death agonist (BID), that induces the release of cytochrome c and second mitochondria-derived activator of caspase (Smac/DIABLO) from the mitochondria into the cytoplasm. Formation of the apoptosome activates caspase-9 and in turn caspase-3, triggering apoptotic cascade. TRAIL-mediated apoptosis inhibitors, such as the cellular FLICE inhibitory protein (cFLIP), inhibitor of apoptosis proteins (IAP), B-cell lymphoma 2 (Bcl-2), Bcl-extra large (Bcl-xL) and myeloid cell leukemia 1 (Mcl-1), can interfere with the two pathways at different levels. Figure is modified from Thapa et al. (2020) [130].

In addition to apoptosis pathway activation, TRAIL could to some extent also promote nonapoptotic signaling. Activation of this noncanonical TRAIL pathway has been detected within TRAIL-mediated apoptosis-resistant cells [125]. Indeed, TRAIL interaction with DR4, DR5 and DcR2 can induce the assembling of a secondary signaling complex composed of

FADD, caspase-8, TNF receptor-associated factor 2 (TRAF2), receptor-interacting serine/threonine-protein kinase 1 (RIPK1) and NF-kB essential modulator (NEMO/IKK), leading to the activation of factor nuclear kappa B (NF-kB), MAPK (e.g., c-jun N-terminal kinase_JNK and ERK) and PI3K/Akt pathways [131,132]. Decision between proapoptotic or pro-survival signaling activation after TRAIL binding may be related to cell-intrinsic features, including different levels of TRAIL-mediated apoptosis inhibitors, such as the cellular FLICE inhibitory protein (cFLIP) and XIAP [133]. However, molecular mechanisms underlying the noncanonical TRAIL signaling need to be further elucidated.

2.4.2 TRAIL signaling in the innate and adaptive immune systems

In view of its physiological expression in several cells of both the innate and adaptive immune system, including macrophages, T lymphocytes, dendritic cells (DC), NK and NK T cells, TRAIL plays a crucial role in immunity and immunoregulation [122]. In particular, endogenous TRAIL binding to its functional receptors acts as a modulator of physiological and pathological events involving the immune system, such as the maintenance of physiological homeostasis and the response to viral infections and autoimmune diseases [134]. It has been reported that TRAIL promotes a monocyte polarization toward an anti-inflammatory M2 phenotype [135] and accelerates neutrophil apoptosis inducing the resolution of inflammation [136]. Moreover, TRAIL induces the deletion of developing autoreactive T and B lymphocytes in central tolerance mechanisms, thereby preserving T cell homeostasis [137], and inhibits Th1 and Th2 cells [138]. TRAIL has a protective role against autoimmune diseases such as autoimmune encephalomyelitis, rheumatoid arthritis, and type I diabetes, preserving peripheral tolerance through the killing of autoreactive T lymphocytes, inhibition of their activation, and promotion of T reg cell proliferation [139]. Furthermore, endogenous TRAIL is involved into immunosurveillance mechanisms against tumors and metastasis, inhibiting tumor development and progression [124]. In tumor immunology, TRAIL can exert its effect directly by inducing apoptosis in tumor cells or indirectly by promoting cytokine secretion by cancer cells stimulating immune system regulation [134]. In particular, TRAIL retains the apoptotic activity of immune effector NK cells that is a prerequisite for immunosurveillance against tumor cells. Indeed, tumor antigen recognition induces NK cell activation that provokes TRAIL release, with a proapoptotic antitumor effect even against disseminated cancer cells [140]. Moreover, monocytes, neutrophils, and immune

effector cytotoxic DC and T cells can activate TRAIL-mediated apoptotic responses in cancer cells [141]. However, the antitumor effects displayed by immune cells expressing TRAIL can be to some extend counteracted by T reg, infiltrating tumor microenvironment, through the secretion of cytokines such as IL-10, TGF-β and IL-35 [142].

2.4.3 TRAIL-based therapy against cancer

Since TRAIL-expressing immune effector cells exhibit a strong anticancer activity, the recombinant human (rh) soluble form of TRAIL molecule (Dulanermin) has attracted significant attention as an antitumor compound due to its ability to selectively trigger apoptotic signaling in tumor cells expressing functional TRAIL receptors, thus sparing healthy tissues [143]. Indeed, functional receptors are often up-regulated on tumor cells, whereas decoy receptors show an increased expression on normal cell. However, decoy receptors are also expressed by tumor cells, without being directly correlated with cell responsiveness to rhTRAIL, suggesting that other mechanisms further regulate TRAIL response in both malignant and non-malignant cells [144]. Along with rhTRAIL, anti-DR4 and -DR5 TRAIL receptor agonist monoclonal antibodies, such as Mapatumumab, Lexatumumab and Conatumumab, have been developed as potential cancer therapy with pre-clinical promising results and subsequently tested in clinical trials. Both rhTRAIL and monoclonal antibodies against TRAIL receptors, alone or combined with chemotherapy, display an evident clinical safety and tolerability. However, their therapeutic response in Phase I/II studies has been lower than expected and their clinical use has been limited due to the suboptimal pharmacokinetics of rhTRAIL, weak apoptotic signaling activated by monoclonal antibodies and intrinsic or acquired TRAIL resistance [130,143]. In particular, half-life of systemically injected rhTRAIL is 0.56 to 1.02 hour in humans because of its rapid renal clearance, whereas monoclonal antibodies display a higher half-life compared to rhTRAIL but mediate receptor dimerization, instead of trimerization, thus resulting into a weak apoptosis induction [143,145]. Therapeutic resistance in TRAIL approach often limits its effectiveness. Indeed, both extrinsic and intrinsic apoptosis pathways are tightly regulated in order to prevent their uncontrolled activation in healthy cells, even if these processes can be also exploited by tumor cells to develop TRAIL-induced apoptosis resistance. Among these regulation mechanisms, high expression of decoy TRAIL receptors could be responsible for TRAIL capture, thus preventing its binding to functional receptors [146]. Moreover,

overexpression of TRAIL-mediated apoptosis inhibitors, such as cFLIP, XIAP and Bcl-2 family proteins, interferes with downstream mediators of TRAIL pathway at different levels and represent the main cause of TRAIL resistance. In particular, cFLIP, whose expression is regulated by NF-kB, MAPK, Akt, and PKC pathways, suppresses caspase-8 activation by binding to FADD, whereas XIAP inhibits effector caspase-3 activation by the mature caspase-9. Anti-apoptotic Bcl-2 family proteins, including Bcl-2, Bcl-extra large (Bcl-xL) and myeloid cell leukemia 1 (Mcl-1), block the mitochondrial depolarization through their interaction with the proapoptotic Bcl-2 family members Bax and Bak [147,148].

Given this scenario, different research groups explored various TRAIL delivery strategies to overcome limitations exhibited by both rhTRAIL and monoclonal antibodies against DR4 and DR5. Among the emerging TRAIL-based strategies, conjugates for TRAIL delivery, TRAIL gene and cell-therapy and combinatory approaches have led to promising results for cancer treatment [130].

2.4.3.1 TRAIL conjugates

Peptide "tags", such as FLAG (FLAG-TRAIL), leucine zipper (LZ-TRAIL) and isoleucine zipper (izTRAIL), have been added to TRAIL, thereby resulting into an increased TRAIL size, with consequent improved stability, and potent apoptotic signaling mediated by TRAIL receptor trimerization [149]. To further reduce their hepatotoxicity and immunogenicity, incorporation of α1 collagen C-pro-peptide (Trimeric-Tag) has been tested, leading to TRAIL homotrimer formation with improved antitumor potential in both in vitro and in vivo cancer models [149]. In addition, a covalent interaction between TRAIL and polyethylene glycol (PEG) or serum albumin, used as NP carriers, also induces better TRAIL pharmacokinetics and pharmacodynamics, stability in serum and longer half-life compared to rhTRAIL in pre-clinical models [150].

2.4.3.2 TRAIL gene therapy

Plasmids expressing different TRAIL variants have been successfully employed for TRAIL gene delivery using both viral and non-viral vectors, allowing a constant production of TRAIL within cancer microenvironment. In systemic administration this delivery system is able to protect TRAIL-expressing plasmids from nuclease activity, avoid a rapid renal clearance and obtain an effective TRAIL concentration within target sites [151]. Among the

non-viral vector-based delivery strategies, systemic administration of liposomes loaded with TRAIL plasmid results into a potent tumor growth inhibition in both in vitro and in vivo models, due to the increased TRAIL half-life, efficient tumor homing capacity and consequent potent activation of TRAIL-induced apoptotic signaling. In particular, the loading of polyamidoamine dendrimers with TRAIL plasmid has been tested for glioma treatment with promising results in mouse models [152].

2.4.3.3 TRAIL cell-based therapy

Among the TRAIL cell-based therapies, the use of genetically modified MSC engineered to constantly product this proapoptotic protein is being currently explored for cancer treatment. The capacity of MSC to be manipulated by viral vectors encoding for therapeutic molecules along with their tropism for tumor sites makes them an efficient vehicle for the delivery of TRAIL in both pre-clinical and clinical settings [153,154]. Moreover, MSC show a low expression of both TRAIL functional receptors, conferring them an intrinsic resistance to TRAIL-induced apoptosis. In the past few years, our group has developed an anticancer gene therapy approach based on AD-MSC as a stable source of the membrane-bound TRAIL, as well as a soluble ligand form (sTRAIL), exhibiting a potent antitumor impact both in vitro and in vivo against several cancer types, including osteosarcoma, rhabdomyosarcoma, Ewing's sarcoma, glioblastoma and pancreatic cancer [3,4,97,155–158].

2.4.3.4 Combinatory strategies

With the aim to overcome the onset of TRAIL resistance mechanisms, combinatory approaches between different therapeutic agents able to synergize with each other have been extensively investigated against cancer [130]. In particular, since apoptosis cascade can be activated through two different pathways, combination of rhTRAIL with chemotherapeutic drugs, such as doxorubicin, irinotecan, GEM and 5-fluorouracil, triggers convergent apoptotic signaling of both extrinsic and intrinsic pathways, thus restoring TRAIL-sensitivity in resistant tumor cells. Moreover, chemotherapy also up-regulates DR4 and DR5 expression on target cells and facilitates TRAIL binding to its receptors [159]. Besides chemotherapeutic agents, inhibitor molecules, such as IAP antagonists, Bcl-2 inhibitors, proteasome inhibitor Bortezomib and cathepsin G, also synergize with TRAIL-based therapy against several types of cancers [130]. Lastly, siRNA silencing Bcl-2, Bcl-xL, XIAP, survivin, cFLIP and TRAIL

decoy receptors can sensitize tumor cells to TRAIL signaling in pre-clinical models, due to their capability to deteriorate target mRNA transcripts or inhibit their translation [160]. Besides the pre-clinical results on combinatory approaches, there have been few Phase I and II clinical studies where rhTRAIL was associated with either chemotherapy agents or monoclonal antibodies [161,162]. These early trials demonstrate the feasibility of combinatory approaches that could also be associated with novel strategies to deliver TRAIL variants.

2.4.4 AD-MSC armed with soluble TRAIL for PDAC treatment

PDAC represents a promising target for TRAIL-based strategies since both PDAC tumor and stromal cells into PDAC tumor tissue show an extensive expression of the two functional TRAIL receptors and a variable expression of decoy receptors. Functional receptors are also expressed by tumor and stromal cells in liver metastasis from PDAC. Evaluation of TRAIL receptor expression has been conducted by immunohistochemistry (IHC) in a retrospective study, that collected tumor specimens from patients affected by PDAC who underwent surgery [40].

Pre-clinical findings prove that PDAC is sensitive to the action of rhTRAIL in both in vitro and in vivo models [163,164]. Furthermore, its association with the current chemotherapeutic agents, including GEM and Nab-Paclitaxel, results into a synergistic impact in pre-clinical investigations for PDAC treatment [165–167]. However, as with most cancers, clinical trials testing rhTRAIL or TRAIL functional receptor agonists reveal limited therapeutic effects against PDAC. Hence, innovative strategies able to overcome rhTRAIL limitations need to be extensively explored to successfully translate pre-clinical evidence into clinical setting [143].

Given this scenario, in our recent studies we have generated AD-MSC delivering a novel TRAIL variant constantly secreted as a soluble ligand (AD-MSC sTRAIL) for PDAC treatment, to bypass the cell-to-cell contact required by MSC engineered with the membrane-bound form of this anticancer agent [3,4,97,158]. sTRAIL armed AD-MSC are characterized by a greater capacity to secrete trimeric and multimeric complexes thanks to the presence of an isoleucine zipper domain. This increased polymerization capacity confers upon sTRAIL superior cytotoxic activity by caspase-8 activation against different PDAC tumor cell lines and primary cells in vitro, compared to the wild-type form. Additionally, AD-MSC sTRAIL peritumorally injected in a subcutaneous mouse model of BxPC-3 PDAC cell line

significantly inhibit PDAC growth, reducing cytokeratin 7 (CK-7) levels and angiogenesis, without off-target effects [3]. We have also demonstrated that Nab-Paclitaxel is able to restore tumor sensitivity to AD-MSC sTRAIL in a TRAIL-resistant in vitro and in vivo model of PDAC, through the downregulation of TRAIL-mediated apoptosis inhibitors such as cFLIP, Bcl-xL and XIAP [4].

So far, no clinical trial for PDAC treatment has been conducted using MSC armed with TRAIL. However, a Phase I/II trial (TACTICAL) with allogenic AD-MSC TRAIL combined with chemotherapeutic agents is currently ongoing to investigate their safety, tolerability, and anticancer efficacy in metastatic nonsmall cell lung cancer (ClinicalTrials.gov, NCT03298763).

In conclusion, based on the reported pre-clinical evidence, the use of AD-MSC armed with sTRAIL in combination with chemotherapeutic drugs, such as GEM or Nab-Paclitaxel, may be a promising therapeutic option to target both the tumor and stromal compartment in PDAC microenvironment, also addressing possible resistance mechanisms and with a potential clinical transferability.

3. AIM OF THE STUDY

Here, we intend to develop an innovative therapeutic approach for PDAC patients combining the standard chemotherapy treatment, represented by GEM, with a novel cell-based gene therapy product based on AD-MSC armed with sTRAIL. The potential clinical transferability of this combinatory strategy was here investigated evaluating the antitumor impact on PDAC and its microenvironment, as well as the safety profile of AD-MSC sTRAIL on white blood cells due to the TRAIL crucial role in immunity and immunoregulation (**Fig. 4**). To achieve these goals, the study has been divided into two sections, each of them with specific aims.

In the first part, we combined treatment of GEM and AD-MSC sTRAIL targeting PDAC, aimed to evaluate the effectiveness and feasibility of the combinatory approach between GEM and AD-MSC sTRAIL targeting both PDAC tumor and stroma by in vitro and in vivo models. In this regard, we assessed the synergistic impact of this strategy on three different PDAC cell lines, characterized by a various sensitivity to TRAIL and GEM, both in 2D and 3D in vitro systems. In addition, a challenging orthotopic PDAC model was here implemented evaluating the efficiency of AD-MSC sTRAIL engraftment and persistence in tumor tissue, along with the antitumor impact of the combined approach (**Fig. 4A**, I). Besides tumor cells, human PDAC primary TAF were also tested for the sensitivity to sTRAIL in combination with GEM, with the aim of investigating the therapeutic potential of this strategy to target PDAC stromal compartment (**Fig. 4A**, II).

In the second part, we evaluated the impact of AD-MSC sTRAIL on white blood cells, aimed to assess the effects of sTRAIL delivered by gene-modified AD-MSC on health and viability of human peripheral white blood cells in vitro. Considering the role played by endogenous TRAIL in regulating both physiological and pathological phenomena of immune system [168] and accounting inflammatory cells as part of tumor microenvironment where mediate the antitumor immune response [49], we wanted to determine any toxic impact displayed by this novel exogenous sTRAIL form on monocytes, polymorphonuclear (PMN) cells and T lymphocytes (**Fig. 4B**).

COMBINATORY STRATEGY FOR PDAC TREATMENT

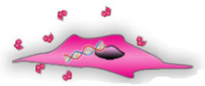
AD-MSC sTRAIL

&

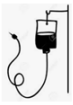
GEM

A. EVALUATION OF ITS ANTITUMOR IMPACT

I) ON PDAC TUMOR CELL LINES

✓ in 2D in vitro system


Cytotoxicity assay (GloMax)

&

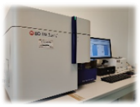
Propidium iodide (PI) staining (FACS)

✓ in 3D in vitro model


BLI signal detection (GloMax)

✓ in in vivo orthotopic PDAC model

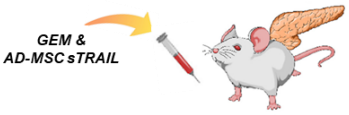


BLI and fluorescence signal detection (IVIS)

&


Ultrasound Imaging System (US)

&


H&E, CK-7 IHC and Basescope assay

II) ON PDAC PRIMARY TAF

✓ in 2D in vitro system


TAF isolation (gentleMACS dissociator)


Cytotoxicity assay (GloMax)

B. EVALUATION OF AD-MSC sTRAIL SAFETY PROFILE ON WHITE BLOOD CELLS

I) IMPACT OF CONDITIONED MEDIUM CONTAINING sTRAIL


Monocyte, PMN and T cell isolation (density gradient)

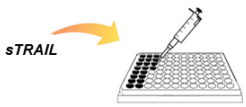


Cytotoxicity assay (GloMax)

II) IMPACT OF CELL-TO-CELL CONTACT WITH AD-MSC sTRAIL

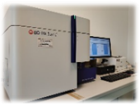
PI staining (FACS)

Figure 4. Overview of experimental workflow of the study

(**A**) Antitumor impact of the combinatory strategy between gemcitabine (GEM) and AD-MSC sTRAIL was investigated on PDAC tumor cell lines (I) in 2D and 3D in vitro systems by cytotoxicity assay (GloMax Discover Microplate Reader), propidium iodide (PI) staining (FACS) and bioluminescence (BLI) signal detection (GloMax), and in a in vivo orthotopic PDAC model via BLI and fluorescence signal detection (IVIS Lumina XRMS), Ultrasound Imaging System (US) and histological analysis, including hematoxylin-and-eosin staining (H&E), IHC analysis of cytokeratin 7 (CK-7) and Basescope^{TM} assay. Proapoptotic effect of the combinatory approach was also assessed on human PDAC primary tumor-associated fibroblasts (TAF) (II) in 2D model by cytotoxicity assay. (**B**) Safety profile of AD-MSC sTRAIL on white blood cells (monocytes, polymorphonuclear_PMN and T lymphocytes) was then investigated, evaluating both the impact of conditioned medium containing sTRAIL released by gene-modified MSC (I) and cell-to-cell contact with AD-MSC sTRAIL (II) via cytotoxicity assay and PI staining respectively.

4. MATERIALS AND METHODS

4.1 Part I: Combined treatment of GEM & AD-MSC sTRAIL targeting PDAC

4.1.1 Cell culture

Three human PDAC cell lines (wild-type BxPC-3, sTRAIL resistant BxPC-3, and MIA PaCa-2) were used. Wild-type BxPC-3 (WT BxPC-3; Interlab Cell Line Collection, ICLC, Genova, Italy) and sTRAIL-resistant BxPC-3 (sT-resistant BxPC-3) [4] were cultured in RPMI (Gibco-Life Technologies, Grand Island, NY, USA) with 10% heat-inactivated fetal bovine serum (FBS; Gibco-Life Technologies, Grand Island, NY, USA), 1% L-glutamine (Euroclone, Milan, Italy), and 1% penicillin/streptomycin (Sigma-Aldrich, Saint Louis, MO, USA). MIA PaCa-2 (ATCC, LGC Standards S.r.l., Milan, Italy) were maintained in DMEM (Gibco-Life Technologies, Grand Island, NY, USA), 10% FBS, 2.5% horse serum (Euroclone, Milan, Italy), 1% penicillin/streptomycin, and 1% L-glutamine. Authentication of PDAC cell lines was performed by the Leibniz Institute DSMZ–German Collection of Microorganisms and Cell Cultures (GmbH, Braunschweig, Germany).

MSC were isolated from lipoaspirate specimens of individuals undergoing aesthetic liposuction after approval from a local ethics committee. Cells were maintained in α-MEM (Gibco-Life Technologies, Grand Island, NY, USA) supplemented with 2.5% human platelet lysate (Macopharma, Tourcoing, France), 1% L-glutamine, 0.5% ciprofloxacin (Fresenius Kabi Italia S.r.l., Verona, Italy), and 0.2% heparin (Sigma-Aldrich, Saint Louis, MO, USA). AD-MSC transduced with a lentiviral vector coding for sTRAIL gene (AD-MSC sTRAIL – Patent Pending Rigenerand Srl) or empty vector as a control (AD-MSC EMPTY) were obtained as described in Spano et al. (2019) [3].

4.1.2 Luciferase transduction of PDAC cell lines

PDAC cell lines were engineered to express a luciferase protein (Lentiviral particles for Firefly Luciferase, GeneCopoeia, MD, USA) per manufacturer instructions. Photon emissions from luciferase-positive (Luc+) PDAC cells were measured via IVIS Lumina XRMS (Perkin

Elmer, Waltham, Massachusetts, USA) with Living Image software (v.4.3.1, Perkin Elmer), used to estimate the level of photon emission per cell.

4.1.3 Cytotoxicity assays

sTRAIL and GEM dose response: PDAC cell lines were seeded in 96-well plates at 5000 cells/well (Corning, New York, USA) and treated the next day with increasing concentrations of GEM (Sandoz, Canada) (0.5–2000 μM) for 24 hours. PDAC cell viability was assessed via Cell Titer AQueous96 One Solution Cell Proliferation assay (Promega, Madison, WI, USA) and quantified via GloMax Discover Microplate Reader (Promega, Madison, WI, USA). Similarly, sTRAIL cytotoxic impact was assessed by treating PDAC cells with conditioned media (CM), collected from engineered MSC and containing increasing concentrations of sTRAIL (50–2500 pg/ml), for 24 hours. CM from AD-MSC EMPTY was collected and used as a control. Tumor cell viability was evaluated via CellTiter-Glo assay (Promega, Madison, WI, USA) and registered via GloMax Discover Microplate Reader.

GEM & sTRAIL combinatory approach in 2D: PDAC cells were seeded in 12-well plates at 21000 cells/well (Day 1) and incubated the following day (Day 2) with 10 μM GEM (WT BxPC-3 and sT-resistant BxPC-3) or 100 μM (MIA PaCa-2). At Day 3, PDAC cell lines were treated for 24 hours more with CM from AD-MSC sTRAIL containing 250 (WT BxPC-3), 500 (MIA PaCa-2), or 300 (sT-resistant BxPC-3) pg/ml of sTRAIL. Death rate was assessed using fluorescent-activated cell sorter (FACS) Aria III (BD, Franklin Lakes, New Jersey, USA) following Propidium Iodide (PI) staining.

GEM & AD-MSC sTRAIL combinatory assay in 3D: Luc+ PDAC cells were seeded in VITVO bioreactor (Rigenerand srl, Medolla, Italy) on Day 1, as described in Candini et al. (2019) [169]. On Day 2, cells were treated with GEM (10 μM for WT BxPC-3 and sT-resistant BxPC-3, 100 μM for MIA PaCa-2) or plain medium for 24 hours. On Day 3, PDAC cells were co-cultured up to 72 hours with AD-MSC sTRAIL at different effector : target ratios (WT BxPC-3 and MIA PaCa-2 E:T = 1:10 and 1:30; sT-resistant BxPC-3 E:T = 1:1 and 1:10). Luciferin substrate (Promega, Madison, WI, USA) was added into co-culture at 10 mg/ml. Tumor cell mortality was quantified based on decrease of Luciferase signal via GloMax Discover Microplate Reader. VITVO loaded with PDAC cells alone or co-cultured with AD-MSC EMPTY were used as controls.

4.1.4 TMRE staining

WT BxPC-3 cells were seeded in 12-well plates at 21000 cells/well and pre-treated with 10 μM GEM, as described above. After 24 hours, CM containing 250 pg/ml of sTRAIL was added, and cells were cultured for 12 more hours. Mitochondrial depolarization was evaluated by MitoStatus TMRE (BD, Franklin Lakes, New Jersey, USA) staining. Samples were acquired via FACS Aria III, and data were analyzed via FACS Diva software (BD, Franklin Lakes, New Jersey, USA).

4.1.5 GEM dose response in WT and engineered MSC

AD-MSC WT or sTRAIL were seeded in 96-well plates at 2500 cells/well. Cells were treated with increasing concentrations of GEM (0.5–2000 μM) for 72 hours. MSC viability was assessed via Cell Titer AQueous96 One Solution Cell Proliferation assay and GloMax Discover Microplate Reader.

4.1.6 ELISA

AD-MSC WT or sTRAIL were cultured with/without GEM (10 or 100 μM) for 72 hours. CM was collected and filtered through a 0.22-μm filter (Euroclone, Milan, Italy). sTRAIL levels from MSC supernatants were measured using a Quantikine Human TRAIL/TNFSF10 kit per manufacturer instructions (Bio-Techne, Minneapolis, MN, USA).

4.1.7 In vivo PDAC orthotopic model and histology

An orthotopic mouse model was used to assess the therapeutic impact of the GEM & AD-MSC sTRAIL combinatory approach after approval by the National Ministry of Health and the local Institutional Animal Care and Use Committee (502/2018-PR. 02/07/2018). $1x10^6$ WT BxPC-3-Luc+ cells in 50 μl of 1:1 Matrigel (Corning, New York, USA) and PBS (Gibco-Life Technologies, Grand Island, NY, USA) suspension were injected into the pancreas of 33 NOD-SCID mice, as previously reported [170,171]. Tumor engraftment was evaluated by bioluminescence 7 days after injection by the IVIS Lumina XRMS system. Tumors were monitored weekly using the ultrasound Vevo 2100 Imaging System (FUJIFILM VisualSonics Inc., Bothell, WA, USA). Before treatment, mice were randomized into four groups by tumor volume. GEM (50 mg/kg) was administered intraperitoneally (i.p.) at Days 25 and 32, followed by an ultrasound-guided intratumor (i.t.) injection of AD-MSC sTRAIL (E:T = 1:30

or 1:10) suspended in 15 µl of PBS at Day 33. AD-MSC sTRAIL were labeled using XenoLight DiR (8 µM; Perkin Elmer, Waltham, Massachusetts, USA), and their biodistribution inside the pancreas was monitored up to 7 days after injection. For tumor necrosis evaluation, tumor and necrotic tissues were quantified using Vevo Lab 3.1.0 software (FUJIFILM VisualSonics Inc., Bothell, WA, USA), and necrosis percentage was calculated as follows: necrotic tissue (mm^3)/total tumor tissue (mm^3) x 100.

Formalin-fixed, paraffin-embedded (FFPE) tumor sections were evaluated via hematoxylin-and-eosin staining (H&E, Carlo Erba, Milan, Italy) and IHC analysis of CK-7, as previously reported [3]. CK-7 expression was analyzed with ImageJ software (NIH, Bethesda, MD), considering all tumor fields per sample at 100X magnification for every individual animal.

4.1.8 Basescope™ Assay

For the detection of AD-MSC sTRAIL in mice tumor samples, we employed the BaseScope™ Assay (ACD Bio-Techne, USA), a novel method of in situ hybridization for visualizing single RNA target molecules in slide-mounted FFPE samples. We designed a specific probe targeting the RNA transcript of the TRAIL transgene and a hybridization-based signal amplification system allowed the detection of TRAIL mRNA inside AD-MSC sTRAIL. Individual sTRAIL RNA transcripts appeared as distinct dots of red chromogen.

4.1.9 Cytotoxicity of GEM & sTRAIL in primary murine stromal cells

A WT BxPC-3 tumor grown in vivo was collected at sacrifice and digested through mechanical and enzymatic dissociation via Tumor Dissociation Kit and the gentleMACS Octo Dissociator (MACS; Miltenyi Biotec, Auburn, CA, USA), following manufacturer instructions. Primary murine stromal cells were isolated and cultured in DMEM low glucose medium (Euroclone, Milan, Italy) with 10% heat-inactivated FBS, 1% L-glutamine, and 1% penicillin/streptomycin. After isolation, murine stromal cells were plated in a 96-well plate at 2500 cells/well. Cells were pre-treated the next day with 10 µM GEM for 24 hours and subsequently treated for 24 hours with CM containing 1000 pg/ml sTRAIL collected from AD-MSC sTRAIL. Cell viability was assessed via CellTiter-Glo assay and registered via GloMax Discover Microplate Reader.

4.1.10 Isolation and immunophenotypic characterization of primary human TAF

Human PDAC tissues were collected from four patients (PZ1 – PZ4) undergoing surgery at the Complex Structure of Hepato-Bilio-Pancreatic Oncological Surgery and Liver Transplant Surgery (University Hospital of Modena), after informed consent. Human PDAC samples were digested as described above. Digested cells were cultured in minimal essential medium with α-MEM containing 2.5% platelet lysate, 1% L-glutamine, 0.5% ciprofloxacin, and 0.2% heparin for 10 days to selectively isolate four primary TAF cell lines. Immunophenotypic characterization of primary human TAF was performed via FACS. Cells were stained using phycoerythrin (PE)-conjugated anti-CD73 (Miltenyi Biotec, Auburn, CA, USA), allophycocyanin (APC)-conjugated anti-CD90 (BD Biosciences, San Jose, CA, USA), fluorescein isothiocyanate (FITC)-conjugated anti-CD105 (BD Biosciences, San Jose, CA, USA), FITC-conjugated anti-CD45 (BD Biosciences, San Jose, CA, USA), PE-conjugated anti-EPCAM (eBioscience, San Diego, CA, USA), FITC-conjugated anti-HLA-DR (eBioscience, San Diego, CA, USA), and BD Via ProbeTM Cell Viability Solution (7-Aminoactinomycin D [7-AAD]; BD Pharmingen, San Diego, CA, USA). To assess TRAIL receptor expression, TAF were tested for PE-conjugated anti-DR4 (BioLegend, San Diego, CA, USA), APC-conjugated anti-DR5 (BioLegend, San Diego, CA, USA), PE-conjugated anti-DcR1 (BioLegend, San Diego, CA, USA), and APC-conjugated anti-DcR2 (R&D Systems, Minneapolis, MN, USA). Isotype control antibodies were used for all cell types and antigens analyzed. Samples were acquired via BD FACSAria III and analyzed via BD FACSDiva software.

4.1.11 Primary human TAF viability assays

Primary TAF from PDAC samples were tested for sensitivity to sTRAIL, alone or with GEM, using a CellTiter-Glo Luminescent Cell Viability assay. Cells were seeded in a 96-well plate at 2500 cells/well in cell culture medium. Cells were next treated with CM from AD-MSC sTRAIL containing increasing doses of sTRAIL (50–2500 pg/ml) or were pre-treated with GEM (10 μM) for 24 hours and incubated with sTRAIL (1000 pg/ml) for 24 hours. TAF viability was assessed via CellTiter-Glo reagent per manufacturer instructions and quantified via GloMax Discover Microplate Reader.

4.1.12 Statistics

Data were expressed as mean values ± standard error of the mean (SEM). An unpaired 2-tailed Student's t-test was used ($p \leq 0.05$ as statistically significant). Fisher's exact test was employed for tumor necrosis quantification in vivo.

4.2 Part II: Impact of AD-MSC sTRAIL on white blood cells

4.2.1 Isolation and cell culture of white blood cells

Human peripheral blood mononuclear cells (PBMC) and PMN were separated by density gradient centrifugation (Lymphoprep; Alere Technologies AS, Oslo, Norway) from the peripheral blood of three healthy donors as approved by the Institutional Review Board.

Monocytes were plated in RPMI 1640 (Gibco-Life Technologies, Grand Island, NY, USA) with 0.5% heat-inactivated defined fetal bovine serum (FBS; HyClone Laboratories, UT, USA) and 1% glutamine (200 mmol/L; Euroclone, Pero, MI, Italy) for 1 hour. Adherent cells were cultivated for 24 hours in RPMI 1640 supplemented with 10% heat-inactivated defined FBS and 1% glutamine and then used for FACS analysis and cell viability assays.

PMN were isolated and used immediately for FACS analysis or plated in RPMI 1640 with 10% heat-inactivated defined FBS and 1% glutamine for cell viability assays.

Lymphocytes were plated in RPMI 1640 with 1% heat-inactivated defined FBS, 1% glutamine, and 1% penicillin-streptomycin (10,000 units penicillin and 10 mg/ml streptomycin in 0.9% sodium chloride; Sigma-Aldrich, Saint Louis, MO, USA) for 2 hours. Non-adherent cells were collected and pre-stimulated for 48 hours in RPMI 1640 supplemented with 10% heat-inactivated defined FBS, 1% glutamine, 1% penicillin-streptomycin, 500 UI/ml rh interleukin-2 (rhIL-2, Proleukin; Clinigen Healthcare Ltd, Stafforshire DE14 2WW, UK), and 7 μg/ml phytohemagglutinin (PHA-M; Sigma-Aldrich, Saint Louis, MO, USA) at a concentration of $1x10^6$ cells/ml. After 48 hours, isolated T lymphocytes were cultured in RPMI 1640 with 10% heat-inactivated defined FBS, 1% glutamine, 1% penicillin-streptomycin, and 500 UI/ml rhIL-2 and used for FACS analysis and cell viability and metabolic activity assays.

4.2.2 FACS analysis

To assess immunophenotype, monocytes were stained using fluorescein isothiocyanate (FITC)-conjugated anti-CD45 (BD Biosciences, San Jose, CA, USA), phycoerythrin (PE)-conjugated anti-CD14 (BD Biosciences, San Jose, CA, USA), peridinin-chlorophyll-protein (PerCP)-conjugated anti-CD3 (BD Biosciences, San Jose, CA, USA), and BD Via ProbeTM Cell Viability Solution (7-Aminoactinomycin D [7-AAD]; BD Pharmingen, San Diego, CA, USA). PMN were stained using FITC-conjugated anti-CD45, allophycocyanin (APC)-conjugated anti-CD10 (BD Biosciences, San Jose, CA, USA), and BD Via ProbeTM Cell Viability Solution (7-AAD). In vitro expanded T lymphocytes were stained using FITC-conjugated anti-CD45, PerCP-conjugated anti-CD3, APC-conjugated anti-CD4 (BD Biosciences, San Jose, CA, USA), PE-conjugated anti-CD8 (BD Biosciences, San Jose, CA, USA), and BD Via ProbeTM Cell Viability Solution (7-AAD). To assess TRAIL receptor expression, monocytes, PMN, and T lymphocytes were tested for PE-conjugated anti-DR4 (BioLegend, San Diego, CA, USA), APC-conjugated anti-DR5 (BioLegend, San Diego, CA, USA), PE-conjugated anti-DcR1 (BioLegend, San Diego, CA, USA), and APC-conjugated anti-DcR2 (R&D Systems, Minneapolis, MN, USA). Isotype control antibodies were used for all cell types and antigens analyzed. All samples were acquired using the BD FACSAria III (BD, Franklin Lakes, NJ, USA) flow cytometer and analyzed using the BD FACSDiva software.

4.2.3 White blood cell viability assays

Monocytes, PMN, and T cells isolated from the three donors were tested in a dose-response assay for sTRAIL cytotoxicity using the CellTiter-Glo Luminescent Cell Viability assay (Promega, Madison, WI, USA). In detail, primary immune cells were seeded in a 96-well plate at a density of 200,000 cells/well in cell culture medium (without IL-2 for T lymphocytes). Supernatants conditioned by AD-MSC secreting sTRAIL or AD-MSC EMPTY as the control were produced as previously reported [3]. The next day, the cell medium was replaced with the supernatants collected from AD-MSC sTRAIL or AD-MSC EMPTY, containing increasing doses of sTRAIL (from 50 to 5000 pg/ml). After 24 hours, treated cells were incubated with the CellTiter-Glo reagent for 10 minutes according to the manufacturer's instructions. The cell viability rate was quantified by measuring the bioluminescence signal using the GloMax Discover microplate reader (Promega, Madison, WI, USA). To assess the

impact of direct cell-to-cell contact with AD-MSC sTRAIL on monocyte and T lymphocyte death, primary immune cells were cultured over a layer of AD-MSC sTRAIL, which were previously allowed to adhere to 12-well plates for 24 hours, at different E:T ratios (1:30, 1:15, 1:10, 1:1, and 10:1; E = AD-MSC, T = T cells) in RPMI 1640 with 10% heat-inactivated defined FBS and 1% glutamine (and 1% penicillin-streptomycin for T lymphocytes). Monocytes or T cells alone (CTL) and co-cultured with AD-MSC EMPTY at a 10:1 E:T ratio were used as controls. Monocyte and T lymphocyte death rate was evaluated by the supravital PI (Sigma-Aldrich, Saint Louis, MO, USA) assay after 24 hours of co-culture. Briefly, non-permeabilized cells were stained using 50 µg/ml PI for 30 minutes [172] and primary immune cell death was quantified by FACS, gating on PI-positive cells.

4.2.4 Metabolic activity assay

The metabolic activity of T lymphocytes isolated from the three donors and treated with sTRAIL was evaluated using the AlamarBlue assay (Invitrogen Corporation, Carlsbad, CA, USA). T cells were treated with increasing doses of sTRAIL (from 50 to 5000 pg/ml) following the same protocol as reported above for the cell viability assay. After 24, 48, and 72 hours of treatment, T lymphocytes were incubated with 10% AlamarBlue for 4 hours at 37 °C. T cell metabolic activity was quantified by measuring the fluorescence signal (λex = 530-560 and λem = 590 nm) using the GloMax Discover microplate reader.

4.2.5 Multiplex ELISA

IL-10, TNFα, IFNγ, VEGF-A, and IL-6 levels were measured in supernatants collected from the co-culture of T cells and AD-MSC sTRAIL (or EMPTY as the control) at different E:T ratios for 24, 48, and 72 hours. The evaluation was done by Labospace Srl using a magnetic Luminex assay (multiplex ELISA; R&D Systems, Minneapolis, MN, USA). Data were reported as fg/ml per T cell for cytokines secreted by T lymphocytes, and fg/ml per AD-MSC for cytokines secreted by AD-MSC.

4.2.6 Statistics

Data are expressed as mean ± SEM. Comparisons of two groups were made with Student's t-test using the Excel 2020 program (Microsoft, Redmond, WA, USA). A two-tailed p-value of ≤ 0.05 was considered statistically significant.

5. RESULTS

5.1 Part I: Combined treatment of GEM & AD-MSC sTRAIL targeting PDAC

5.1.1 sTRAIL released by AD-MSC and GEM display variable cytotoxic activity in PDAC cell lines

To test PDAC cell sensitivity to sTRAIL produced by engineered AD-MSC (courtesy of Rigenerand Srl) or GEM single treatments, dose-response assays were carried out for each drug using two PDAC cell lines, WT BxPC-3 and Mia PaCa-2, and a previously generated sTRAIL-resistant clone of BxPC-3 (sT-resistant BxPC-3) [4] (**Fig. 5**). Regarding sTRAIL activity evaluation, we formerly demonstrated through FACS the high expression of the DR5 functional receptor and the low expression of decoy receptors DcR1 and DcR2 in all selected cell lines [3,4]. Here, PDAC cells were cultured for 24 hours with CM from engineered AD-MSC containing increasing concentrations of sTRAIL (0–2500 pg/ml) (**Fig. 5A**, **5C** and **5E**). Over 60% cell viability decrease compared to the control was observed in WT BxPC-3 and MIA PaCa-2 after incubation with 250 and 500 pg/ml sTRAIL, respectively (**Fig. 5A** and **5C**). Conversely, sT-resistant BxPC-3 showed a weak response to sTRAIL treatment, and over half of tumor cells were still viable at a ten-times higher concentration (2500 pg/ml) of sTRAIL (58 ± 1%) (**Fig. 5E**). Unsurprisingly, CM collected by AD-MSC EMPTY did not induce apoptosis in any tested cell lines. TRAIL resistance did not affect GEM sensitivity in PDAC cell lines, and both WT and sT-resistant BxPC-3 were more sensitive than MIA PaCa-2 to this chemotherapeutic agent (**Fig. 5B**, **5D** and **5F**). After 48 hours of incubation, GEM was able to significantly reduce WT BxPC-3 and sT-resistant BxPC-3 viability even at the lowest tested concentration (i.e., 0.5 μM). This effect increased at 72 hours, with a drop of tumor cell viability to 42 ± 3% for WT BxPC-3 and 56 ± 0% for sT-resistant BxPC-3 at 0.5 μM GEM (**Fig. 5B** and **5F**, respectively). Conversely, MIA PaCa-2 demonstrated higher resistance to GEM treatment, with no significant tumor cell mortality observed after 48 hours of incubation. After 72 hours, a slight decrease in tumor cell viability was observed alongside an increase in GEM concentration. However, at the highest GEM concentration (2000 μM), 52% of tumor cells remained alive (**Fig. 5D**).

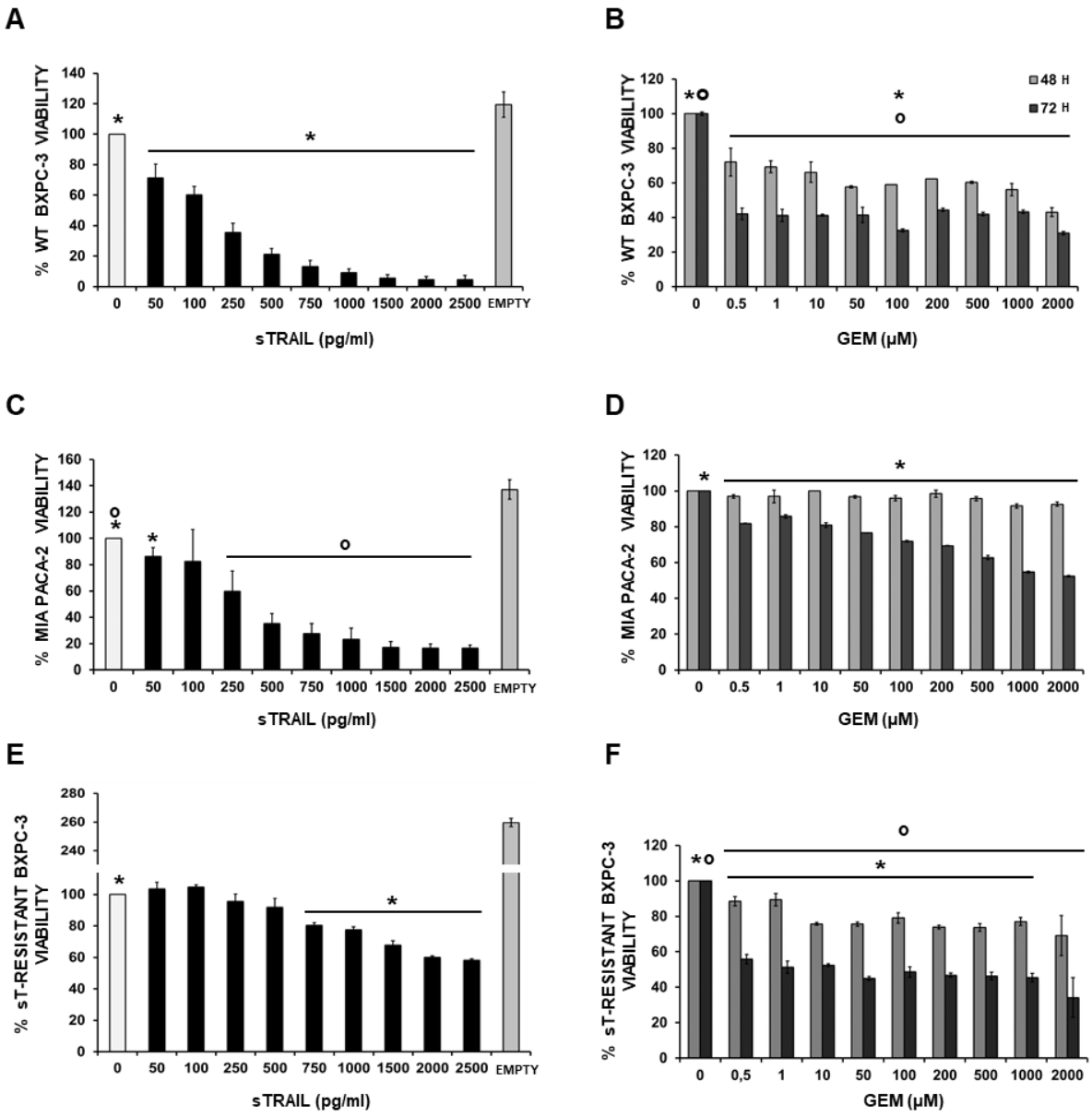

Figure 5. PDAC cell lines display different sensitivities to sTRAIL and GEM

Cytotoxicity assays by evaluation of luminescent viability. Different concentrations of sTRAIL (50–2500 pg/ml) (**A, C, E**) and gemcitabine (GEM; 0.5–2000 µM) (**B, D, F**) were tested on WT BxPC-3 (A-B), MIA PaCa-2 (C-D), and sT-resistant BxPC-3 (E-F) cell lines (sTRAIL treatment: 24 hours; GEM treatment: 48 and 72 hours). For sTRAIL dose response, unconditioned medium (0 pg/ml) and conditioned medium from AD-MSC EMPTY (EMPTY) were used as a negative control. p-values by t-test: A, *p < 0.0007; B, *p < 0.05, °p <0 .0001; C, *p < 0.01, °p < 0.005; D, *p < 0.05; E, *p < 0.005; F, *p < 0.05, °p < 0.005.

5.1.2 GEM synergizes with sTRAIL to induce apoptosis in both TRAIL-sensitive and resistant PDAC cells

Differing sensitivities to single agents registered in PDAC cell lines reflect the clinical heterogeneity in therapeutic responses of PDAC patients and thus a reliable platform to investigate the impact of a combinatorial regimen based on co-treatment with GEM & sTRAIL in the presence of high sensitivity to both single agents (as in WT BxPC-3) or in the presence of resistance to sTRAIL (as in sT-resistant BxPC-3) or GEM (as in MIA PaCa-2).

Given single-drug screening results, we selected appropriate concentrations of GEM and sTRAIL for each PDAC cell line and assessed the synergistic potential of their combination in vitro (**Fig. 6**). The combined treatment of GEM (10 µM) and sTRAIL (250 pg/ml) yielded a significant increase in WT BxPC-3 cell death rate versus either sTRAIL or GEM alone (**Fig. 6A**). Similarly, co-treatment of MIA PaCa-2 with GEM (100 µM) and sTRAIL (500 pg/ml) doubled tumor cell death rate compared to uncombined drugs (**Fig. 6B**). Enhanced proapoptotic effects were also observed in sT-resistant BxPC-3 cell lines after combination of GEM (10 µM) and sTRAIL (300 pg/ml) compared to single treatments (**Fig. 6C**). Overall, the combinatorial approach significantly increased cell death in all treated cell lines compared to single-drug approaches, overcoming resistance.

To explore molecular mechanisms behind the synergy between GEM and sTRAIL against PDAC, we performed TMRE staining and FACS quantification on treated WT BxPC-3, evaluating the loss of mitochondrial membrane potential (**Fig. 6D**). The induction of mitochondrial membrane permeabilization, resulting in release of cytochrome C and subsequent activation of downstream caspase cascade, is a mechanism by which GEM and TRAIL mediate tumor cell apoptosis [173,174]. The combination of these two proapoptotic molecules may cumulatively impact mitochondria membrane permeability, as reported for rhTRAIL and GEM [166], and significantly increase tumor cell death. The combinatory approach with GEM (24 hours) plus sTRAIL (12 hours) yielded massive mitochondrial depolarization compared to treatment with single agents, supporting the observed cooperation of the combinatorial approach in inducing apoptosis (**Fig. 6D**).

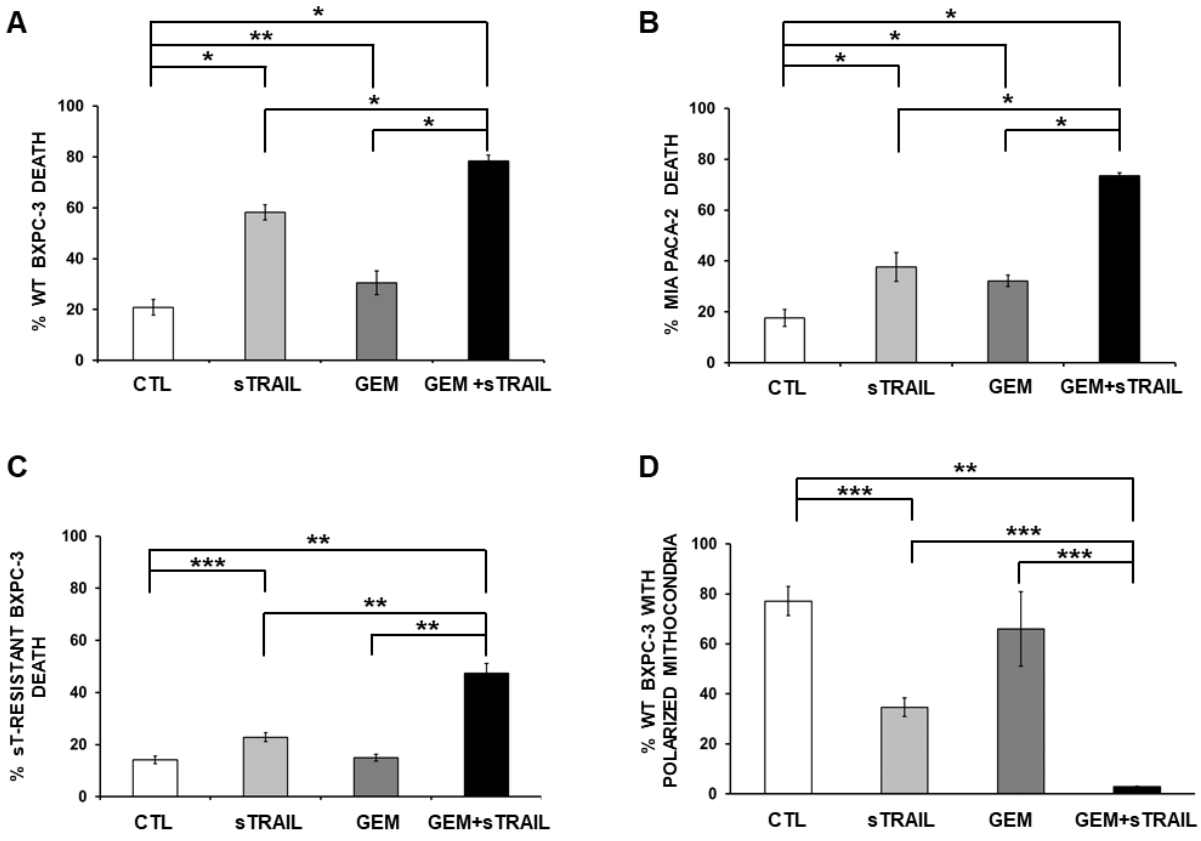

Figure 6. GEM & sTRAIL approach on PDAC cell lines in 2D and molecular mechanism of combinatorial treatment

(**A**-**C**) Cytotoxicity assay performed in 2D by propidium iodide (PI) staining (FACS analysis) on WT BxPC-3 (**A**), MIA PaCa-2 (**B**), and sT-resistant BxPC-3 (**C**) pre-treated with 10 μM (WT BxPC-3 and sT-resistant BxPC-3) or 100 μM (MIA PaCa-2) GEM for 24 hours and subsequently treated for 24 more hours with conditioned media collected from AD-MSC sTRAIL containing 250 (WT BxPC-3), 500 (MIA PaCa-2), or 300 (sT-resistant BxPC-3) pg/ml sTRAIL, respectively. (**D**) TMRE staining by FACS analysis allowed quantification of cells with depolarized mitochondria. WT BxPC-3 were pre-treated for 24 hours with GEM (10uM) alone or cultured for 12 additional hours with sTRAIL (250 pg/ml). Culture media alone was used as a control (CTL). p-values by t-test: *$p < 0.00001$, **$p < 0.005$, ***$p < 0.05$.

5.1.3 AD-MSC sTRAIL and GEM combinatorial regimen generates massive antitumor effect in 3D in vitro models of PDAC

Having obtained significant antitumor efficacy in 2D using CM from AD-MSC producing sTRAIL in combination with GEM, we challenged the therapeutic potency of this combinatorial approach in an in vitro PDAC model. VITVO bioreactor was employed to recreate a tridimensional tumor cell culture mimicking the in vivo tumor burden (**Fig. 7**) [169]. Briefly, Luc+ PDAC cell lines were loaded into VITVO and cells pre-treated with

GEM (10 µM for WT- and sT-resistant BxPC-3, 100 µM for MIA PaCa-2) for 24 hours; AD-MSC sTRAIL were then delivered into the bioreactor at different E:T ratios (1:1 and 1:10 for sT-resistant BxPC-3, 1:10 and 1:30 for other cell lines) (**Fig. 7A**). Notably, for sT-resistant BxPC-3, we selected higher E:T ratios due to resistance of this cell clone to sTRAIL treatment. We confirmed the potent synergistic effect of the GEM & AD-MSC sTRAIL combination for all PDAC cell lines, independent of their respective sensitivities to sTRAIL or GEM alone (**Fig. 7B-D**). For WT BxPC-3, the combination was much more efficient in inducing tumor cell death versus single drugs after only 24 hours of treatment. GEM was able to increase sTRAIL sensitivity of tumor cells, and GEM and AD-MSC sTRAIL combined at the lowest dose (1:30) yielded a cell death rate of 90 ± 2%, while only half (49 ± 7%) of WT BxPC-3 cells were killed by AD-MSC sTRAIL 1:30 alone (**Fig. 7B**). Similarly, GEM & AD-MSC sTRAIL 1:10 and 1:30 provoked apoptosis in 98 ± 0% (1:10) and 97 ± 0% (1:30) of MIA PaCa-2 cells after 72 hours of treatment, improving GEM-mediated cytotoxic impact (51 ± 2%, **Fig. 7C**). GEM alone did not determine a significant cell death percentage in sT-resistant BxPC-3 (48 hours, 21 ± 10%; 72 hours, 24 ± 6%) but was able to revoke sTRAIL resistance displayed by tumor cells, and after 48 hours of treatment with GEM & AD-MSC sTRAIL 1:10, we observed a cell death rate of 83 ± 2% (**Fig. 7D**).

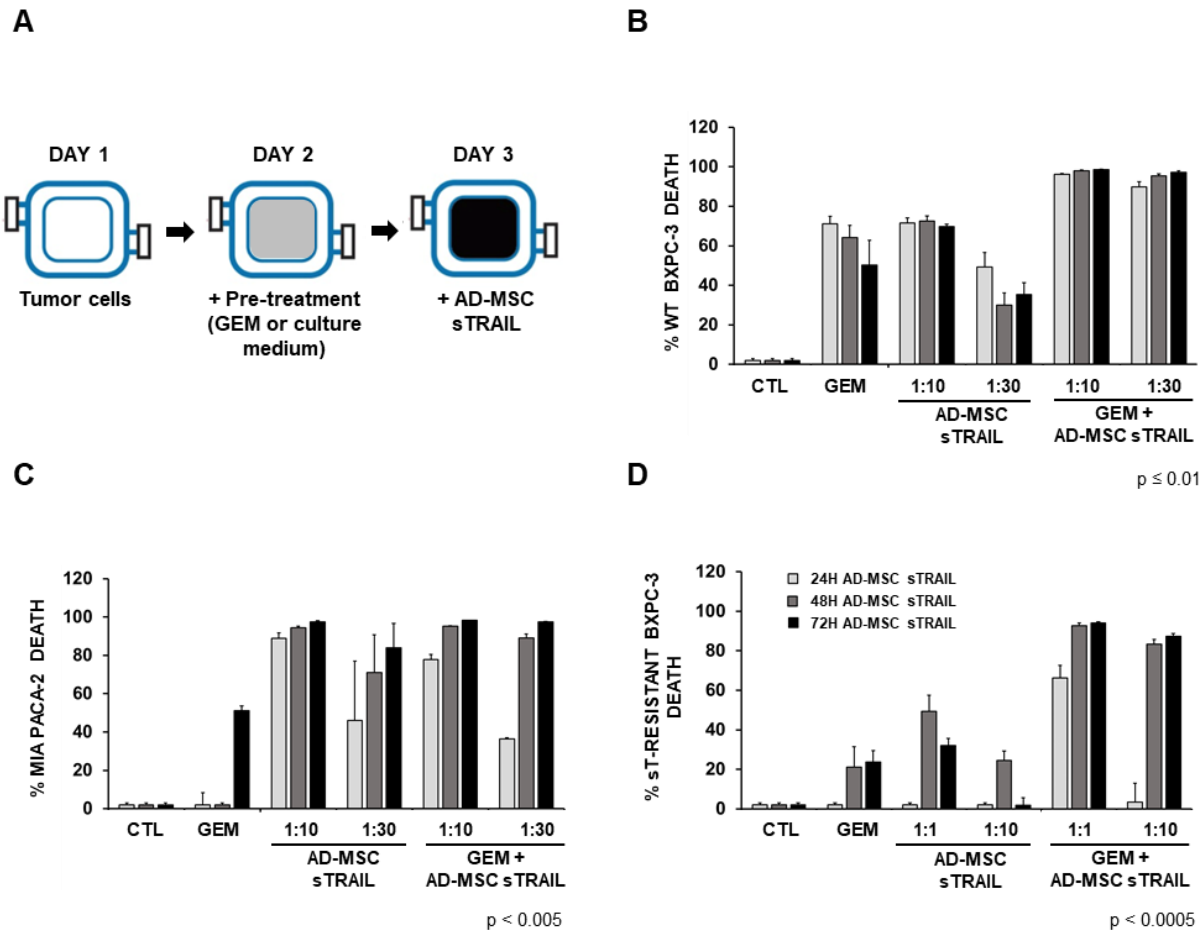

Figure 7. Combinatory approach of GEM & AD-MSC sTRAIL on PDAC cell lines in a 3D system

(**A**) Scheme of the experimental layout: Luc+ PDAC cell lines (**B**, WT BxPC-3; **C**, MIA PaCa-2; **D**, sT-resistant BxPC-3) were cultured in VITVO (Day 1), pre-treated (Day 2) with GEM (10 µM for WT BxPC-3 and sT-resistant BxPC-3, 100 µM for MIA PaCa-2) or plain medium for 24 hours, and subsequently treated (Day 3) up to 72 hours with different effector : target (E:T) ratios of AD-MSC sTRAIL (WT BxPC-3 and MIA PaCa-2 E:T = 1:10 and 1:30; sT-resistant BxPC-3 E:T = 1:1 and 1:10). p-values by t-test: **B**, CTL/GEM/AD-MSC sTRAIL (1:30 and 1:10) vs. GEM+AD-MSC sTRAIL (1:30 and 1:10) 24 h $p \leq 0.01$, 48 h $p < 0.005$, 72 h $p < 0.01$; **C**, CTL/GEM vs. GEM+AD-MSC sTRAIL (1:30 and 1:10) 24 h $p < 0.005$, 48 h $p < 0.0005$, 72 h $p < 0.005$; **D**, CTL/GEM/AD-MSC sTRAIL 1:1 vs. GEM+AD-MSC sTRAIL 1:1 24 h $p < 0.0005$; CTL/GEM/AD-MSC sTRAIL (1:10 and 1:1) vs. GEM+AD-MSC sTRAIL (1:10 and 1:1) 48 h $p < 0.0005$, 72 h $p < 0.00001$.

In hopes of transferring this promising combinatorial approach to a clinical setting, we also investigated whether GEM affected AD-MSC sTRAIL viability with negative effects on possible combinations of drug and cell therapy (**Fig. 8**). Notably, AD-MSC sTRAIL were less sensitive than AD-MSC WT up to 200 µM GEM, with over 60% viability after 72 hours of exposure (**Fig. 8A**). Furthermore, sTRAIL release by AD-MSC sTRAIL was not

compromised by GEM treatment (**Fig. 8B**). Indeed, sTRAIL levels were comparable in CM harvested after 48 hours from cells exposed and unexposed to 10 µM GEM, while 100 µM GEM doubled sTRAIL secretion levels (**Fig. 8B**).

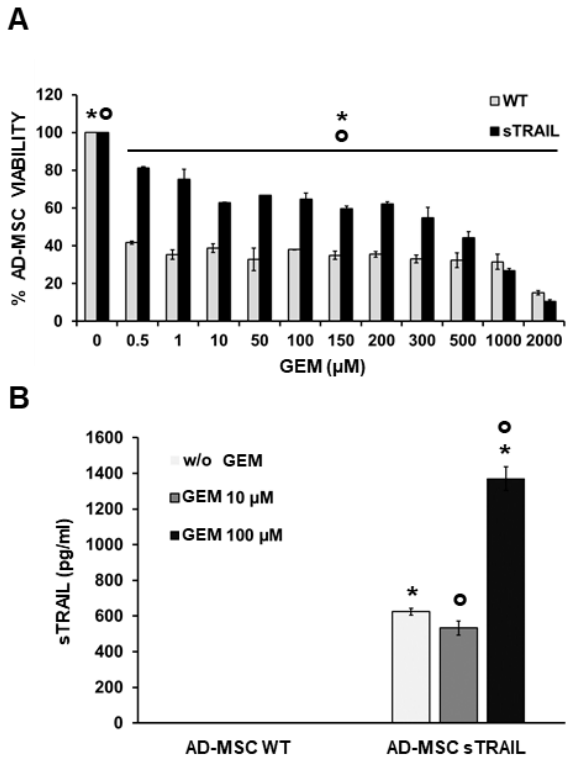

Figure 8. MSC sensitivity to GEM

(**A**) Cytotoxicity assay of GEM (0.5–2000 µM) on AD-MSC wild-type (WT) or sTRAIL (GEM treatment: 72 hours). p-values by t-test: *p < 0.001; °p < 0.01; other comparisons: WT vs sTRAIL from 0.5 to 200 µM, p < 0.004. (**B**) sTRAIL production in AD-MSC sTRAIL after 48 hours of incubation, with or without GEM (10 and 100 uM). As expected, no production of sTRAIL was detected in the supernatant of AD-MSC WT. p-values by t-test: *, °p < 0.01.

5.1.4 Establishment of a predictive orthotopic in vivo model of PDAC and evaluation of AD-MSC sTRAIL biodistribution after eco-guided intratumor administration

A PDAC orthotopic xenotransplant murine model was developed to mimic the clinical situation and both assess the efficiency of AD-MSC sTRAIL engraftment and persistence into the pancreatic tumor and confirm the anticancer efficacy of the combined GEM & AD-MSC sTRAIL. At Day 0, we injected $1x10^6$ WT BxPC-3-Luc+ cells into the pancreas of 5-week-old NOD-SCID mice (**Fig. 9A**). Cells were implanted in the pancreas tail, and a pocket was visible inside the pancreas after surgery (**Fig. 9B**, I). Tumor engraftment and localization were

verified by in vivo bioluminescence imaging at Day 7 (**Fig. 9B**, II). GEM (50 mg/kg) was administered i.p. at Days 25 and 32, while AD-MSC sTRAIL were delivered at Day 33 by ultrasound-guided i.t. injection (**Fig. 9A** and **9C**). Ultrasound imaging enabled precise location of the syringe needle inside the tumor and monitoring of cell distribution during injection (**Fig. 9C**, I-III). The presence of fluorescent areas in the tumor burden, indicating the engraftment and stable persistence of DiR-labeled AD-MSC sTRAIL in the PDAC microenvironment, was detected up to 7 days after AD-MSC sTRAIL injection in all treated tumors (**Fig. 9C**, IV). The fluorescence intensity registered in tumor samples collected from mice who received AD-MSC sTRAIL at the 1:10 dose was three times higher compared to the 1:30 dose, according to the three times higher number of injected cells (**Fig. 9D**). Notably, no other tissues showed fluorescence, suggesting that AD-MSC sTRAIL did not migrate into other organs after intra-tumor administration (data not shown). A Basescope^{TM} Assay also demonstrated that, once engrafted into the PDAC microenvironment, AD-MSC sTRAIL cells appeared as either spindle-shaped viable cells organized in small groups or as single cellular elements (**Fig. 9E**, I-IV). The staining intensity and presence of numerous red dots inside the cytoplasm suggested that engineered MSC expressed the sTRAIL gene in vivo even after intra-tumor delivery (**Fig. 9E**, III-IV).

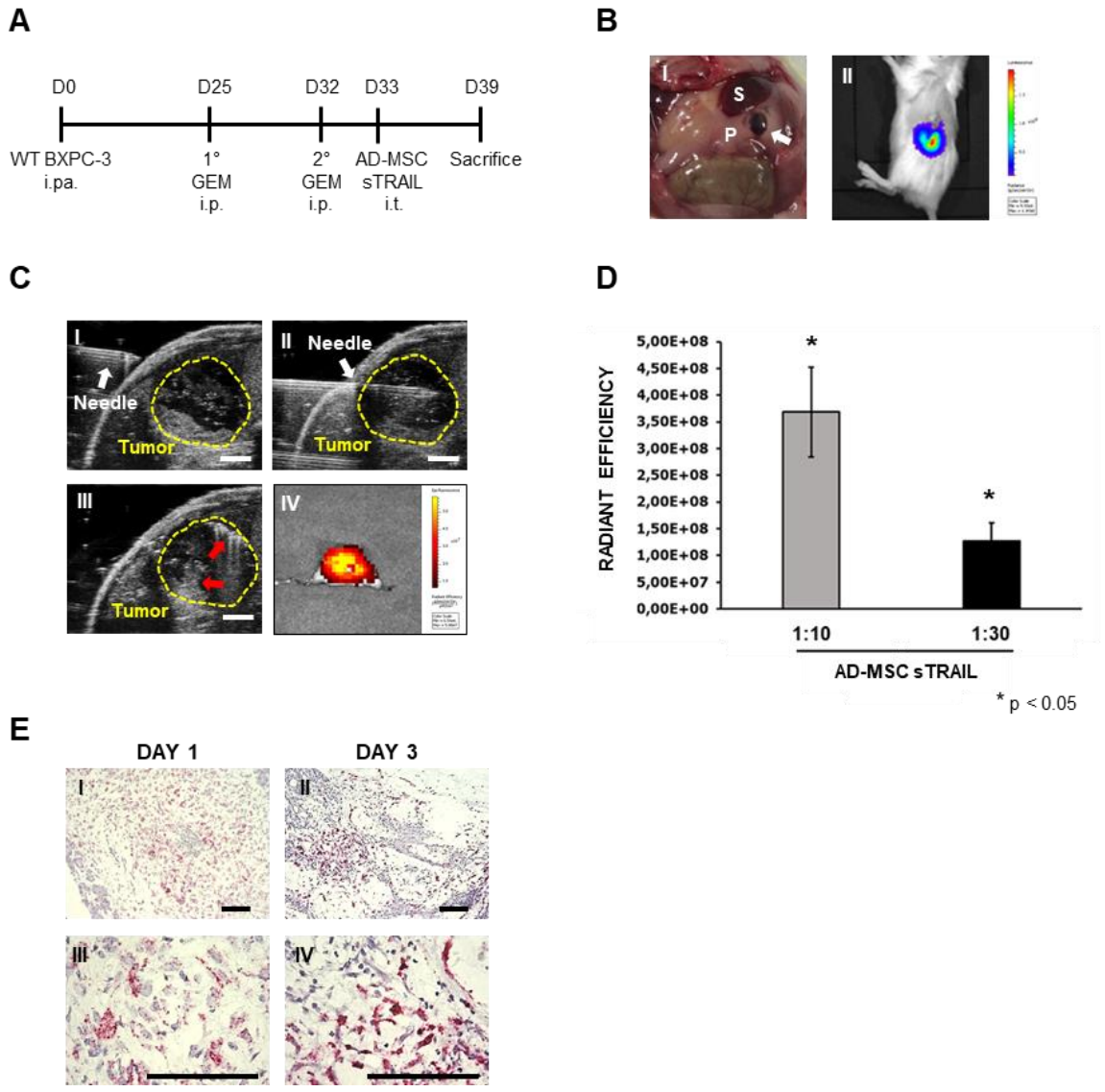

Figure 9. Set-up of PDAC orthotopic model

(**A**) Experimental schedule. WT BxPC-3-Luc+ cells ($1x10^6$) were injected in NOD-SCID mice pancreas at Day 0. GEM was administered intraperitoneally (i.p.) at Days 25 and 32, followed by ultrasound-guided intratumor injection of AD-MSC sTRAIL in two different concentrations (E:T = 1:30 and 1:10) at Day 33. Number of mice/group: CTL, N = 9; GEM, N = 9; GEM+sTRAIL 1:30, N = 7; GEM+sTRAIL 1:10, N = 8. (**B**) I, after WT BxPC-3 injection by surgical procedure, a pocket within the mice pancreas was visible (white arrow). P, pancreas; S, spleen; II, representative image of tumor bioluminescence signal 7 days after WT BxPC-3 injection. (**C**) Representative images of AD-MSC sTRAIL ultrasound-guided injection in orthotopic pancreatic tumor. I, the syringe needle is entering mouse skin; II, the needle is inside the tumor; III, AD-MSC sTRAIL (red arrows) are located inside the tumor after injection. Yellow dashed line surrounds the tumor area. Scale bar 2 mm. IV, Representative fluorescence image of a mouse pancreas with intrapancreatic tumor explanted 7 days after injection of AD-MSC sTRAIL labeled by DiR. (**D**) Mean fluorescence signal in GEM+sTRAIL groups of mice (1:10 and 1:30) generated by DiR-labeled AD-MSC sTRAIL engrafted into pancreatic tumor 7 days post-

injection. p-value by t test. (**E**) Representative images of Basescope™ Assay on WT BxPC-3 tumors one (I and III) or three (II and IV) days after AD-MSC sTRAIL 1:10 injection. Individual sTRAIL RNA transcripts appear as distinct dots of red chromogen precipitate. I-II, magnification 100X; III-IV magnification 400X. Scale bar 100 µm.

5.1.5 GEM synergizes with AD-MSC sTRAIL in shredding tumor tissue in PDAC orthotopic model

Ultrasound imaging allowed non-invasive and realistic real-time analysis of tumor volume and neoplastic tissue composition over time (**Fig. 10A**). Areas of necrosis and serum were visible in ultrasound images as intense hypoechoic (dark) regions. A small amount of necrosis was observed in the control group, while treated mice displayed a higher degree of hypoechoic areas due to tumor tissue shredding (**Fig. 10A**). Three categories of hypoechoic/empty areas in tumors were considered: tumor with 0–20% empty area (low necrotic), tumor with 20–30% empty area (intermediate necrotic), and tumor with over 30% empty area (high necrotic) (**Fig. 10B**). Most mice in control and GEM groups displayed a level of black/hypoechoic/empty tissue between 0–20% (78% and 56% of mice, respectively). However, the latter demonstrated an increase in number of mice with a range of black/hypoechoic/empty between 20–30% and > 30%, suggesting an antitumor effect of GEM. In combinatory groups (both 1:30/1:10), most mice (72/63%, respectively) displayed black/hypoechoic/empty areas greater than 20%. Particularly, in the group treated with GEM & AD-MSC sTRAIL 1:10, 50% of mice presented a necrotic area higher than 30%, with a frequency increase quadruple and double that of control and GEM/GEM & AD-MSC STRAIL 1:30 groups, respectively. However, due to the limited number of mice employed in the study, these differences were not statistically significant (Fisher's exact test).

Observations made with ultrasound images were validated using histological analyses (**Fig. 10A** and **10C**). Images of the H&E sections were compared to those acquired with ultrasound, and the presence of large necrotic areas in treated samples was confirmed (**Fig. 10A**). Hypoechoic regions detected by ultrasound corresponded to degenerated and necrotic areas in tumor burden. All treatments modified the tumor microenvironment structure, inducing the formation of empty holes due to tumor cell degeneration and tissue integrity loss. However, the combinatorial regimen was able to reinforce the anticancer effect with the chemotherapeutic drug, provoking the formation of larger, more numerous areas of necrosis together with empty space in tumor parenchyma (**Fig. 10A** and **10C**). A significant reduction

of CK-7 expression was also observed in all treated tumors compared to the control group, but the combinatorial regimen (at both E:T ratios) resulted in a higher reduction of tumor cell amount compared to GEM alone (CK-7 positive cells: CTL = 54 ± 1%; GEM = 45 ± 2%; GEM+sTRAIL 1:30 = 39 ± 2%; GEM+sTRAIL 1:10 = 41 ± 2%), further confirming the synergistic antitumor impact observed in H&E analysis (**Fig. 10D**). Additionally, histological analysis revealed that PDAC tumors were composed primarily of tumor cells (i.e., WT BxPC-3) organized into tumor "islets," but infiltrating murine stromal cells were also present (**Fig. 10C**).

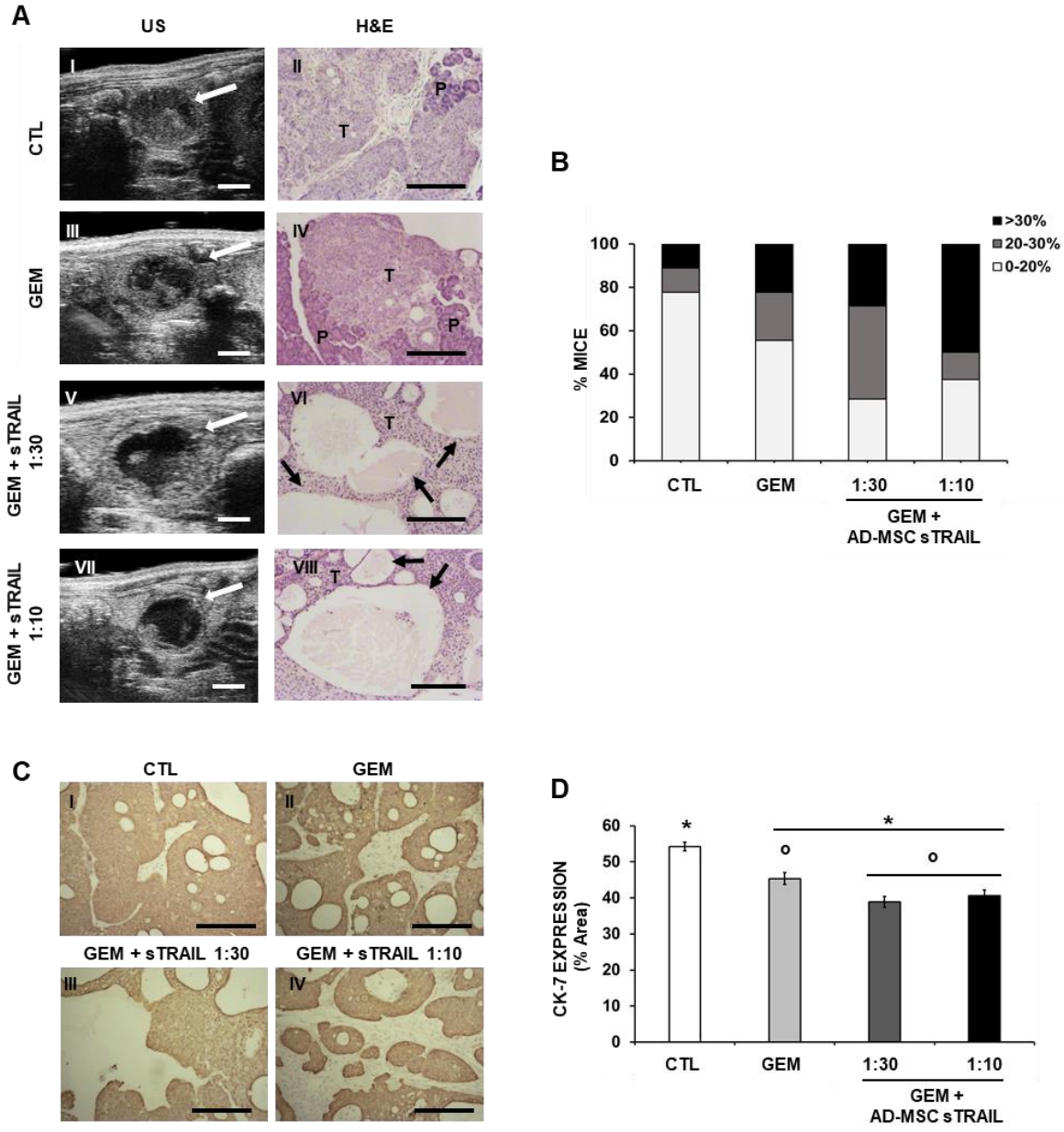

Figure 10. Antitumor efficacy of GEM+AD-MSC sTRAIL on PDAC orthotopic model

(**A**) (I, III, V, VII) Representative ultrasound images of orthotopic-implanted pancreatic tumors, control (CTL; I) or treated with GEM alone (III) or with GEM+AD-MSC sTRAIL 1:30 (V) or 1:10 (VII). Compact and trophic neoplastic tissue was visible as bright hyperechoic regions, while degenerated tumor tissue appeared as hypoechoic (dark) regions via ultrasound. White arrows indicate the intrapancreatic tumor. Scale bar 2 mm. (II, IV, VI, VIII) Representative microphotographs of H&E staining of tumors. T, tumor parenchyma; P, pancreas; black arrow, necrotic areas. Magnification 100X, scale bar 200 µm. (**B**) Percentage of mice with black/hypoechoic/empty areas in the different groups measured by ultrasound. (**C**) Representative images of the histological analysis of pancreatic tumor tissue in mice by anti-cytokeratin 7 (CK-7) IHC. Magnification 100X, scale bar 200 µm. (**D**) Histogram representing the quantification of CK-7-positive areas within different groups. p-values by t-test: *$p < 0.00001$; °$p < 0.05$.

Hence, as part of tumor mass, we also evaluated the impact of the combinatorial regimen on murine stroma, isolating a murine stromal primary cell line from a WT BxPC-3 tumor grown in vivo and performing a cytotoxicity assay. Murine stromal cells displayed resistance to both single and combined treatments in respect to WT BxPC-3 (**Fig. 6A** and **11**), with 95 ± 0% of murine stromal cells still viable after incubation with sTRAIL CM, while a lower, yet notable, percentage of stromal cells were resistant to GEM and GEM & sTRAIL (51 ± 5% and 44 ± 3%, respectively).

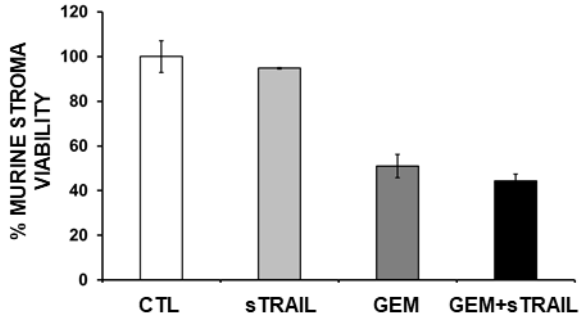

Figure 11. Murine stroma sensitivity to the combinatorial approach

A WT BxPC-3 tumor grown in vivo was digested and murine stroma were isolated. A cytotoxicity assay in 2D was performed on murine stromal cells with a pre-treatment with 10 µM GEM for 24 hours; murine cells were subsequently treated for 24 more hours with conditioned media (CM) collected from AD-MSC sTRAIL containing 1000 pg/ml sTRAIL. p-values by t-test: CTL/sTRAIL vs. GEM $p < 0.05$; CTL/sTRAIL vs. GEM+sTRAIL $p < 0.01$.

5.1.6 Pre-treatment with GEM sensitizes patient derived TAF to sTRAIL apoptotic effect

Human primary TAF were obtained from four patients affected by PDAC (PZ1–PZ4) through mechanical and enzymatic digestion. Isolated cells were cultured in selective medium and, ten days after in vitro culture, a population composed of spindle shape cells displaying typical fibroblast morphology was visible (**Fig. 12A**). Immunophenotype of primary TAF was characterized by flow cytometry [99]. Most of the isolated cells demonstrated the typical mesenchymal antigen expression profile, expressing CD73 (98 ± 1%), CD90 (99%), and CD105 (87 ± 12%) and lacking CD45, EPCAM, and HLA-DR markers, proving their stromal cell lineage and confirming the absence of leukocyte or epithelial contaminant subpopulations (**Fig. 12B**). Moreover, to predict sensitivity of TAF to the sTRAIL apoptotic effect, expression of both functional (DR4, DR5) and decoy (DcR1, DcR2) TRAIL receptors was evaluated on the cell membrane of isolated cells. PDAC TAF displayed high levels of DR5 (60 ± 3%) and negligible expression of DR4 and decoy receptors DcR1 and DcR2 (less than 10%, **Fig. 12C**).

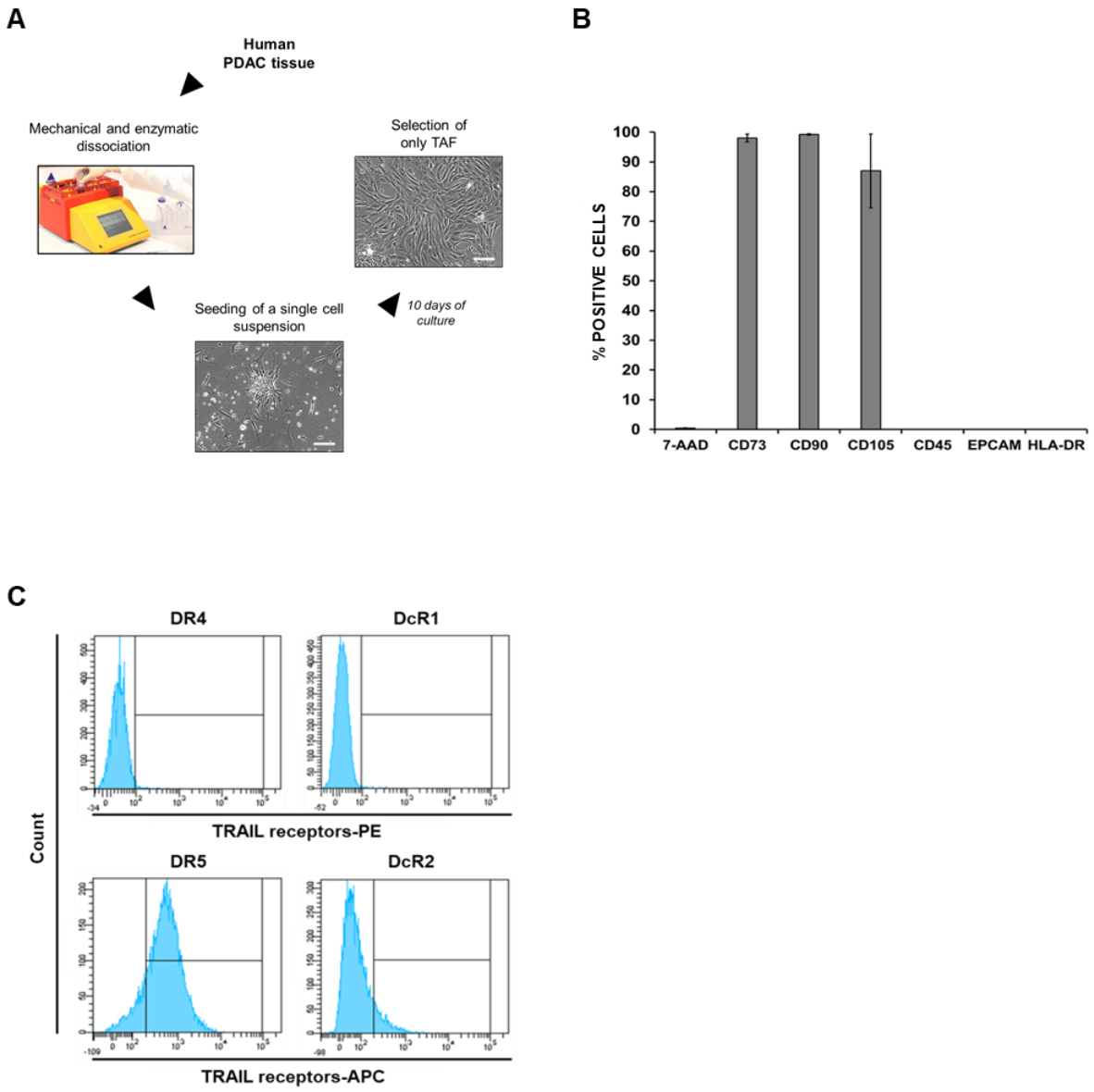

Figure 12. Isolation and characterization of TAF from four primary PDAC samples

(**A**) Experimental workflow of primary TAF isolation from four human samples collected from patients affected by PDAC (PZ1 – PZ4). (**B**) Stromal origin of primary TAF was confirmed by FACS based on the expression of CD73, CD90, and CD105 markers. Contaminant leucocytes populations were excluded based on lack of CD45, EPCAM, and HLA-DR antigen expression. (**C**) The presence of both functional (DR4 and DR5) and decoy (DcR1 and DcR2) TRAIL receptors was also investigated in primary TAF by FACS.

To investigate whether sTRAIL released by AD-MSC sTRAIL triggers apoptosis in human TAF from PDAC samples, TAF viability was evaluated by testing increasing doses of sTRAIL (0–2500 pg/ml). For all tested conditions, TAF viability after 24 hours was not significantly reduced compared to untreated cells (**Fig. 13A**, **13C**, **13E** and **13G**), indicating

resistance to the cytotoxic effect mediated by sTRAIL despite the high expression of DR5 on cell membranes. After demonstrating the synergistic impact of GEM and sTRAIL on both TRAIL-sensitive and resistant PDAC cells, we investigated whether pre-treatment with GEM was also able to revert TRAIL resistance in primary human tumor stromal cells. Human TAF were pre-treated with GEM (10 µM) for 24 hours; sTRAIL (1000 pg/ml) was then added to culture media for 24 more hours. Cell priming with GEM remarkably enhanced TAF sensitivity to sTRAIL, demonstrating a potent synergistic antitumor effect in 80% of analyzed stromal samples (**Fig. 13B**, **13D**, **13F** and **13H**). Additionally, despite the relative cytotoxic effect of GEM as a single treatment (more than 40% of TAF death), the combinatory approach of GEM & sTRAIL significantly reinforced the toxic effect mediated by GEM, increasing TAF mortality compared to the chemotherapeutic drug alone (**Fig. 13B**, **13D**, **13F** and **13H**). These results suggest that a combinatory approach based on GEM & sTRAIL may present an effective therapeutic option for targeting both tumor and stromal compartments in PDAC.

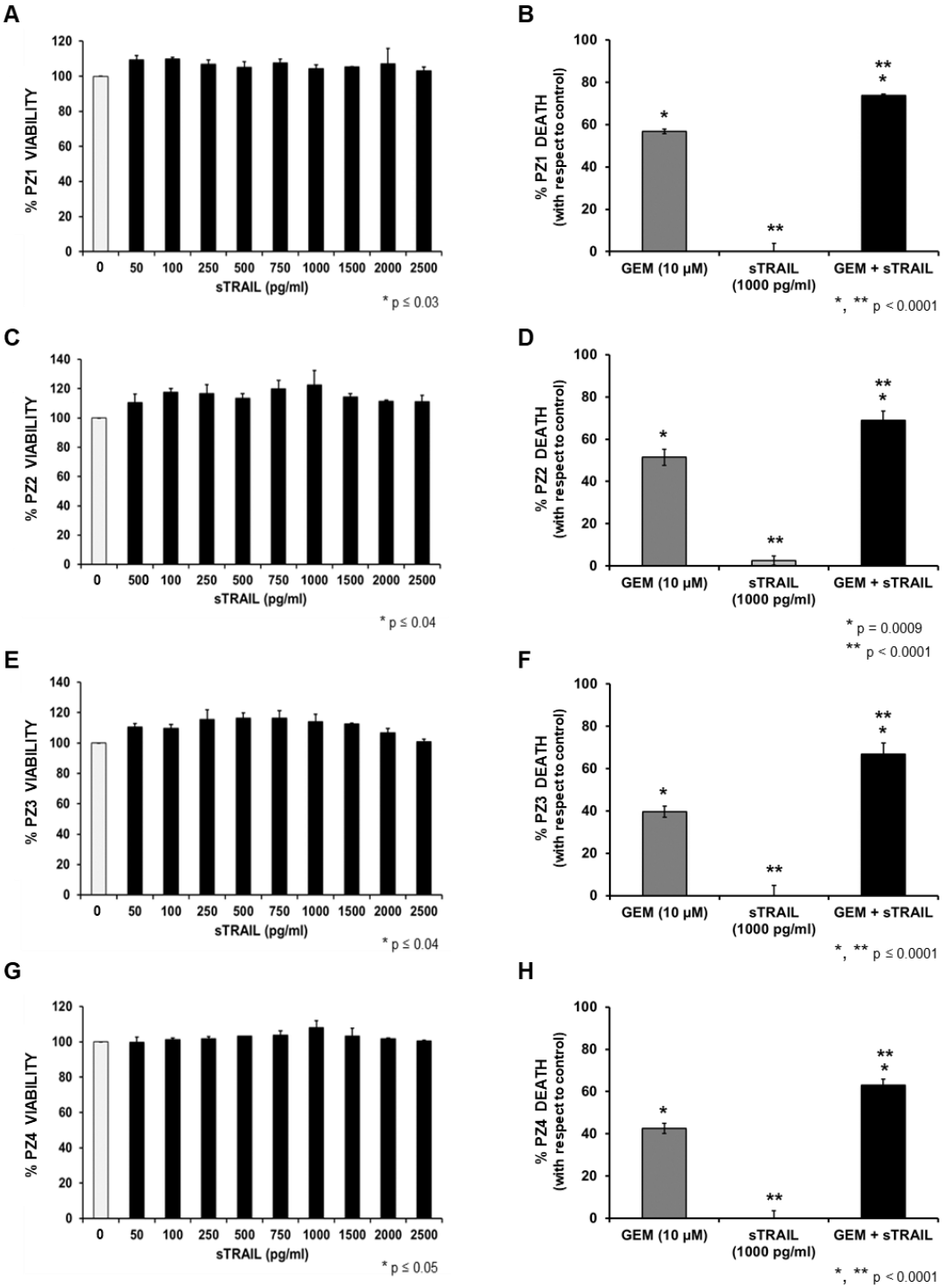

Figure 13. GEM & sTRAIL approach on primary TAF isolated from human PDAC samples

(**A, C, E, G**) Cells were treated with increasing concentrations of sTRAIL (50–2500 pg/ml) for 24 h, with cell viability evaluated by CellTiter-Glo assay. Culture media alone was used as a negative control. (**B, D, F, H**) Cytotoxicity of primary stromal cells performed by CellTiter-Glo Assay. Primary TAF were pre-treated with 10 µM GEM for 24 hours, and CM containing sTRAIL (1000 pg/ml) was added for 24 more hours. GEM (10 µM) or sTRAIL (1000 pg/ml) alone were used as a control. p-values by t-test.

5.2 Part II: Impact of AD-MSC sTRAIL on white blood cells

5.2.1 Evaluation of TRAIL receptor expression on white blood cells

White blood cells were obtained from the peripheral blood of three healthy donors. After density gradient centrifugation, monocytes, PMN, and T lymphocytes were isolated and grown separately in vitro under different culture conditions. For each leukocyte subpopulation, the immunophenotype was assessed by flow cytometry to confirm the purity and the lineage of in vitro expanded cells. Cultured primary monocytes were characterized and quantified based on the co-expression of CD45 and CD14 antigens (**Fig. 14A**, left). The analysis revealed that most cells (63±2%) displayed the antigen profile typical of monocytes. Despite the selective culture conditions, a small fraction of lymphocytes (14±10%) was still present within the monocyte cell culture as revealed by the co-expression of CD45 and CD3 (**Fig. 14A**, right). Therefore, contaminant T cells were excluded from the following analysis by gating on CD45+/CD3− cellular elements. After isolation, both CD45 and CD10 antigens were detected on the cell membrane in 85±5% of viable PMN, thus confirming their neutrophil lineage (**Fig. 14B**). T lymphocytes were cultured with IL-2 in vitro before being used in further experiments. In vitro expanded T lymphocytes were analyzed by gating on viable 7AAD− cells (73±14%, data not shown). The number of CD4+ helper and CD8+ cytotoxic T lymphocytes within the CD45+/CD3+ population was quantified (**Fig. 14C**, left). FACS analysis revealed that within the T cell population, most lymphocytes were positive for the CD8 antigen (71±9%), whereas only 14±1% of cells expressed CD4 (**Fig. 14C**, right).

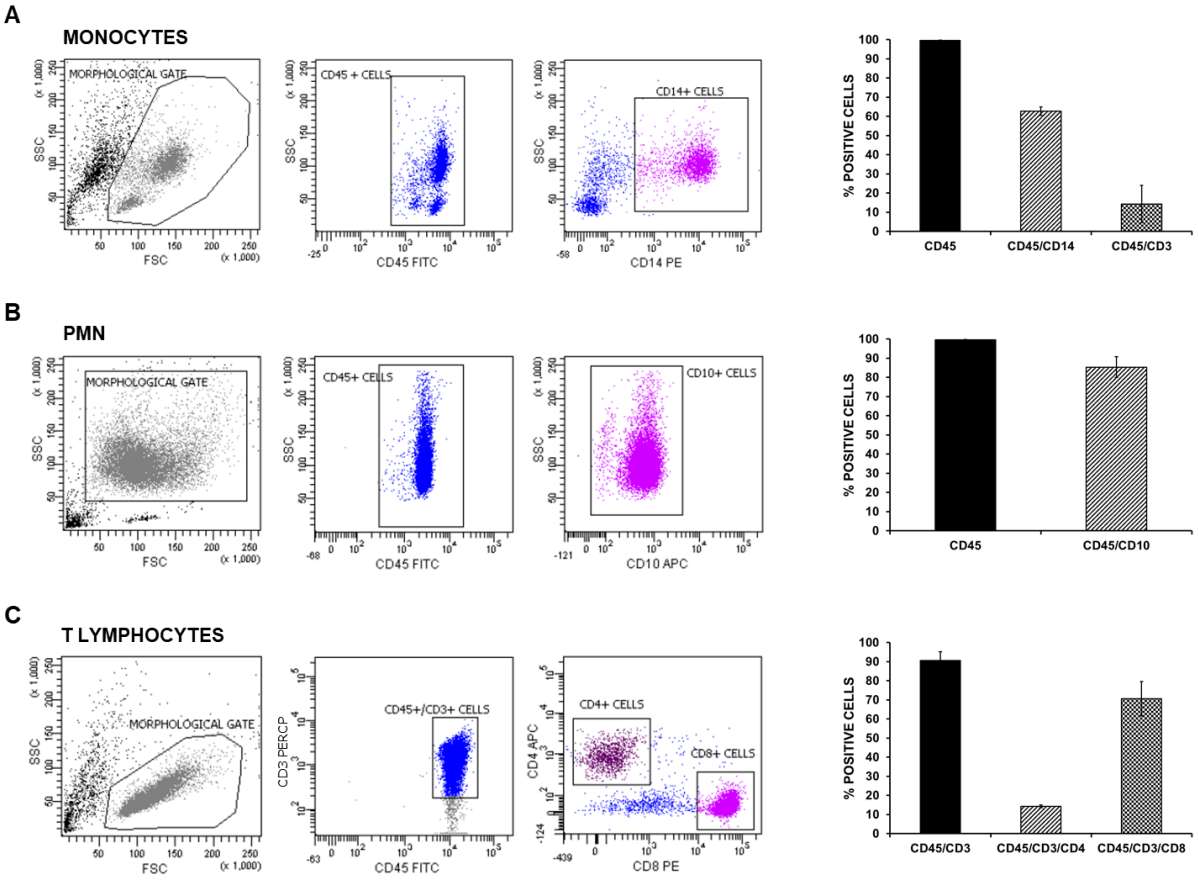

Figure 14. Immunophenotype of monocytes, polymorphonuclear cells, and T lymphocytes from three donors

For each isolated cell type, a representative FACS analysis of one donor is depicted on the left and mean percentage values of the three donors are shown in the histogram on the right. (**A**) Monocytes isolated from three donors were quantified by FACS based on the identification of CD45+/CD14+ cells. Contaminant T lymphocytes were detected by the co-expression of CD45 and CD3 antigens, quantified, and excluded from the following analysis. Error bars = SEM. (**B**) Polymorphonuclear cells (PMN) from three donors were quantified by FACS based on the identification of CD45+/CD10+ cells. (**C**) T lymphocytes isolated from three donors were detected by the co-expression of CD45 and CD3 antigens and quantified by FACS. The expression of both CD4+ helper and CD8+ cytotoxic T cells was quantified within the CD45+/CD3+ subpopulation.

To predict the potential sensitivity of white blood cells to the cytotoxic effects of sTRAIL, the presence of both functional (DR4 and DR5) and decoy (DcR1 and DcR2) TRAIL receptors was investigated on the cell membrane of all three leukocyte subpopulations (**Fig. 15A**, **15B**, and **15C**, left panels).

Monocytes showed high positivity for DR5 (77±4%), whereas the presence of DR4 and decoy receptors was negligible (DR4: 1±0.5%; DcR1: 4±2%; DcR2: 1±0.1%; **Fig. 15A**, right). After

isolation, PMN revealed weak expression of both functional and DcR1 receptors (less than 25%); in contrast, the presence of decoy receptor DcR2 was detected in 62±14% of neutrophils (**Fig. 15B**, right). T cells were negative or slightly positive for all TRAIL receptors (DR4: 7±4%; DR5: 13±5%; DcR1: 3±2%; DcR2: 1±1%) after in vitro culture (**Fig. 15C**, right).

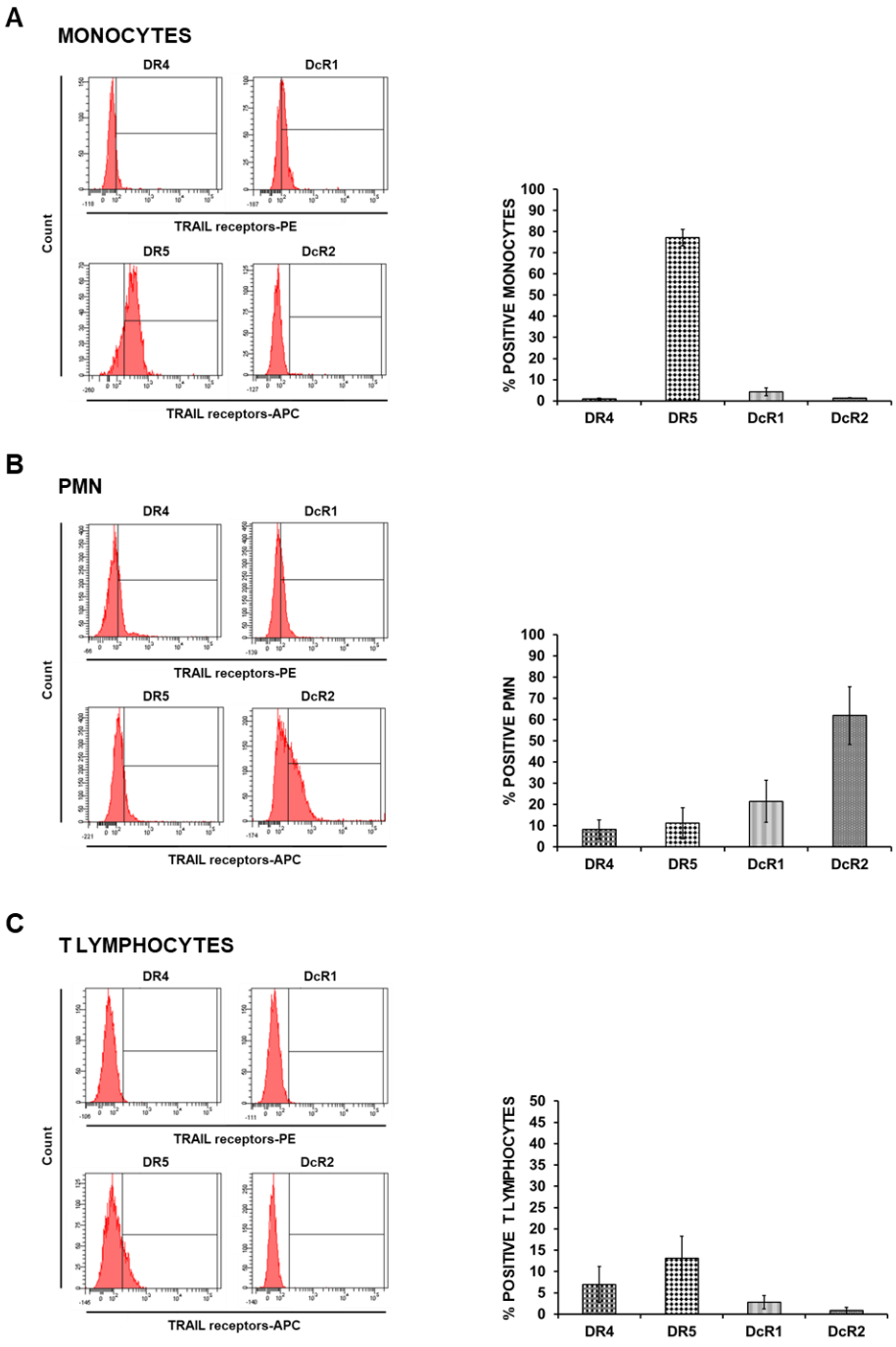

Figure 15. Expression of TRAIL receptors on monocytes, PMN, and T lymphocytes from three donors

Expression of both functional (DR4 and DR5) and decoy (DcR1 and DcR2) TRAIL receptors evaluated by FACS on (**A**) monocytes, (**B**) PMN, and (**C**) T lymphocytes isolated from three donors. Representative FACS analysis of one donor is depicted on the left; the histograms on the right present the mean values of the three donors.

5.2.2 Conditioned medium containing sTRAIL protein secreted by gene-modified AD-MSC does not alter the viability of white blood cells

To evaluate if sTRAIL variant secreted by gene-modified AD-MSC and characterized by an improved trimerization capacity could be associated with an increased cytotoxic profile on white blood cells, the viability of monocytes, PMN, and T cells was assessed in a dose-response assay testing AD-MSC sTRAIL - CM containing increasing doses of sTRAIL (from 0 to 5000 pg/ml; **Fig. 16**). The analysis revealed that the number of living monocytes and PMN was not reduced by sTRAIL treatment; rather, after 24 hours, cell viability progressively increased with increasing concentrations of sTRAIL in the CM compared to the control (up to 2-fold increase; **Fig. 16A** and **16B**, $p \leq 0.02$ and $p \leq 0.05$ for monocytes and PMN, respectively). Similarly, supernatant collected from AD-MSC EMPTY could significantly boost monocyte and PMN proliferation compared to the control (**Fig. 16A** and **16B**). These results suggest that, regardless of the presence of sTRAIL, CM collected from AD-MSC favors the growth of monocytes and PMN, and this effect may be due to the release of soluble factors and cytokines by MSC into the culture medium (**Fig. 16A** and **16B**). Additionally, after 24 hours and for all tested doses of sTRAIL, T cell viability did not show significant variations compared to the negative controls (T lymphocytes untreated or treated with CM from AD-MSC EMPTY; **Fig. 16C**). Collectively, these results indicate that irrespective of the expression of functional TRAIL receptors on the different cell types, resting leukocytes are refractory to the proapoptotic effect displayed by sTRAIL secreted by AD-MSC.

Moreover, the impact of sTRAIL on the health condition of T cells was further investigated by the AlamarBlue assay. AlamarBlue is a nontoxic viability compound that exploits the natural reducing power of healthy and metabolically active cells to convert a non-fluorescent substrate to a highly fluorescent molecule that can be evaluated quantitatively based on absorbance or fluorescence signals, returning a snapshot of cellular metabolic activity. Hence, a reduction in the AlamarBlue signal may signify an impairment of cellular metabolism or

mitochondrial dysfunction provoked by cytotoxic stimuli [175]. At 24 hours, starting from the lowest sTRAIL dose (50 pg/ml), a slight decrease in T cell metabolism was recorded compared to untreated cells. This trend was completely reversed at later time points of 48 and 72 hours, at which no statistically significant variations in AlamarBlue reduction were observed compared to the control. In addition, at the highest sTRAIL dose (5000 pg/ml) and for all tested time points, CM from both AD-MSC sTRAIL and EMPTY significantly increased T cell metabolic activity compared to that of untreated cells (**Fig. 16D**). Collectively, these data indicate that both the viability and health condition of T cells, which are characterized by the negligible expression of TRAIL receptors, are not negatively affected by sTRAIL. Rather, trophic factors released by AD-MSC in the CM may favor lymphocyte growth in culture.

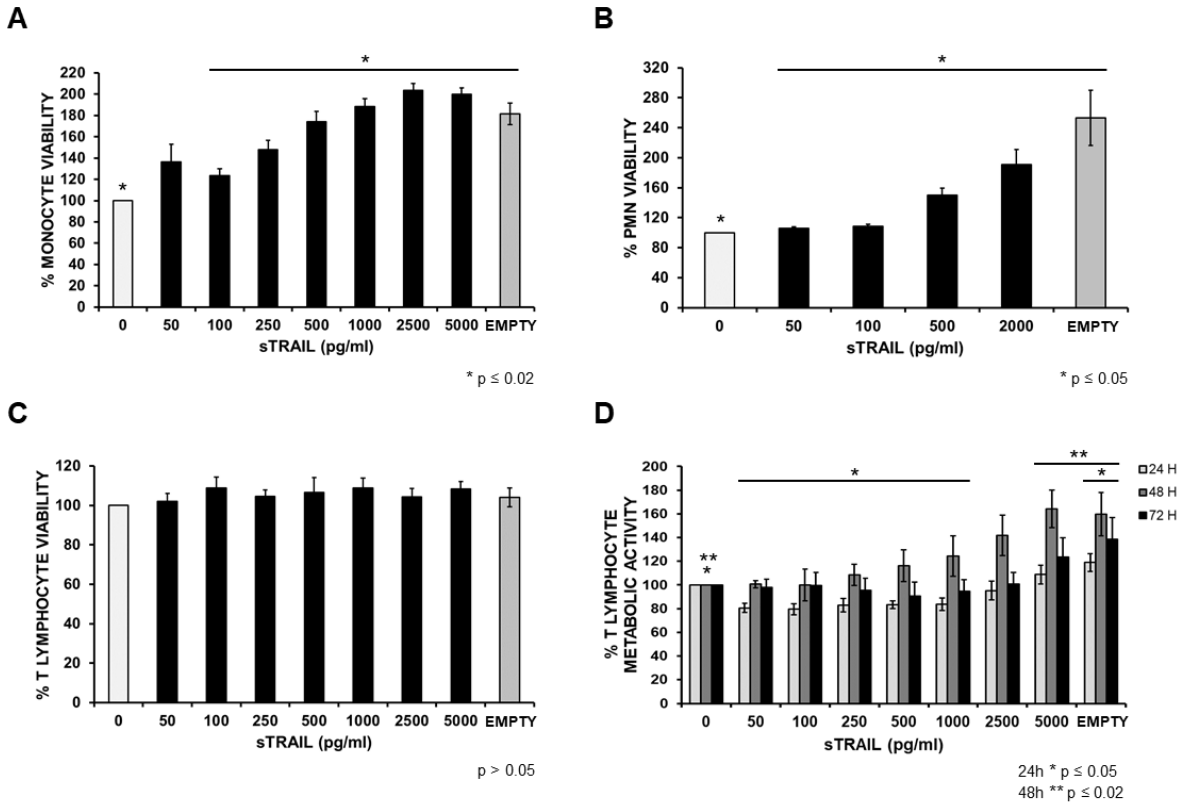

Figure 16. Quantification of the cytotoxic effect of different doses of sTRAIL on monocytes, PMN, and T lymphocytes from three donors

(**A**) Monocyte, (**B**) PMN, and (**C**) T lymphocyte viability evaluated by the CellTiter-Glo Luminescent Cell Viability assay after 24 hours of treatment with conditioned medium (CM) from AD-MSC sTRAIL containing increasing sTRAIL doses (0 to 5000 pg/ml for monocytes and T cells; 0 to 2000 pg/ml for PMN). CM from AD-MSC EMPTY (EMPTY) was used as a control. Mean values of the three donors are reported. p-value by t-test.

(**D**) T lymphocyte metabolic activity percentage as a function of sTRAIL doses (0 to 5000 pg/ml) after 24, 48, and 72 hours, evaluated by the AlamarBlue assay. CM from AD-MSC EMPTY (EMPTY) was used as a control. p-value by t-test. Mean values of the three donors are shown.

5.2.3 Direct cell-to-cell contact with AD-MSC expressing sTRAIL does not negatively impact monocyte and T cell viability in vitro

To investigate if direct cell-to-cell contact with AD-MSC sTRAIL compromises the number of living white blood cells, monocytes as well as T cells were further cultured in the presence of AD-MSC sTRAIL at different E:T ratios (1:30, 1:15, 1:10, 1:1, and 10:1) for 24 hours (**Fig. 17**). Leukocytes alone (CTL) or co-cultured with AD-MSC EMPTY at the highest E:T ratio were used as the control. The reason for testing such a wide range of E:T ratios (from 1:30 to 10:1) is that in this study we explored in vitro any toxic effect on immune cells caused by exposure to an anticancer medicinal product based on AD-MSC expressing sTRAIL.

No statistically significant variations in monocyte viability were recorded at any of the tested E:T ratios compared to CTL, confirming that direct cell-to-cell contact with AD-MSC sTRAIL did not provoke cytotoxicity in primary monocytes (**Fig. 17A**) despite the high expression of DR5 on the cell membrane.

From E:T ratios of 1:30 to 1:10, T cell viability was not affected by the presence of AD-MSC sTRAIL, whereas a progressive slight increase in T cell mortality (less than 20% over CTL) was registered at higher doses (E:T ratios of 1:1 and 10:1; **Fig. 17B**). The modest but appreciable reduction of T cell viability can be specifically ascribed to the apoptotic effect mediated by sTRAIL released in the supernatant by AD-MSC sTRAIL since it was not observed in co-culture with AD-MSC EMPTY. The amount of sTRAIL detected by ELISA in culture media collected from samples having E:T ratios of 1:1: and 10:1 was 75±2 pg/ml and 251±2 pg/ml, respectively. Both these concentrations are sufficient to induce relevant cytotoxic effects in TRAIL-sensitive tumor cells (data not shown). In particular, we have reported that a 250 pg/ml dose of sTRAIL can provoke apoptosis in more than 50% of Ewing's sarcoma and pancreatic tumor cell lines [3,158]. Lastly, to evaluate whether AD-MSC sTRAIL equally targeted both CD4+ and CD8+ T lymphocytes, T cell immunophenotype after co-culture with AD-MSC sTRAIL at E:T ratios of 1:1 and 10:1 was assessed, and no variations were detected compared to T cells alone (**Fig. 17C**).

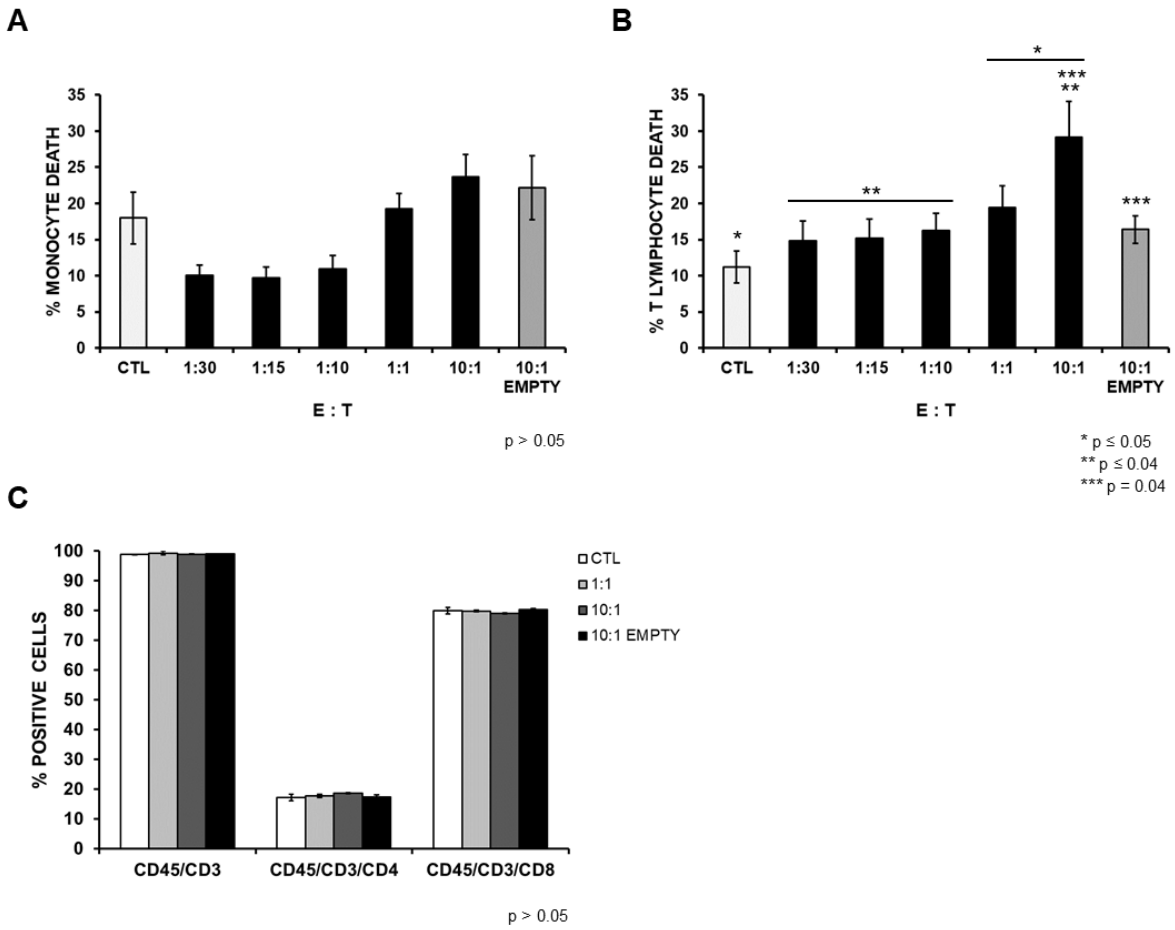

Figure 17. Quantification of the cytotoxic impact of direct cell-to-cell contact with AD-MSC sTRAIL on monocytes and T lymphocytes from three donors

AD-MSC sTRAIL and EMPTY co-culture with (**A**) monocytes or (**B**) T lymphocytes at different effector:target ratios (1:30, 1:15, 1:10, 1:1, and 10:1; E:T, E = AD-MSC sTRAIL or EMPTY as a control, T = target cells, i.e., monocytes or T cells). After 24 hours, leukocyte death was quantified by supravital propidium iodide (PI) staining and FACS analysis. p-value by t-test. Mean values of the three donors are reported. CTL = monocytes or T cells alone. (**C**) The expression of both CD4+ and CD8+ T cells after co-culture with AD-MSC sTRAIL and EMPTY at E:T ratios of 1:1 and 10:1 was quantified within the CD45+/CD3+ subpopulation by FACS. p-value by t-test. CTL = T cells alone.

5.2.4 Impact of sTRAIL-producing AD-MSC on T cell cytokine release

To investigate cellular crosstalk between T lymphocytes and AD-MSC sTRAIL, the secretion of several anti-inflammatory and tumor-related cytokines was investigated in supernatants collected from T cell–MSC co-cultures at different E:T ratios (1:30, 1:15, 1:10, 1:1, and 10:1) for 24, 48, and 72 hours. Five cytokines secreted by either T lymphocytes (IL-10, TNFα, and IFNγ) or AD-MSC (VEGF-A and IL-6) were analyzed. T lymphocytes alone or AD-MSC

alone were used as controls. The evaluation was done by multiplex ELISA. Since different T cell–MSC ratios were tested in co-culture, thus creating differences in the absolute number of T cells in each culture condition, the amount of IL-10, TNFα, and IFNγ was divided by the real number of T cells in the plate to make all conditions comparable with each other; a similar approach was used to normalize the amount of VEFG-A and IL-6 produced by MSC. Data were reported as fg/ml per T cell for cytokines secreted by T lymphocytes and fg/ml per AD-MSC for cytokines secreted by AD-MSC. The collected results revealed the highest statistically significant increase in IL-10 (**Fig. 18A**), TNFα (**Fig. 18B**), and IFNγ (**Fig. 18C**) secretion by T cells when co-cultured with AD-MSC sTRAIL (or EMPTY) at a 10:1 E:T ratio. T lymphocytes, in turn, induced a peak of VEGF-A (**Fig. 18D**) and IL-6 (**Fig. 18E**) secretion by AD-MSC after 72 hours of co-culture at a 1:30 E:T ratio, an effect probably mediated by TNFα and IFNγ released by the T cells themselves. No difference in VEGF-A and IL-6 secretion was detected between AD-MSC sTRAIL (or EMPTY) co-cultured with T lymphocytes at a 10:1 E:T ratio and AD-MSC sTRAIL (or EMPTY) alone (data not shown). Collectively, these data highlight the cytokine crosstalk between T lymphocytes and AD-MSC sTRAIL in co-culture: AD-MSC sTRAIL stimulate IL-10, TNFα, and IFNγ secretion by T cells, and T lymphocytes, in turn, induce VEGF-A and IL-6 secretion by AD-MSC, probably mediated by TNFα and IFNγ.

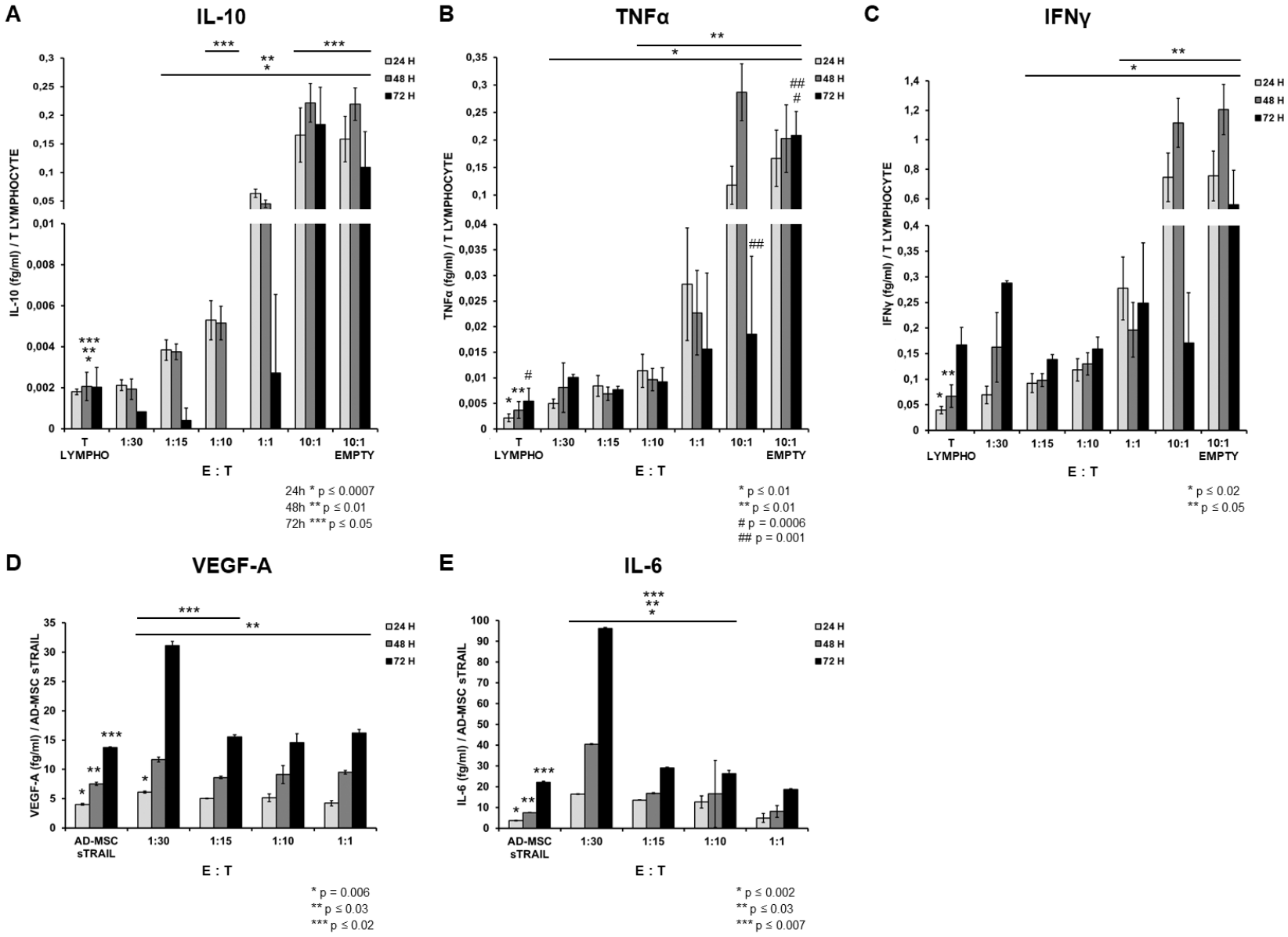
A
IL-10
IL-10 (fg/ml) / T LYMPHOCYTE
24 H
48 H
72 H
T LYMPHO
1:30
1:15
1:10
1:1
10:1
10:1 EMPTY
E : T
24h * p ≤ 0.0007
48h ** p ≤ 0.01
72h *** p ≤ 0.05
B
TNFα
TNFα (fg/ml) / T LYMPHOCYTE
* p ≤ 0.01
** p ≤ 0.01
# p = 0.0006
p = 0.001
C
IFNγ
IFNγ (fg/ml) / T LYMPHOCYTE
* p ≤ 0.02
** p ≤ 0.05
D
VEGF-A
VEGF-A (fg/ml) / AD-MSC sTRAIL
AD-MSC sTRAIL
* p = 0.006
** p ≤ 0.03
*** p ≤ 0.02
E
IL-6
IL-6 (fg/ml) / AD-MSC sTRAIL
* p ≤ 0.002
** p ≤ 0.03
*** p ≤ 0.007

Figure 18. Cytokine profile in co-cultures of T lymphocytes and AD-MSC sTRAIL

Evaluation of (**A**) IL-10, (**B**) TNFα, and (**C**) IFNγ protein levels (fg/ml) per T lymphocyte in co-culture supernatants of T lymphocytes with AD-MSC sTRAIL at different E:T ratios (1:30, 1:15, 1:10, 1:1, and 10:1; E = AD-MSC sTRAIL or EMPTY as a control, T = T cells) after 24, 48, and 72 hours by multiplex ELISA. Results from three donors are presented together. p-value by t-test. (**D**) VEGF-A and (**E**) IL-6 protein levels (fg/ml) per AD-MSC sTRAIL in co-culture supernatants of T lymphocytes with AD-MSC sTRAIL at different E:T ratios (1:30, 1:15, 1:10, and 1:1; E = AD-MSC sTRAIL, T = T cells) after 24, 48, and 72 hours by multiplex ELISA. Results from three donors are presented together. p-value by t-test.

6. DISCUSSION

6.1 Combined treatment of GEM & AD-MSC sTRAIL targeting PDAC

For decades, GEM has represented the standard treatment for advanced PDAC, but drug resistance development severely limits patient outcomes [176]. PDAC chemoresistance has been ascribed to both intrinsic mechanisms of tumor cells and desmoplastic stroma [177,178]. Indeed, stromal abundance represents a physical barrier to tumors, hampering neoplastic growth and dissemination and restricting tumor vasculature, with subsequent compromising of chemotherapy delivery into neoplastic tissue [2,179]. An intense and dynamic biochemical and molecular crosstalk has been described in PDAC between neoplastic cells and TAF. This intercellular network contributes to tumor development and progression, desmoplastic stroma production, and multi-drug resistance [45,67,180].

Besides conventional chemotherapy, the proapoptotic molecule TRAIL emerged as a highly specific, barely toxic anticancer molecule. However, some tumors show low sensitivity to solo treatment with rhTRAIL both in vitro and in vivo, and rhTRAIL antitumor approaches display some limitations in a clinical setting [181,182]. Recently, many combinatorial approaches to overcome TRAIL resistance have been evaluated, but few pre-clinical and clinical studies focused on GEM plus TRAIL therapy for pancreatic cancer. Two in vitro studies demonstrated that the combined use of GEM and rhTRAIL enhances inhibition of pancreatic cancer cell viability [166,183]. Hylander et al. (2005) showed in vivo that the combination GEM & rhTRAIL overcomes rhTRAIL tumor resistance in patient-derived pancreatic tumors [163]. The same group later showed that treatment with rhTRAIL decompresses in vivo the microenvironment by killing tumor cells in MIA PaCa-2 tumors, and that priming with rhTRAIL enables an increase in GEM uptake and improved efficacy versus treatment with GEM alone in a colon adenocarcinoma model [184]. In a clinical setting, treatment with GEM plus agonistic DR4 and DR5 antibodies in patients affected by solid tumors does not determine major toxicities, and partial responses to the combinatory approach were observed [185,186].

Considering previous work, the current study proposed a GEM & TRAIL approach using a more stable form of TRAIL (sTRAIL vs rhTRAIL) delivered by AD-MSC [3], targeting both tumor and stromal cells in PDAC. AD-MSC sTRAIL represent a promising anticancer

therapy, taking advantage of MSC attraction to inflamed tissues (including tumor microenvironments) and the constant production of sTRAIL, which enables stable bioavailability in tumor sites [3,97,187]. Importantly, treatment with GEM did not impact sTRAIL release by MSC, and almost 50% of AD-MSC sTRAIL remained alive after 72 hours in the presence of high GEM concentrations (500 μM).

Considering these aims, we selected a panel of PDAC cell lines that represented the possible clinical heterogeneity in PDAC therapeutic responses. In all tumor cell lines considered, independent of sensitivity levels to either GEM or sTRAIL, we observed a synergistic cytotoxic effect of the combinatory approach both in 2D and in 3D that overcame GEM and TRAIL resistance after single-drug treatment. Notably, in 2D we obtained a higher apoptotic combinatory effect on WT BxPC-3 and MIA PaCa-2 versus that demonstrated in Elia et al. (2017) [183], with the same GEM concentrations and 1000-times lower TRAIL concentrations, confirming the greater stability and toxicity of sTRAIL versus rhTRAIL [3]. We furthermore evaluated GEM & sTRAIL by employing for the first time AD-MSC sTRAIL in a VITVO 3D co-culture with PDAC tumor cells.

After encouraging in vitro results, we tested the combinatorial approach on a PDAC orthotopic model, which better mimics the situation of human PDAC patients compared to commonly employed subcutaneous models. Ultrasound imaging provided crucial information concerning tumor composition, enabling eco-guided injections and real-time distribution of therapeutic agents. Up to seven days after injection, AD-MSC sTRAIL remained detectable in treated tumors as viable, metabolically active cells. The combinatory approach led to shredding of tumor architecture, with significant reduction in CK-7 expression and increase in tumor necrosis without a significant impact on tumor desmoplastic reaction. This is probably due to the large amount of murine stromal cells infiltrating damaged neoplastic tissue in response to combinatory treatment. We thus tested the impact of the combinatory approach on isolated primary murine stromal cells, showing for the first time their resistance to GEM & AD-MSC sTRAIL therapy. Given these data, we hypothesized that presence of murine stroma, as part of tumor mass, partially hindered tumor volume analysis.

Many recent efforts have focused on developing PDAC anti-stroma treatments. However, given the limited benefits of these therapeutic strategies in clinical trials, it has been suggested that simple depletion of stromal compartments could result in PDAC progression induction

rather than inhibition [1,2]. Therefore, development of novel therapeutic combinatorial approaches able to target both malignant and stromal cells is needed.

The current study thus investigated GEM & sTRAIL efficacy against human primary PDAC TAF. After isolation from four human PDAC samples, we confirmed the typical TAF mesenchymal immunophenotype [42]. Although TAF molecular definition remains controversial, TAF are understood to comprise cellular components within PDAC microenvironments that are distinct from leukocytes and endothelial, epithelial, and tumor cells, as confirmed by the lack of CD45, HLA-DR, and EPCAM antigens on TAF cell membranes [44].

We moreover showed the high expression of functional DR5 by TAF. This result was unsurprising considering data reported by Dall'Ora et al. (2021) indicating that histologically, human PDAC stromal tissue stains positive for DR5 and negative for DR4 [40]. Additionally, human fibroblasts in vitro reportedly express moderate levels of DR5 but not DR4 [188]. Despite high DR5 expression on their cell membranes, all four TAF cell lines were resistant to sTRAIL alone, even at the highest tested concentration (2500 pg/ml). Szegezdi et al. (2010) showed that human fibroblasts are not sensitive to rhTRAIL apoptotic induction [188]. It was additionally reported that full-length transmembrane TRAIL does not induce pancreatic stellate cell death within the PDAC microenvironment, unlike with nearby tumor cells [189]. However, no other studies have reported data on the cytotoxic effect of multimeric sTRAIL complexes on pancreatic TAF. Subsequently, we registered a synergistic proapoptotic impact of combined treatment on primary TAF versus either sTRAIL or chemotherapeutic agent alone. Aligning with our results, emerging evidence suggests that TAF and normal fibroblasts do not display much sensitivity to GEM alone and that TAF contribute to GEM resistance of pancreatic tumors [190,191].

Future perspectives of the current study include the validation of the in vivo results using innovative 3D models able to faithfully recapitulate in vivo cancer biology, including TAF and ECM components of PDAC microenvironment. The tumor/stroma compartment, deeply explored and characterized by Dall'Ora et al. (2021) in human PDAC histological samples, could be recreated into VITVO 3D bioreactor co-culturing human primary TAF and PDAC tumor cells at the same percentage measured in tumour microenvironment of PDAC samples (45% of primary TAF and 55% of malignant cells) [40]. The same ratio between stromal and tumor components in co-culture was applied by other groups in previous studies [189,192].

As reported by De la Pena et al. (2021), bioengineered 3D models of human pancreatic cancer, based on a co-culture between primary tumor, stromal and immune cells encapsulated into a cell culture matrix composed of self-assembling peptides and ECM macromolecules, might be also used to recapitulate the PDAC tumor microenvironment, thus reflecting in vivo treatment responses [193]. Moreover, for both in vitro and in vivo experiments of our work we have employed PDAC tumor cell lines showing different sensitivity levels to either GEM or sTRAIL to summarize the interpatient heterogeneity. However, with the aim of enhancing the biological relevance of our study and reproducing patient clinical response, we also planned to isolate and expand in vitro PDAC tumor primary cells to be used in vivo to further improve the PDAC orthotopic murine model.

To conclude, the present work demonstrates the therapeutic potential of combining an sTRAIL gene therapy approach with the gold standard of chemotherapy for PDAC treatment. The combinatory approach is able to strongly potentiate in vitro single-drug treatment in PDAC cell lines, and the synergistic effect is further demonstrated in vivo using a PDAC orthotopic model. Although further investigation is needed, these encouraging findings support the synergistic effect of GEM & sTRAIL on PDAC TAF, suggesting that future studies should consider this proposed therapeutic regimen for integrated therapy toward both tumor and stromal components in PDAC.

6.2 Impact of AD-MSC sTRAIL on white blood cells

The use of TRAIL as an anticancer agent has aroused great interest in oncology research due to its tumor-selective activity, which triggers the apoptotic signaling cascade preferentially in cancer cells with little-to-no effect in normal cells (e.g., lung fibroblasts, skeletal muscle cells, epidermal keratinocytes, and melanocytes) [143,194]. However, the antitumor cell therapy approach developed by our group is based on gene-modified AD-MSC expressing a novel secreted variant of TRAIL characterized by the presence of an isoleucine zipper domain that confers the capacity to form more stable multimeric complexes of TRAIL, thus resulting in higher cytotoxic activity on tumor cells compared to the recombinant human molecule [3]. In view of this, the assessment of the immunological safety of AD-MSC sTRAIL is crucial considering both the immunomodulatory activity displayed by MSC on immune cells and the role played by TRAIL in the regulation of innate and adaptive immune responses [122,168].

Indeed, TRAIL can be expressed by immune cells based on their activation status, with the upregulation of TRAIL on both innate and adaptive immune cells, such as monocytes, neutrophils, T and B lymphocytes, and NK cells, when stimulated with type I IFN. In addition to TRAIL expression, activated immune cells can also express decoy TRAIL receptors, thereby creating resistance to TRAIL-mediated apoptotic signaling [125]. TRAIL has been referred to as a guardian against pathogen infections, autoimmunity, and cancer onset and progression, playing a crucial role in immunosurveillance mechanisms [134]. More, it has been reported that TRAIL expressed by neutrophils, CD8+ T lymphocytes, and NK cells promotes the elimination of pathogen-infected cells expressing functional TRAIL receptors, thus containing infections [125]. Against autoimmunity, TRAIL inhibits the activation of autoreactive T cells but promotes Treg proliferation in diabetes, rheumatoid arthritis, and autoimmune encephalomyelitis [139]. Moreover, monocytes stimulated with IFNγ, CD4+ T cells, and NK cells expressing TRAIL can recognize and then neutralize transformed cells, inhibiting tumor growth and preventing tumor metastases within the immunosurveillance process [195].

For the first time, we have also evaluated the impact of a novel form of sTRAIL released by AD-MSC on the viability, metabolic activity, and cytokine release of white blood cells. At first, we evaluated by flow cytometry the expression of both functional and decoy TRAIL receptors responsible for inducing or inhibiting TRAIL signaling, respectively, on freshly isolated purified blood leukocytes from healthy donors. As reported by Liguori et al. (2016), we observed heterogeneous expression of TRAIL receptors on resting white blood cells: DR5 was mainly expressed on monocytes, whereas the decoy receptors (DcR1 and DcR2) were essentially expressed on neutrophils. On the contrary, resting T cells revealed weak expression of all TRAIL receptors [196].

Since our MSC-based cell product releases multimeric sTRAIL complexes into the cell culture medium [3], we first investigated the biological impact of supernatant collected from AD-MSC sTRAIL on primary resting leukocytes. For all considered immune cell subtypes, we did not observe any toxicity even at the highest tested sTRAIL concentration (5000 pg/ml); on the contrary, we registered a relevant and significant increase of cell viability for monocytes and PMN after exposure to CM collected from engineered AD-MSC. This effect was visible in cells treated with supernatant collected from both AD-MSC sTRAIL and AD-MSC EMPTY, suggesting that soluble trophic factors and cytokines secreted by MSC within

the supernatant, such as GM-CSF, IL-6, and IL-8, could support monocyte and PMN growth and survival [197,198]. In addition, no significant variations were revealed in the viability of T cells treated with CM from AD-MSC sTRAIL compared to the control. In the literature, it is well established that resting peripheral T cells are resistant to TRAIL-mediated apoptosis, in contrast to T lymphocytes activated by antigenic stimulation and autoreactive T cells, as a mechanism to prevent potentially dangerous autoimmune damage [138,199]. This result is not unexpected considering both the low expression of DR4 and DR5 revealed and the data reported by Clancy et al. (2005) indicating that in T lymphocytes, decoy receptors mediate resistance to TRAIL-induced apoptosis by creating mixed functional-decoy receptor complexes that do not efficiently trigger TRAIL signaling [200]. The health status of T cells was also assessed by evaluating their metabolic activity after exposure to increasing doses of sTRAIL released by AD-MSC in CM at different time points (24, 48, and 72 hours). A significant but slight reduction in T cell metabolism was observed at 24 hours with 50–2500 pg/ml sTRAIL, but this trend was completely reversed with both CM from AD-MSC sTRAIL with the highest sTRAIL concentration (containing 5000 pg/ml of sTRAIL) and from AD-MSC EMPTY and at later time points (48 and 72 hours). This suggests that, similar to what was observed for T cell proliferation, lymphocyte metabolism may be more influenced by trophic factors secreted by MSC than by the toxic impact of sTRAIL. More, this tells that non-activated T cells would be resistant to sTRAIL released by engineered AD-MSC thanks to the high expression of TRAIL-mediated apoptosis inhibitors, such as cFLIP, as already reported for the wild-type form of TRAIL [201–203].

To further investigate if the cellular crosstalk between MSC and white blood cells could modify TRAIL sensitivity in leucocytes, we established co-culture experiments. Monocyte viability was confirmed as not being influenced by cell-to-cell interactions with engineered AD-MSC secreting sTRAIL despite the high expression of DR5 registered by FACS analysis. On T lymphocytes, we instead observed a slight increase in cell death at higher E:T doses (E:T ratios of 1:1 and 10:1) compared to CTL and co-culture with AD-MSC EMPTY. The modest (less than 20%) but significant reduction in T cell viability registered at the 10:1 E:T ratio is likely due to the 251±2 pg/ml of sTRAIL secreted by AD-MSC since it was not observed in co-culture with AD-MSC EMPTY. In addition, TRAIL-mediated apoptosis did not selectively affect T cell subtypes since no significant variations in CD4+ versus CD8+ cell ratios were observed in co-culture with gene-modified AD-MSC and lymphocytes alone. The

biological reason for the same amount of sTRAIL not having any cytotoxic impact on T cells when used as CM from AD-MSC sTRAIL may be the release of specific cytokines able to sensitize T cells to TRAIL apoptosis during cell-to-cell interaction. In this sense, it has been reported that IFNγ and TNFα enhance TRAIL sensitivity on target cells [204–206].

Therefore, cytokine crosstalk accounting for MSC immunomodulatory properties was investigated in co-cultures of T cells and AD-MSC sTRAIL. The levels of the IL-10, TNFα, and IFNγ cytokines released by T cells in co-culture with AD-MSC (both sTRAIL and EMPTY) were massively increased at the 10:1 E:T ratio, suggesting that the secretion of these molecules could be indirectly stimulated by MSC as already reported in the literature [207].Therefore, the relevant increase in TNFα and IFNγ amounts registered in the culture medium at the highest E:T ratios may be responsible for the increased sensitivity of lymphocytes to the apoptotic impact of TRAIL, justifying the enhanced T cell death after direct exposure to AD-MSC sTRAIL. Similarly, cytokines secreted by MSC, such as VEGF-A and IL-6, were also evaluated. VEGF-A is a key promoter of blood vessel growth and vascular permeability as well as an inhibitor of lymphocyte activation, thus stimulating tumor neoangiogenesis, progression, and metastasis [208]. We observed the most relevant increase in both VEGF-A and IL-6 secretion per AD-MSC at the 1:30 E:T ratio after 72 hours of co-culture with T lymphocytes, which is probably related to the release of TNFα and IFNγ by T cells as shown by Nagineni et al. (2016) [88,209]. Moreover, it is known that IL-6 (alone or in combination with TNFα) can induce VEGF-A secretion by AD-MSC through the ERK, JNK, and PI3K pathways [210]. Therefore, we highlighted the cytokine crosstalk between T cells and AD-MSC sTRAIL in co-culture. In particular, AD-MSC induced IL-10, TNFα, and IFNγ secretion by T lymphocytes, and TNFα and IFNγ, in turn, promoted VEGF-A and IL-6 release by AD-MSC.

To conclude, these data demonstrate that white blood cells are refractory to the proapoptotic effect displayed by sTRAIL and that direct cell-to-cell contact with AD-MSC sTRAIL has a negligible impact on T cell and monocyte viability, confirming the immunological safety and thus the clinical feasibility of an anticancer gene therapy strategy based on AD-MSC expressing sTRAIL.

7. CONCLUSIONS

Collectively, these data demonstrate the therapeutic efficacy of combining a gene therapy strategy with chemotherapy to target both the tumor and stromal compartment in PDAC microenvironment. Indeed, synergy between GEM and AD-MSC sTRAIL against malignant compartment was confirmed both in vitro on TRAIL-resistant and sensitive PDAC cell lines and in vivo using an orthotopic PDAC murine model. Similarly, GEM was able to restore sTRAIL sensitivity of human primary PDAC TAF, showing a significant synergistic effect.

Moreover, in addition to the therapeutic potential, this thesis also proves the immunological safety of this strategy against white blood cells, supporting the clinical feasibility of an antitumor gene therapy based on AD-MSC armed with sTRAIL.

8. REFERENCES

1. Lafaro KJ, Melstrom LG. The Paradoxical Web of Pancreatic Cancer Tumor Microenvironment. Am J Pathol. 2019 Jan;189(1):44–57.

2. Sun Q, Zhang B, Hu Q, Qin Y, Xu W, Liu W, Yu X, Xu J. The impact of cancer-associated fibroblasts on major hallmarks of pancreatic cancer. Theranostics. 2018;8(18):5072–87.

3. Spano C, Grisendi G, Golinelli G, Rossignoli F, Prapa M, Bestagno M, Candini O, Petrachi T, Recchia A, Miselli F, Rovesti G, Orsi G, Maiorana A, Manni P, Veronesi E, Piccinno MS, Murgia A, Pinelli M, Horwitz EM, Cascinu S, Conte P, Dominici M. Soluble TRAIL Armed Human MSC As Gene Therapy For Pancreatic Cancer. Sci Rep. 2019 Dec;9(1):1788.

4. Rossignoli F, Spano C, Grisendi G, Foppiani EM, Golinelli G, Mastrolia I, Bestagno M, Candini O, Petrachi T, Recchia A, Miselli F, Rovesti G, Orsi G, Veronesi E, Medici G, Petocchi B, Pinelli M, Horwitz EM, Conte P, Dominici M. MSC-Delivered Soluble TRAIL and Paclitaxel as Novel Combinatory Treatment for Pancreatic Adenocarcinoma. Theranostics. 2019;9(2):436–48.

5. Hidalgo M, Cascinu S, Kleeff J, Labianca R, Löhr J-M, Neoptolemos J, Real FX, Van Laethem J-L, Heinemann V. Addressing the challenges of pancreatic cancer: Future directions for improving outcomes. Pancreatology. 2015 Jan;15(1):8–18.

6. Vincent A, Herman J, Schulick R, Hruban RH, Goggins M. Pancreatic cancer. The Lancet. 2011 Aug;378(9791):607–20.

7. Bray F, Ferlay J, Soerjomataram I, Siegel RL, Torre LA, Jemal A. Global cancer statistics 2018: GLOBOCAN estimates of incidence and mortality worldwide for 36 cancers in 185 countries. CA Cancer J Clin. 2018 Nov;68(6):394–424.

8. Davoodi SH, Malek-Shahabi T, Malekshahi-Moghadam A, Shahbazi R, Esmaeili S. Obesity as an Important Risk Factor for Certain Types of Cancer. Iran J Cancer Prev. 2013;6(4):9.

9. Rawla P, Sunkara T, Gaduputi V. Epidemiology of Pancreatic Cancer: Global Trends, Etiology and Risk Factors. World J Oncol. 2019;10(1):10–27.

10. Siegel RL, Miller KD, Jemal A. Cancer statistics, 2018. CA Cancer J Clin. 2018 Jan;68(1):7–30.

11. Yonezawa S, Higashi M, Yamada N, Goto M. Precursor Lesions of Pancreatic Cancer. Gut Liver. 2008 Dec;2(3):137–54.

12. Hruban RH, Albores J, Garrett ES, Kern SE, Longnecker DS, Offerhaus GJA. Pancreatic Intraepithelial Neoplasia. Am J Surg Pathol. 2001;25(5):8.

13. Nakamura A, Horinouchi M, Goto M, Nagata K, Sakoda K, Takao S, Imai K, Kim YS, Sato E, Yonezawa S. New classification of pancreatic intraductal papillary-mucinous tumour by mucin expression: its relationship with potential for malignancy. J Pathol. 2002 Jun;197(2):201–10.

14. Jones S, Zhang X, Parsons DW, Lin JC-H, Leary RJ, Angenendt P, Mankoo P, Carter H, Kamiyama H, Jimeno A, Hong S-M, Fu B, Lin M-T, Calhoun ES, Kamiyama M, Walter K, Nikolskaya T, Nikolsky Y, Hartigan J, Smith DR, Hidalgo M, Leach SD, Klein AP, Jaffee EM, Goggins M, Maitra A, Iacobuzio-Donahue C, Eshleman JR, Kern SE, Hruban RH, Karchin R, Papadopoulos N, Parmigiani G, Vogelstein B, Velculescu VE, Kinzler KW. Core Signaling Pathways in Human Pancreatic Cancers Revealed by Global Genomic Analyses. Science. 2008 Sep 26;321(5897):1801–6.

15. Maitra A, Fukushima N, Takaori K, Hruban RH. Precursors to Invasive Pancreatic Cancer. Adv Anat Pathol. 2005;12(2):11.

16. Freelove R, Walling AD. Pancreatic Cancer: Diagnosis and Management. Pancreat Cancer. 2006;73(3):8.

17. Kalser MH, Barkin J, Macintyre JM. Pancreatic cancer. Assessment of prognosis by clinical presentation. Cancer. 1985 Jul 15;56(2):397–402.

18. Singhi AD, Koay EJ, Chari ST, Maitra A. Early Detection of Pancreatic Cancer: Opportunities and Challenges. Gastroenterology. 2019 May;156(7):2024–40.

19. Li J, He R, Li Y, Cao G, Ma Q, Yang W. Endoscopic Ultrasonography for Tumor Node Staging and Vascular Invasion in Pancreatic Cancer: A Meta-Analysis. Dig Surg. 2014;31(4–5):297–305.

20. Lee ES. Imaging diagnosis of pancreatic cancer: A state-of-the-art review. World J Gastroenterol. 2014;20(24):7864.

21. Ballehaninna UK, Chamberlain RS. Serum CA 19-9 as a Biomarker for Pancreatic Cancer—A Comprehensive Review. Indian J Surg Oncol. 2011 Jun;2(2):88–100.

22. McGuigan A, Kelly P, Turkington RC, Jones C, Coleman HG, McCain RS. Pancreatic cancer: A review of clinical diagnosis, epidemiology, treatment and outcomes. World J Gastroenterol. 2018 Nov 21;24(43):4846–61.

23. Demir IE, Jäger C, Schlitter AM, Konukiewitz B, Stecher L, Schorn S, Tieftrunk E, Scheufele F, Calavrezos L, Schirren R, Esposito I, Weichert W, Friess H, Ceyhan GO. R0 Versus R1 Resection Matters after Pancreaticoduodenectomy, and Less after Distal or Total Pancreatectomy for Pancreatic Cancer. Ann Surg. 2018 Dec;268(6):1058–68.

24. Anderson EM, Thomassian S, Gong J, Hendifar A, Osipov A. Advances in Pancreatic Ductal Adenocarcinoma Treatment. Cancers. 2021 Nov 3;13(21):5510.

25. Mini E, Nobili S, Caciagli B, Landini I, Mazzei T. Cellular pharmacology of gemcitabine. Ann Oncol. 2006 May;17:v7–12.

26. Jain A, Bhardwaj V. Therapeutic resistance in pancreatic ductal adenocarcinoma: Current challenges and future opportunities. World J Gastroenterol. 2021 Oct 21;27(39):6527–50.

27. Conroy T, Hammel P, Hebbar M, Abdelghani MB, Wei AC, Raoul J-L, Chone L, Francois E, Artru P, Biagi JJ, Lecomte T, Assenat E, Faroux R, Ychou M, Volet J, Sauvanet A, Jouffroy-Zeller C, Rat P, Castan F, Bachet J-B. Unicancer GI PRODIGE 24/CCTG PA.6 trial: A multicenter international randomized phase III trial of adjuvant mFOLFIRINOX versus gemcitabine (gem) in patients with resected pancreatic ductal adenocarcinomas. J Clin Oncol. 2018;36(18).

28. Von Hoff DD, Ervin T, Arena FP, Chiorean EG, Infante J, Moore M, Seay T, Tjulandin SA, Ma WW, Saleh MN, Harris M, Reni M, Dowden S, Laheru D, Bahary N, Ramanathan RK, Tabernero J, Hidalgo M, Goldstein D, Van Cutsem E, Wei X, Iglesias J, Renschler MF. Increased Survival in Pancreatic Cancer with nab-Paclitaxel plus Gemcitabine. N Engl J Med. 2013 Oct 31;369(18):1691–703.

29. Neoptolemos JP, Palmer DH, Ghaneh P, Psarelli EE, Valle JW, Halloran CM, Faluyi O, O'Reilly DA, Cunningham D, Wadsley J, Darby S, Meyer T, Gillmore R, Anthoney A, Lind P, Glimelius B, Falk S, Izbicki JR, Middleton GW, Cummins S, Ross PJ, Wasan H, McDonald A, Crosby T, Ma YT, Patel K, Sherriff D, Soomal R, Borg D, Sothi S, Hammel P, Hackert T, Jackson R, Büchler MW. Comparison of adjuvant gemcitabine and capecitabine with gemcitabine monotherapy in patients with resected pancreatic cancer (ESPAC-4): a multicentre, open-label, randomised, phase 3 trial. The Lancet. 2017 Mar;389(10073):1011–24.

30. Thomas AG, Awasthi N. Targeted therapy for pancreatic cancer: lessons learned and future opportunities. Dig Med Res. 2021 Jun;4:32–32.

31. Annese T, Tamma R, Ruggieri S, Ribatti D. Angiogenesis in Pancreatic Cancer: Pre-Clinical and Clinical Studies. Cancers. 2019 Mar 18;11(3):381.

32. Brahmer JR, Tykodi SS, Chow LQM, Hwu W-J, Topalian SL, Hwu P, Drake CG, Camacho LH, Kauh J, Odunsi K, Pitot HC, Hamid O, Bhatia S, Martins R, Eaton K, Chen S, Salay TM, Alaparthy S, Grosso JF, Korman AJ, Parker SM, Agrawal S, Goldberg SM, Pardoll DM, Gupta A, Wigginton JM. Safety and Activity of Anti–PD-L1 Antibody in Patients with Advanced Cancer. N Engl J Med. 2012 Jun 28;366(26):2455–65.

33. Montemagno, Cassim, Trichanh, Savary, Pouyssegur, Pagès, Fagret, Broisat, Ghezzi. 99mTc-A1 as a Novel Imaging Agent Targeting Mesothelin-Expressing Pancreatic Ductal Adenocarcinoma. Cancers. 2019 Oct 10;11(10):1531.

34. Tongu M, Harashima N, Monma H, Inao T, Yamada T, Kawauchi H, Harada M. Metronomic chemotherapy with low-dose cyclophosphamide plus gemcitabine can induce anti-tumor T cell immunity in vivo. Cancer Immunol Immunother. 2013 Feb;62(2):383–91.

35. Fan J, Wang M-F, Chen H-L, Shang D, Das JK, Song J. Current advances and outlooks in immunotherapy for pancreatic ductal adenocarcinoma. Mol Cancer. 2020 Dec;19(1):32.

36. Sato-Dahlman M, Wirth K, Yamamoto M. Role of Gene Therapy in Pancreatic Cancer—A Review. Cancers. 2018 Apr 3;10(4):103.

37. Shashkova EV, Kuppuswamy MN, Wold WSM, Doronin K. Anticancer activity of oncolytic adenovirus vector armed with IFN-α and ADP is enhanced by pharmacologically controlled expression of TRAIL. Cancer Gene Ther. 2008 Feb;15(2):61–72.

38. Poutou J, Bunuales M, Gonzalez-Aparicio M, Garcia-Aragoncillo E, Quetglas JI, Casado R, Bravo-Perez C, Alzuguren P, Hernandez-Alcoceba R. Safety and antitumor effect of oncolytic and helper-dependent adenoviruses expressing interleukin-12 variants in a hamster pancreatic cancer model. Gene Ther. 2015 Sep;22(9):696–706.

39. Ventura A, Kirsch DG, McLaughlin ME, Tuveson DA, Grimm J, Lintault L, Newman J, Reczek EE, Weissleder R, Jacks T. Restoration of p53 function leads to tumour regression in vivo. Nature. 2007 Feb;445(7128):661–5.

40. Dall'Ora M, Rovesti G, Bonetti LR, Casari G, Banchelli F, Veronesi E, Petrachi T, Magistri P, Benedetto FD, Spallanzani A, Chiavelli C, Spano MC, Maiorana A, Dominici M, Grisendi G. TRAIL receptors are expressed in both malignant and stromal cells in pancreatic ductal adenocarcinoma. Am J Cancer Res. 2021 Sep 30;11(9):4500–14.

41. Group Young Researchers in Inflammatory Carcinogenesis, Wandmacher AM, Mehdorn A-S, Sebens S. The Heterogeneity of the Tumor Microenvironment as Essential Determinant of Development, Progression and Therapy Response of Pancreatic Cancer. Cancers. 2021 Sep 30;13(19):4932.

42. Awaji M, Singh R. Cancer-Associated Fibroblasts' Functional Heterogeneity in Pancreatic Ductal Adenocarcinoma. Cancers. 2019 Mar 1;11(3):290.

43. Moir JAG, Mann J, White SA. The role of pancreatic stellate cells in pancreatic cancer. Surg Oncol. 2015 Sep;24(3):232–8.

44. Öhlund D, Elyada E, Tuveson D. Fibroblast heterogeneity in the cancer wound. J Exp Med. 2014 Jul 28;211(8):1503–23.

45. Hwang RF, Moore T, Arumugam T, Ramachandran V, Amos KD, Rivera A, Ji B, Evans DB, Logsdon CD. Cancer-Associated Stromal Fibroblasts Promote Pancreatic Tumor Progression. Cancer Res. 2008 Feb 1;68(3):918–26.

46. Kadaba R, Birke H, Wang J, Hooper S, Andl CD, Di Maggio F, Soylu E, Ghallab M, Bor D, Froeling FE, Bhattacharya S, Rustgi AK, Sahai E, Chelala C, Sasieni P, Kocher HM. Imbalance of desmoplastic stromal cell numbers drives aggressive cancer processes: Cancer-stroma interactions. J Pathol. 2013 May;230(1):107–17.

47. Masamune A, Kikuta K, Watanabe T, Satoh K, Hirota M, Shimosegawa T. Hypoxia stimulates pancreatic stellate cells to induce fibrosis and angiogenesis in pancreatic cancer. Am J Physiol-Gastrointest Liver Physiol. 2008 Oct;295(4):G709–17.

48. Shalapour S, Karin M. Immunity, inflammation, and cancer: an eternal fight between good and evil. J Clin Invest. 2015 Sep 1;125(9):3347–55.

49. Protti MP, De Monte L. Immune infiltrates as predictive markers of survival in pancreatic cancer patients. Front Physiol. 2013 Aug 9;4(210).

50. Foucher ED, Ghigo C, Chouaib S, Galon J, Iovanna J, Olive D. Pancreatic Ductal Adenocarcinoma: A Strong Imbalance of Good and Bad Immunological Cops in the Tumor Microenvironment. Front Immunol. 2018 May 14;9:1044.

51. Nomi T, Sho M, Akahori T, Hamada K, Kubo A, Kanehiro H, Nakamura S, Enomoto K, Yagita H, Azuma M, Nakajima Y. Clinical Significance and Therapeutic Potential of the Programmed Death-1 Ligand/Programmed Death-1 Pathway in Human Pancreatic Cancer. Clin Cancer Res. 2007 Apr 1;13(7):2151–7.

52. Suzuki D, Furukawa K, Kimura F, Shimizu H, Yoshidome H, Ohtsuka M, Kato A, Yoshitomi H, Miyazaki M. Effects of perioperative immunonutrition on cell-mediated immunity, T helper type 1 (Th1)/Th2 differentiation, and Th17 response after pancreaticoduodenectomy. Surgery. 2010 Sep;148(3):573–81.

53. Peng Y-P, Xi C-H, Zhu Y, Yin L-D, Wei J-S, Zhang J-J, Liu X-C, Guo S, Fu Y, Miao Y. Altered expression of CD226 and CD96 on natural killer cells in patients with pancreatic cancer. Oncotarget. 2016 Oct 11;7(41):66586–94.

54. Helm O, Held-Feindt J, Grage-Griebenow E, Reiling N, Ungefroren H, Vogel I, Krüger U, Becker T, Ebsen M, Röcken C, Kabelitz D, Schäfer H, Sebens S. Tumor-associated macrophages exhibit pro- and anti-inflammatory properties by which they impact on pancreatic tumorigenesis: Role of macrophages in pancreatic cancer. Int J Cancer. 2014 Aug 15;135(4):843–61.

55. Cui R, Yue W, Lattime EC, Stein MN, Xu Q, Tan X-L. Targeting tumor-associated macrophages to combat pancreatic cancer. Oncotarget. 2016 Aug 2;7(31):50735–54.

56. Powell DR, Huttenlocher A. Neutrophils in the Tumor Microenvironment. Trends Immunol. 2016 Jan;37(1):41–52.

57. Qu P, Wang L, Lin PC. Expansion and functions of myeloid-derived suppressor cells in the tumor microenvironment. Cancer Lett. 2016 Sep;380(1):253–6.

58. Hwang HK, Kim H-I, Kim SH, Choi J, Kang CM, Kim KS, Lee WJ. Prognostic impact of the tumor-infiltrating regulatory T-cell (Foxp3+)/activated cytotoxic T lymphocyte (granzyme B+) ratio on resected left-sided pancreatic cancer. Oncol Lett. 2016 Dec;12(6):4477–84.

59. Whiteside T. The role of regulatory T cells in cancer immunology. ImmunoTargets Ther. 2015 Aug;159.

60. Guéry L, Hugues S. Th17 Cell Plasticity and Functions in Cancer Immunity. BioMed Res Int. 2015;2015:1–11.

61. Daley D, Zambirinis CP, Seifert L, Akkad N, Mohan N, Werba G, Barilla R, Torres-Hernandez A, Hundeyin M, Mani VRK, Avanzi A, Tippens D, Narayanan R, Jang J-E, Newman E, Pillarisetty VG, Dustin ML, Bar-Sagi D, Hajdu C, Miller G. γδ T Cells Support Pancreatic Oncogenesis by Restraining αβ T Cell Activation. Cell. 2016 Sep;166(6):1485-1499.e15.

62. Tian C, Clauser KR, Öhlund D, Rickelt S, Huang Y, Gupta M, Mani DR, Carr SA, Tuveson DA, Hynes RO. Proteomic analyses of ECM during pancreatic ductal adenocarcinoma progression reveal different contributions by tumor and stromal cells. Proc Natl Acad Sci. 2019 Sep 24;116(39):19609–18.

63. Perez VM, Kearney JF, Yeh JJ. The PDAC Extracellular Matrix: A Review of the ECM Protein Composition, Tumor Cell Interaction, and Therapeutic Strategies. Front Oncol. 2021 Oct 6;11:751311.

64. Hamidi H, Ivaska J. Every step of the way: integrins in cancer progression and metastasis. Nat Rev Cancer. 2018 Sep;18(9):533–48.

65. Pan S, Chen R, Tamura Y, Crispin DA, Lai LA, May DH, McIntosh MW, Goodlett DR, Brentnall TA. Quantitative Glycoproteomics Analysis Reveals Changes in N-Glycosylation Level Associated with Pancreatic Ductal Adenocarcinoma. J Proteome Res. 2014 Mar 7;13(3):1293–306.

66. Fraser JRE, Laurent TC, Laurent UBG. Hyaluronan: its nature, distribution, functions and turnover. J Intern Med. 1997 Jul;242(1):27–33.

67. Bailey JM, Swanson BJ, Hamada T, Eggers JP, Singh PK, Caffery T, Ouellette MM, Hollingsworth MA. Sonic Hedgehog Promotes Desmoplasia in Pancreatic Cancer. Clin Cancer Res. 2008 Oct 1;14(19):5995–6004.

68. Ferrara B, Pignatelli C, Cossutta M, Citro A, Courty J, Piemonti L. The Extracellular Matrix in Pancreatic Cancer: Description of a Complex Network and Promising Therapeutic Options. Cancers. 2021 Sep 3;13(17):4442.

69. Weniger M, Honselmann K, Liss A. The Extracellular Matrix and Pancreatic Cancer: A Complex Relationship. Cancers. 2018 Sep 6;10(9):316.

70. Froeling FEM, Feig C, Chelala C, Dobson R, Mein CE, Tuveson DA, Clevers H, Hart IR, Kocher HM. Retinoic Acid–Induced Pancreatic Stellate Cell Quiescence Reduces Paracrine Wnt–β-Catenin Signaling to Slow Tumor Progression. Gastroenterology. 2011 Oct;141(4):1486-1497.e14.

71. Dolor A, Szoka FC. Digesting a Path Forward: The Utility of Collagenase Tumor Treatment for Improved Drug Delivery. Mol Pharm. 2018 Jun 4;15(6):2069–83.

72. Zion O, Genin O, Kawada N, Yoshizato K, Roffe S, Nagler A, Iovanna JL, Halevy O, Pines M. Inhibition of Transforming Growth Factor A Signaling by Halofuginone as a Modality for Pancreas Fibrosis Prevention. 2009;38(4):9.

73. Winer A, Adams S, Mignatti P. Matrix Metalloproteinase Inhibitors in Cancer Therapy: Turning Past Failures Into Future Successes. Mol Cancer Ther. 2018 Jun;17(6):1147–55.

74. Thompson CB, Shepard HM, O'Connor PM, Kadhim S, Jiang P, Osgood RJ, Bookbinder LH, Li X, Sugarman BJ, Connor RJ, Nadjsombati S, Frost GI. Enzymatic Depletion of Tumor Hyaluronan Induces Antitumor Responses in Preclinical Animal Models. Mol Cancer Ther. 2010 Nov;9(11):3052–64.

75. Ramanathan RK, McDonough SL, Philip PA, Hingorani SR, Lacy J, Kortmansky JS, Thumar J, Chiorean EG, Shields AF, Behl D, Mehan PT, Gaur R, Seery T, Guthrie KA, Hochster HS. Phase IB/II Randomized Study of FOLFIRINOX Plus Pegylated Recombinant Human Hyaluronidase Versus FOLFIRINOX Alone in Patients With Metastatic Pancreatic Adenocarcinoma: SWOG S1313. J Clin Oncol. 2019 May 1;37(13):1062–9.

76. Gilles M-E, Maione F, Cossutta M, Carpentier G, Caruana L, Di Maria S, Houppe C, Destouches D, Shchors K, Prochasson C, Mongelard F, Lamba S, Bardelli A, Bouvet P, Couvelard A, Courty J, Giraudo E, Cascone I. Nucleolin Targeting Impairs the Progression of Pancreatic Cancer and Promotes the Normalization of Tumor Vasculature. Cancer Res. 2016 Dec 15;76(24):7181–93.

77. Yamahatsu K, Matsuda Y, Ishiwata T, Uchida E, Naito Z. Nestin as a novel therapeutic target for pancreatic cancer via tumor angiogenesis. Int J Oncol. 2012 Jan 13;40:1345–57.

78. Friedenstein AJ, Chailakhyan RK, Latsinik NV, Panasyuk AF, Keiliss-Borok IV. Stromal cells responsible for transferring the microenvironment of the hemopoietic tissues: cloning in vitro and retransplantation in vivo. Transplantation. 1973 Sep 14;17(4):331–40.

79. Caplan AI. Mesenchymal stem cells. J Orthop Res. 1991 Sep;9(5):641–50.

80. Andrzejewska A, Lukomska B, Janowski M. Concise Review: Mesenchymal Stem Cells: From Roots to Boost. Stem Cells. 2019 Jul 1;37(7):855–64.

81. Fraser JK, Wulur I, Alfonso Z, Hedrick MH. Fat tissue: an underappreciated source of stem cells for biotechnology. Trends Biotechnol. 2006 Apr;24(4):150–4.

82. Heo JS, Choi Y, Kim H-S, Kim HO. Comparison of molecular profiles of human mesenchymal stem cells derived from bone marrow, umbilical cord blood, placenta and adipose tissue. Int J Mol Med. 2016 Jan;37(1):115–25.

83. Dominici M, Le Blanc K, Mueller I, Slaper-Cortenbach I, Marini FC, Krause DS, Deans RJ, Keating A, Prockop DJ, Horwitz EM. Minimal criteria for defining

multipotent mesenchymal stromal cells. The International Society for Cellular Therapy position statement. Cytotherapy. 2006;8(4):315–7.

84. Cantinieaux D, Quertainmont R, Blacher S, Rossi L, Wanet T, Noël A, Brook G, Schoenen J, Franzen R. Conditioned Medium from Bone Marrow-Derived Mesenchymal Stem Cells Improves Recovery after Spinal Cord Injury in Rats: An Original Strategy to Avoid Cell Transplantation. Rameshwar P, editor. PLoS ONE. 2013 Aug 27;8(8):e69515.

85. Monguió-Tortajada M, Roura S, Gálvez-Montón C, Franquesa M, Bayes-Genis A, Borràs FE. Mesenchymal Stem Cells Induce Expression of CD73 in Human Monocytes In Vitro and in a Swine Model of Myocardial Infarction In Vivo. Front Immunol. 2017 Nov 20;8:1577.

86. Cassatella MA, Mosna F, Micheletti A, Lisi V, Tamassia N, Cont C, Calzetti F, Pelletier M, Pizzolo G, Krampera M. Toll-Like Receptor-3-Activated Human Mesenchymal Stromal Cells Significantly Prolong the Survival and Function of Neutrophils. Stem Cells. 2011 Jun 1;29(6):1001–11.

87. Brandau S, Jakob M, Bruderek K, Bootz F, Giebel B, Radtke S, Mauel K, Jäger M, Flohé SB, Lang S. Mesenchymal Stem Cells Augment the Anti-Bacterial Activity of Neutrophil Granulocytes. Jacobs R, editor. PLoS ONE. 2014 Sep 19;9(9):e106903.

88. Najar M, Rouas R, Raicevic G, Boufker HI, Lewalle P, Meuleman N, Bron D, Toungouz M, Martiat P, Lagneaux L. Mesenchymal stromal cells promote or suppress the proliferation of T lymphocytes from cord blood and peripheral blood: the importance of low cell ratio and role of interleukin-6. Cytotherapy. 2009 Jan;11(5):570–83.

89. Demircan PC, Sariboyaci AE, Unal ZS, Gacar G, Subasi C, Karaoz E. Immunoregulatory effects of human dental pulp-derived stem cells on T cells: comparison of transwell co-culture and mixed lymphocyte reaction systems. Cytotherapy. 2011 Nov;13(10):1205–20.

90. Corcione A, Benvenuto F, Ferretti E, Giunti D, Cappiello V, Cazzanti F, Risso M, Gualandi F, Mancardi GL, Pistoia V, Uccelli A. Human mesenchymal stem cells modulate B-cell functions. Blood. 2006 Jan 1;107(1):367–72.

91. Golinelli G, Mastrolia I, Aramini B, Masciale V, Pinelli M, Pacchioni L, Casari G, Dall'Ora M, Soares MBP, Damasceno PKF, Silva DN, Dominici M, Grisendi G. Arming Mesenchymal Stromal/Stem Cells Against Cancer: Has the Time Come? Front Pharmacol. 2020 Sep 29;11:529921.

92. Chen X, Song E. Turning foes to friends: targeting cancer-associated fibroblasts. Nat Rev Drug Discov. 2019 Feb;18(2):99–115.

93. Moniri MR, Dai L-J, Warnock GL. The challenge of pancreatic cancer therapy and novel treatment strategy using engineered mesenchymal stem cells. Cancer Gene Ther. 2014 Jan;21(1):12–23.

94. Mastrolia I, Foppiani EM, Murgia A, Candini O, Samarelli AV, Grisendi G, Veronesi E, Horwitz EM, Dominici M. Challenges in Clinical Development of Mesenchymal Stromal/Stem Cells: Concise Review. Stem Cells Transl Med. 2019 Nov 1;8(11):1135–48.

95. Silva LHA, Cruz FF, Morales MM, Weiss DJ, Rocco PRM. Magnetic targeting as a strategy to enhance therapeutic effects of mesenchymal stromal cells. Stem Cell Res Ther. 2017 Dec;8(1):58.

96. Hakkarainen T, Särkioja M, Lehenkari P, Miettinen S, Ylikomi T, Suuronen R, Desmond RA, Kanerva A, Hemminki A. Human Mesenchymal Stem Cells Lack Tumor Tropism but Enhance the Antitumor Activity of Oncolytic Adenoviruses in Orthotopic Lung and Breast Tumors. Hum Gene Ther. 2007 Jul;18(7):627–41.

97. Golinelli G, Grisendi G, Prapa M, Bestagno M, Spano C, Rossignoli F, Bambi F, Sardi I, Cellini M, Horwitz EM, Feletti A, Pavesi G, Dominici M. Targeting GD2-positive glioblastoma by chimeric antigen receptor empowered mesenchymal progenitors. Cancer Gene Ther. 2020 Aug;27(7–8):558–70.

98. Kidd S, Caldwell L, Dietrich M, Samudio I, Spaeth EL, Watson K, Shi Y, Abbruzzese J, Konopleva M, Andreeff M, Marini FC. Mesenchymal stromal cells alone or expressing interferon-β suppress pancreatic tumors in vivo, an effect countered by anti-inflammatory treatment. Cytotherapy. 2010 Sep;12(5):615–25.

99. Grisendi G, Bussolari R, Veronesi E, Piccinno S, Burns JS, Santis GD, Loschi P, Pignatti M, Benedetto FD, Ballarin R, Gregorio CD, Piccinini L, Horwitz EM, Paolucci P, Conte P, Dominici M. Understanding tumor-stroma interplays for targeted therapies by armed mesenchymal stromal progenitors: the Mesenkillers. Am J Cancer Res. 2011 Jun 30;1(6):787–805.

100. Kidd S, Spaeth E, Watson K, Burks J, Lu H, Klopp A, Andreeff M, Marini FC. Origins of the Tumor Microenvironment: Quantitative Assessment of Adipose-Derived and Bone Marrow–Derived Stroma. Rameshwar P, editor. PLoS ONE. 2012 Feb 20;7(2):e30563.

101. Norozi F, Ahmadzadeh A, Shahrabi S, Vosoughi T, Saki N. Mesenchymal stem cells as a double-edged sword in suppression or progression of solid tumor cells. Tumor Biol. 2016 Sep;37(9):11679–89.

102. Pessina A, Coccè V, Pascucci L, Bonomi A, Cavicchini L, Sisto F, Ferrari M, Ciusani E, Crovace A, Falchetti ML, Zicari S, Caruso A, Navone S, Marfia G, Benetti A, Ceccarelli P, Parati E, Alessandri G. Mesenchymal stromal cells primed with Paclitaxel attract and kill leukaemia cells, inhibit angiogenesis and improve survival of leukaemia-bearing mice. Br J Haematol. 2013 Mar;160(6):766–78.

103. Pascucci L, Coccè V, Bonomi A, Ami D, Ceccarelli P, Ciusani E, Viganò L, Locatelli A, Sisto F, Doglia SM, Parati E, Bernardo ME, Muraca M, Alessandri G, Bondiolotti G, Pessina A. Paclitaxel is incorporated by mesenchymal stromal cells and released in

exosomes that inhibit in vitro tumor growth: A new approach for drug delivery. J Controlled Release. 2014 Oct;192:262–70.

104. Bonomi A, Steimberg N, Benetti A, Berenzi A, Alessandri G, Pascucci L, Boniotti J, Coccè V, Sordi V, Pessina A, Mazzoleni G. Paclitaxel-releasing mesenchymal stromal cells inhibit the growth of multiple myeloma cells in a dynamic 3D culture system: 3D myeloma inhibition by drug releasing MSCs. Hematol Oncol. 2017 Dec;35(4):693–702.

105. Aggarwal S, Pittenger MF. Human mesenchymal stem cells modulate allogeneic immune cell responses. Blood. 2005 Feb 15;105(4):1815–22.

106. Layek B, Sadhukha T, Panyam J, Prabha S. Nano-Engineered Mesenchymal Stem Cells Increase Therapeutic Efficacy of Anticancer Drug Through True Active Tumor Targeting. Mol Cancer Ther. 2018 Jun;17(6):1196–206.

107. Bruno S, Chiabotto G, Favaro E, Deregibus MC, Camussi G. Role of extracellular vesicles in stem cell biology. Am J Physiol-Cell Physiol. 2019 Aug 1;317(2):C303–13.

108. Pessina A, Bonomi A, Coccè V, Invernici G, Navone S, Cavicchini L, Sisto F, Ferrari M, Viganò L, Locatelli A, Ciusani E, Cappelletti G, Cartelli D, Arnaldo C, Parati E, Marfia G, Pallini R, Falchetti ML, Alessandri G. Mesenchymal Stromal Cells Primed with Paclitaxel Provide a New Approach for Cancer Therapy. Tjwa M, editor. PLoS ONE. 2011 Dec 20;6(12):e28321.

109. Nakashima H, Kaur B, Chiocca EA. Directing systemic oncolytic viral delivery to tumors via carrier cells. Cytokine Growth Factor Rev. 2010 Apr;21(2–3):119–26.

110. Shah K. Mesenchymal stem cells engineered for cancer therapy. Adv Drug Deliv Rev. 2012 Jun;64(8):739–48.

111. Zhang J, Kale V, Chen M. Gene-Directed Enzyme Prodrug Therapy. AAPS J. 2015 Jan;17(1):102–10.

112. Kucerova L, Altanerova V, Matuskova M, Tyciakova S, Altaner C. Adipose Tissue–Derived Human Mesenchymal Stem Cells Mediated Prodrug Cancer Gene Therapy. Cancer Res. 2007 Jul 1;67(13):6304–13.

113. Chen X, Lin X, Zhao J, Shi W, Zhang H, Wang Y, Kan B, Du L, Wang B, Wei Y, Liu Y, Zhao X. A Tumor-selective Biotherapy With Prolonged Impact on Established Metastases Based on Cytokine Gene-engineered MSCs. Mol Ther. 2008 Apr;16(4):749–56.

114. Bonomi A, Sordi V, Dugnani E, Ceserani V, Dossena M, Coccè V, Cavicchini L, Ciusani E, Bondiolotti G, Piovani G, Pascucci L, Sisto F, Alessandri G, Piemonti L, Parati E, Pessina A. Gemcitabine-releasing mesenchymal stromal cells inhibit in vitro proliferation of human pancreatic carcinoma cells. Cytotherapy. 2015 Dec;17(12):1687–95.

115. Wu D-M, Wen X, Han X-R, Wang S, Wang Y-J, Shen M, Fan S-H, Zhang Z-F, Shan Q, Li M-Q, Hu B, Lu J, Chen G-Q, Zheng Y-L. Bone Marrow Mesenchymal Stem Cell-Derived Exosomal MicroRNA-126-3p Inhibits Pancreatic Cancer Development by Targeting ADAM9. Mol Ther - Nucleic Acids. 2019 Jun;16:229–45.

116. Xu Y, Liu N, Wei Y, Zhou D, Lin R, Wang X, Shi B. Anticancer effects of miR-124 delivered by BM-MSC derived exosomes on cell proliferation, epithelial mesenchymal transition, and chemotherapy sensitivity of pancreatic cancer cells. Aging. 2020 Oct 11;12(19):19660–76.

117. Kaczorowski A, Hammer K, Liu L, Villhauer S, Nwaeburu C, Fan P, Zhao Z, Gladkich J, Groß W, Nettelbeck DM, Herr I. Delivery of improved oncolytic adenoviruses by mesenchymal stromal cells for elimination of tumorigenic pancreatic cancer cells. Oncotarget. 2016 Feb 23;7(8):9046–59.

118. Jing W, Chen Y, Lu L, Hu X, Shao C, Zhang Y, Zhou X, Zhou Y, Wu L, Liu R, Fan K, Jin G. Human Umbilical Cord Blood–Derived Mesenchymal Stem Cells Producing IL15 Eradicate Established Pancreatic Tumor in Syngeneic Mice. Mol Cancer Ther. 2014 Aug;13(8):2127–37.

119. Niess H, von Einem JC, Thomas MN, Michl M, Angele MK, Huss R, Günther C, Nelson PJ, Bruns CJ, Heinemann V. Treatment of advanced gastrointestinal tumors with genetically modified autologous mesenchymal stromal cells (TREAT-ME1): study protocol of a phase I/II clinical trial. BMC Cancer. 2015 Dec;15(1):237.

120. von Einem JC, Peter S, Günther C, Volk H-D, Grütz G, Salat C, Stoetzer O, Nelson PJ, Michl M, Modest DP, Holch JW, Angele M, Bruns C, Niess H, Heinemann V. Treatment of advanced gastrointestinal cancer with genetically modified autologous mesenchymal stem cells - TREAT-ME-1 - a phase I, first in human, first in class trial. Oncotarget. 2017 Oct 6;8(46):80156–66.

121. Liabakk N-B, Sundan A, Torp S, Aukrust P, Frøland SS, Espevik T. Development, characterization and use of monoclonal antibodies against sTRAIL: measurement of sTRAIL by ELISA. J Immunol Methods. 2002 Jan;259(1–2):119–28.

122. Falschlehner C, Schaefer U, Walczak H. Following TRAIL's path in the immune system. Immunology. 2009 Jun;127(2):145–54.

123. Song K, Chen Y, Göke R, Wilmen A, Seidel C, Göke A, Hilliard B, Chen Y. Tumor Necrosis Factor–Related Apoptosis-Inducing Ligand (Trail) Is an Inhibitor of Autoimmune Inflammation and Cell Cycle Progression. J Exp Med. 2000 Apr 3;191(7):1095–104.

124. Cretney E, Takeda K, Yagita H, Glaccum M, Peschon JJ, Smyth MJ. Increased Susceptibility to Tumor Initiation and Metastasis in TNF-Related Apoptosis-Inducing Ligand-Deficient Mice. J Immunol. 2002 Feb 1;168(3):1356–61.

125. Cardoso Alves L, Corazza N, Micheau O, Krebs P. The multifaceted role of TRAIL signaling in cancer and immunity. FEBS J. 2021 Oct;288(19):5530–54.

126. Bodmer J-L, Holler N, Reynard S, Vinciguerra P, Schneider P, Juo P, Blenis J, Tschopp J. TRAIL receptor-2 signals apoptosis through FADD and caspase-8. Nat Cell Biol. 2000 Apr;2(4):241–3.

127. Saraste A. Morphologic and biochemical hallmarks of apoptosis. Cardiovasc Res. 2000 Feb;45(3):528–37.

128. Yuan S, Akey CW. Apoptosome Structure, Assembly, and Procaspase Activation. Structure. 2013 Apr;21(4):501–15.

129. Lowe SW, Bodis S, McClatchey A, Remington L, Ruley HE, Fisher DE, Housman DE, Jacks T. p53 Status and the Efficacy of Cancer Therapy in Vivo. Science. 1994 Nov 4;266(5186):807–10.

130. Thapa B, Kc R, Uludağ H. TRAIL therapy and prospective developments for cancer treatment. J Controlled Release. 2020 Oct;326:335–49.

131. Azijli K, Weyhenmeyer B, Peters GJ, de Jong S, Kruyt FAE. Non-canonical kinase signaling by the death ligand TRAIL in cancer cells: discord in the death receptor family. Cell Death Differ. 2013 Jul;20(7):858–68.

132. Kreuz S, Siegmund D, Rumpf J-J, Samel D, Leverkus M, Janssen O, Häcker G, Dittrich-Breiholz O, Kracht M, Scheurich P, Wajant H. NFκB activation by Fas is mediated through FADD, caspase-8, and RIP and is inhibited by FLIP. J Cell Biol. 2004 Aug 2;166(3):369–80.

133. Song JH, Tse MCL, Bellail A, Phuphanich S, Khuri F, Kneteman NM, Hao C. Lipid Rafts and Nonrafts Mediate Tumor Necrosis Factor–Related Apoptosis-Inducing Ligand–Induced Apoptotic and Nonapoptotic Signals in Non–Small Cell Lung Carcinoma Cells. Cancer Res. 2007 Jul 15;67(14):6946–55.

134. Beyer, Baukloh, Stoyanova, Kamphues, Sattler, Kotsch. Interactions of Tumor Necrosis Factor–Related Apoptosis-Inducing Ligand (TRAIL) with the Immune System: Implications for Inflammation and Cancer. Cancers. 2019 Aug 13;11(8):1161.

135. Hartwig T, Montinaro A, von Karstedt S, Sevko A, Surinova S, Chakravarthy A, Taraborrelli L, Draber P, Lafont E, Arce Vargas F, El-Bahrawy MA, Quezada SA, Walczak H. The TRAIL-Induced Cancer Secretome Promotes a Tumor-Supportive Immune Microenvironment via CCR2. Mol Cell. 2017 Feb;65(4):730-742.e5.

136. Kamohara H, Matsuyama W, Shimozato O, Abe K, Galligan C, Hashimoto S-I, Matsushima K, Yoshimura T. Regulation of tumour necrosis factor-related apoptosis-inducing ligand (TRAIL) and TRAIL receptor expression in human neutrophils. Immunology. 2004 Feb;111(2):186–94.

137. Bossi F, Bernardi S, Zauli G, Secchiero P, Fabris B. TRAIL Modulates the Immune System and Protects against the Development of Diabetes. J Immunol Res. 2015;2015:1–12.

138. Ikeda T, Hirata S, Fukushima S, Matsunaga Y, Ito T, Uchino M, Nishimura Y, Senju S. Dual Effects of TRAIL in Suppression of Autoimmunity: The Inhibition of Th1 Cells and the Promotion of Regulatory T Cells. J Immunol. 2010 Nov 1;185(9):5259–67.

139. Rossin A, Miloro G, Hueber A-O. TRAIL and FasL Functions in Cancer and Autoimmune Diseases: Towards an Increasing Complexity. Cancers. 2019 May 8;11(5):639.

140. Prager I, Watzl C. Mechanisms of natural killer cell-mediated cellular cytotoxicity. J Leukoc Biol. 2019 Jun;105(6):1319–29.

141. de Looff M, de Jong S, Kruyt FAE. Multiple Interactions Between Cancer Cells and the Tumor Microenvironment Modulate TRAIL Signaling: Implications for TRAIL Receptor Targeted Therapy. Front Immunol. 2019 Jul 3;10:1530.

142. Zhao H, Liao X, Kang Y. Tregs: Where We Are and What Comes Next? Front Immunol. 2017 Nov 24;8:1578.

143. Lemke J, von Karstedt S, Zinngrebe J, Walczak H. Getting TRAIL back on track for cancer therapy. Cell Death Differ. 2014 Sep;21(9):1350–64.

144. Held J, Schulze-Osthoff K. Potential and caveats of TRAIL in cancer therapy. Drug Resist Updat. 2001 Aug;4(4):243–52.

145. Herbst RS, Eckhardt SG, Kurzrock R, Ebbinghaus S, O'Dwyer PJ, Gordon MS, Novotny W, Goldwasser MA, Tohnya TM, Lum BL, Ashkenazi A, Jubb AM, Mendelson DS. Phase I Dose-Escalation Study of Recombinant Human Apo2L/TRAIL, a Dual Proapoptotic Receptor Agonist, in Patients With Advanced Cancer. J Clin Oncol. 2010 Jun 10;28(17):2839–46.

146. Zhang XD, Franco AV, Nguyen T, Gray CP, Hersey P. Differential Localization and Regulation of Death and Decoy Receptors for TNF-Related Apoptosis-Inducing Ligand (TRAIL) in Human Melanoma Cells. J Immunol. 2000 Apr 15;164(8):3961–70.

147. Fulda S, Meyer E, Debatin K-M. Inhibition of TRAIL-induced apoptosis by Bcl-2 overexpression. Oncogene. 2002 Apr;21(15):2283–94.

148. Vogler M, Dürr K, Jovanovic M, Debatin K-M, Fulda S. Regulation of TRAIL-induced apoptosis by XIAP in pancreatic carcinoma cells. Oncogene. 2007 Jan;26(2):248–57.

149. Liu H, Su D, Zhang J, Ge S, Li Y, Wang F, Gravel M, Roulston A, Song Q, Xu W, Liang JG, Shore G, Wang X, Liang P. Improvement of Pharmacokinetic Profile of TRAIL via Trimer-Tag Enhances its Antitumor Activity in vivo. Sci Rep. 2017 Dec;7(1):8953.

150. Kim TH, Youn YS, Jiang HH, Lee S, Chen X, Lee KC. PEGylated TNF-Related Apoptosis-Inducing Ligand (TRAIL) Analogues: Pharmacokinetics and Antitumor Effects. Bioconjug Chem. 2011 Aug 17;22(8):1631–7.

151. Goklany S, Lu P, Godeshala S, Hall A, Garrett-Mayer E, Voelkel-Johnson C, Rege K. Delivery of TRAIL-expressing plasmid DNA to cancer cells *in vitro* and *in vivo* using aminoglycoside-derived polymers. J Mater Chem B. 2019;7(44):7014–25.

152. Luo C, Miao L, Zhao Y, Musetti S, Wang Y, Shi K, Huang L. A novel cationic lipid with intrinsic antitumor activity to facilitate gene therapy of TRAIL DNA. Biomaterials. 2016 Sep;102:239–48.

153. Stuckey DW, Shah K. Stem cell-based therapies for cancer treatment: separating hope from hype. Nat Rev Cancer. 2014 Oct;14(10):683–91.

154. Hammer K, Kazcorowski A, Liu L, Behr M, Schemmer P, Herr I, Nettelbeck DM. Engineered adenoviruses combine enhanced oncolysis with improved virus production by mesenchymal stromal carrier cells: Oncolytic adenoviruses for MSC delivery to pancreatic cancer. Int J Cancer. 2015 Aug 15;137(4):978–90.

155. Grisendi G, Bussolari R, Cafarelli L, Petak I, Rasini V, Veronesi E, De Santis G, Spano C, Tagliazzucchi M, Barti-Juhasz H, Scarabelli L, Bambi F, Frassoldati A, Rossi G, Casali C, Morandi U, Horwitz EM, Paolucci P, Conte P, Dominici M. Adipose-Derived Mesenchymal Stem Cells as Stable Source of Tumor Necrosis Factor–Related Apoptosis-Inducing Ligand Delivery for Cancer Therapy. Cancer Res. 2010 May 1;70(9):3718–29.

156. Grisendi G, Spano C, D'souza N, Rasini V, Veronesi E, Prapa M, Petrachi T, Piccinno S, Rossignoli F, Burns JS, Fiorcari S, Granchi D, Baldini N, Horwitz EM, Guarneri V, Conte P, Paolucci P, Dominici M. Mesenchymal progenitors expressing TRAIL induce apoptosis in sarcomas. STEM CELLS. 2015 Mar;33(3):859–69.

157. Golinelli G, Grisendi G, Spano C, Dominici M. Surrounding Pancreatic Adenocarcinoma by Killer Mesenchymal Stromal/Stem Cells. Hum Gene Ther. 2014 May;25(5):406–7.

158. Golinelli G, Grisendi G, Dall'Ora M, Casari G, Spano C, Talami R, Banchelli F, Prapa M, Chiavelli C, Rossignoli F, Candini O, D'Amico R, Nasi M, Cossarizza A, Casarini L, Dominici M. Anti-GD2 CAR MSCs against metastatic Ewing's sarcoma. Transl Oncol. 2022 Jan;15(1):101240.

159. Woo SM, Seo SU, Kim SH, Nam J-O, Kim S, Park J-W, Min K, Kwon TK. Hispidulin Enhances TRAIL-Mediated Apoptosis via CaMKKβ/AMPK/USP51 Axis-Mediated Bim Stabilization. Cancers. 2019 Dec 6;11(12):1960.

160. Thapa B, Bahadur KC R, Uludağ H. Novel targets for sensitizing breast cancer cells to TRAIL-induced apoptosis with siRNA delivery: Novel targets for sensitizing breast cancer cells. Int J Cancer. 2018 Feb 1;142(3):597–606.

161. Soria J-C, Smit E, Khayat D, Besse B, Yang X, Hsu C-P, Reese D, Wiezorek J, Blackhall F. Phase 1b Study of Dulanermin (recombinant human Apo2L/TRAIL) in Combination With Paclitaxel, Carboplatin, and Bevacizumab in Patients With

Advanced Non-Squamous Non–Small-Cell Lung Cancer. J Clin Oncol. 2010 Mar 20;28(9):1527–33.

162. Yee L, Fanale M, Dimick K, Calvert S, Robins C, IngJ. Ling J, Novotny W, Ashkenazi A, Burris III H. A phase IB safety and pharmacokinetic (PK) study of recombinant human Apo2L/TRAIL in combination with rituximab in patients with low-grade non-Hodgkin lymphoma. J Clin Oncol. 2007 Jun 20;25(18):8078–8078.

163. Hylander BL, Pitoniak R, Penetrante RB, Gibbs JF, Oktay D, Cheng J, Repasky EA. The anti-tumor effect of Apo2L/TRAIL on patient pancreatic adenocarcinomas grown as xenografts in SCID mice. J Transl Med. 2005 Dec;3(1):22.

164. Sharma R, Buitrago S, Pitoniak R, Gibbs JF, Curtin L, Seshadri M, Repasky EA, Hylander BL. Influence of the Implantation Site on the Sensitivity of Patient Pancreatic Tumor Xenografts to Apo2L/TRAIL Therapy. Pancreas. 2014 Mar;43(2):298–305.

165. Nogueira DR, Yaylim I, Aamir Q, Kahraman O, Fayyaz S, Naqvi SK-U-H, Farooqi AA. TRAIL Mediated Signaling in Pancreatic Cancer. Asian Pac J Cancer Prev. 2014 Aug 15;15(15):5977–82.

166. Zhao B, Li L, Cui K, Wang C-L, Wang A-L, Zhang B, Zhou W-Y, Niu Z-X, Tian H, Xue Y, Li S. Mechanisms of TRAIL and Gemcitabine Induction of Pancreatic Cancer Cell Apoptosis. Asian Pac J Cancer Prev. 2011;12:2675–8.

167. Min SY, Byeon HJ, Lee C, Seo J, Lee ES, Shin BS, Choi H-G, Lee KC, Youn YS. Facile one-pot formulation of TRAIL-embedded paclitaxel-bound albumin nanoparticles for the treatment of pancreatic cancer. Int J Pharm. 2015 Oct;494(1):506–15.

168. Kupcova Skalnikova H. Proteomic techniques for characterisation of mesenchymal stem cell secretome. Biochimie. 2013 Dec;95(12):2196–211.

169. Candini O, Grisendi G, Foppiani EM, Brogli M, Aramini B, Masciale V, Spano C, Petrachi T, Veronesi E, Conte P, Mari G, Dominici M. A Novel 3D In Vitro Platform for Pre-Clinical Investigations in Drug Testing, Gene Therapy, and Immuno-oncology. Sci Rep. 2019 Dec;9(1):7154.

170. Qiu W, Su GH. Development of Orthotopic Pancreatic Tumor Mouse Models. Methods Mol Biol. 2013;980:215–23.

171. Kim MP, Evans DB, Wang H, Abbruzzese JL, Fleming JB, Gallick GE. Generation of orthotopic and heterotopic human pancreatic cancer xenografts in immunodeficient mice. Nat Protoc. 2009 Nov;4(11):1670–80.

172. Zamai L, Canonico B, Luchetti F, Ferri P, Melloni E, Guidotti L, Cappellini A, Cutroneo G, Vitale M, Papa S. Supravital exposure to propidium iodide identifies apoptosis on adherent cells. Cytometry. 2001 May 1;44(1):57–64.

173. Suzuki S, Okada M, Shibuya K, Seino M, Sato A, Takeda H, Seino S, Yoshioka T, Kitanaka C. JNK suppression of chemotherapeutic agents-induced ROS confers chemoresistance on pancreatic cancer stem cells. Oncotarget. 2015 Jan 1;6(1):458–70.

174. Chen S-H, Li D-L, Yang F, Wu Z, Zhao Y-Y, Jiang Y. Gemcitabine-induced pancreatic cancer cell death is associated with MST1/Cyclophilin D mitochondrial complexation. Biochimie. 2014 Aug;103:71–9.

175. Rampersad SN. Multiple Applications of Alamar Blue as an Indicator of Metabolic Function and Cellular Health in Cell Viability Bioassays. Sensors. 2012 Sep 10;12(9):12347–60.

176. Zeng, Pöttler, Lan, Grützmann, Pilarsky, Yang. Chemoresistance in Pancreatic Cancer. Int J Mol Sci. 2019 Sep 11;20(18):4504.

177. Chu GC, Kimmelman AC, Hezel AF, DePinho RA. Stromal biology of pancreatic cancer. J Cell Biochem. 2007 Jul 1;101(4):887–907.

178. Veenstra V, Garcia-Garijo A, van Laarhoven H, Bijlsma M. Extracellular Influences: Molecular Subclasses and the Microenvironment in Pancreatic Cancer. Cancers. 2018 Jan 27;10(2):34.

179. Liang C, Shi S, Meng Q, Liang D, Ji S, Zhang B, Qin Y, Xu J, Ni Q, Yu X. Do anti-stroma therapies improve extrinsic resistance to increase the efficacy of gemcitabine in pancreatic cancer? Cell Mol Life Sci. 2018 Mar;75(6):1001–12.

180. Carvalho TMA, Di Molfetta D, Greco MR, Koltai T, Alfarouk KO, Reshkin SJ, Cardone RA. Tumor Microenvironment Features and Chemoresistance in Pancreatic Ductal Adenocarcinoma: Insights into Targeting Physicochemical Barriers and Metabolism as Therapeutic Approaches. Cancers. 2021 Dec 6;13(23):6135.

181. Todaro M, Lombardo Y, Francipane MG, Alea MP, Cammareri P, Iovino F, Di Stefano AB, Di Bernardo C, Agrusa A, Condorelli G, Walczak H, Stassi G. Apoptosis resistance in epithelial tumors is mediated by tumor-cell-derived interleukin-4. Cell Death Differ. 2008 Apr;15(4):762–72.

182. Soria J-C, Márk Z, Zatloukal P, Szima B, Albert I, Juhász E, Pujol J-L, Kozielski J, Baker N, Smethurst D, Hei Y, Ashkenazi A, Stern H, Amler L, Pan Y, Blackhall F. Randomized Phase II Study of Dulanermin in Combination With Paclitaxel, Carboplatin, and Bevacizumab in Advanced Non–Small-Cell Lung Cancer. J Clin Oncol. 2011 Nov 20;29(33):4442–51.

183. Elia A, Henry-Grant R, Adiseshiah C, Marboeuf C, Buckley RJ, Clemens MJ, Mudan S, Pyronnet S. Implication of 4E-BP1 protein dephosphorylation and accumulation in pancreatic cancer cell death induced by combined gemcitabine and TRAIL. Cell Death Dis. 2017 Dec;8(12):3204.

184. Hylander BL, Sen A, Beachy SH, Pitoniak R, Ullas S, Gibbs JF, Qiu J, Prey JD, Fetterly GJ, Repasky EA. Tumor priming by Apo2L/TRAIL reduces interstitial fluid

pressure and enhances efficacy of liposomal gemcitabine in a patient derived xenograft tumor model. J Controlled Release. 2015 Nov;217:160–9.

185. Oldenhuis C, Mom C, Sleijfer S, Gietema JA, Fox NL, Corey A, Eskens F, Loos W, De Vries EG, Verweij J. A phase I study with the agonistic TRAIL-R1 antibody, mapatumumab, in combination with gemcitabine and cisplatin. J Clin Oncol. 2008 May 20;26(15):3540–3540.

186. Sikic BI, Wakelee HA, Von Mehren M, Lewis N, Calvert AH, Plummer ER, Fox NL, Howard T, Jones SF, Burris III HA. A phase Ib study to assess the safety of lexatumumab, a human monoclonal antibody that activates TRAIL-R2, in combination with gemcitabine, pemetrexed, doxorubicin or FOLFIRI. J Clin Oncol. 2007 Jun 20;25(18):14006–14006.

187. Razeghian E, Suksatan W, Sulaiman Rahman H, Bokov DO, Abdelbasset WK, Hassanzadeh A, Marofi F, Yazdanifar M, Jarahian M. Harnessing TRAIL-Induced Apoptosis Pathway for Cancer Immunotherapy and Associated Challenges. Front Immunol. 2021 Aug 20;12:699746.

188. Szegezdi E, O'Reilly A, Davy Y, Vawda R, Taylor DL, Murphy M, Samali A, Mehmet H. Stem cells are resistant to TRAIL receptor-mediated apoptosis. J Cell Mol Med. 2009 Nov;13(11–12):4409–14.

189. Jiang H, Wang S, Zhou X, Wang L, Ye L, Zhou Z, Tang J, Liu X, Teng L, Shen Y. New path to treating pancreatic cancer: TRAIL gene delivery targeting the fibroblast-enriched tumor microenvironment. J Controlled Release. 2018 Sep;286:254–63.

190. Fang Y, Zhou W, Rong Y, Kuang T, Xu X, Wu W, Wang D, Lou W. Exosomal miRNA-106b from cancer-associated fibroblast promotes gemcitabine resistance in pancreatic cancer. Exp Cell Res. 2019 Oct;383(1):111543.

191. Wei L, Ye H, Li G, Lu Y, Zhou Q, Zheng S, Lin Q, Liu Y, Li Z, Chen R. Cancer-associated fibroblasts promote progression and gemcitabine resistance via the SDF-1/SATB-1 pathway in pancreatic cancer. Cell Death Dis. 2018 Nov;9(11):1065.

192. Ligorio M, Sil S, Malagon-Lopez J, Nieman LT, Misale S, Di Pilato M, Ebright RY, Karabacak MN, Kulkarni AS, Liu A, Vincent Jordan N, Franses JW, Philipp J, Kreuzer J, Desai N, Arora KS, Rajurkar M, Horwitz E, Neyaz A, Tai E, Magnus NKC, Vo KD, Yashaswini CN, Marangoni F, Boukhali M, Fatherree JP, Damon LJ, Xega K, Desai R, Choz M, Bersani F, Langenbucher A, Thapar V, Morris R, Wellner UF, Schilling O, Lawrence MS, Liss AS, Rivera MN, Deshpande V, Benes CH, Maheswaran S, Haber DA, Fernandez-Del-Castillo C, Ferrone CR, Haas W, Aryee MJ, Ting DT. Stromal Microenvironment Shapes the Intratumoral Architecture of Pancreatic Cancer. Cell. 2019 Jun;178(1):160-175.e27.

193. Osuna de la Peña D, Trabulo SMD, Collin E, Liu Y, Sharma S, Tatari M, Behrens D, Erkan M, Lawlor RT, Scarpa A, Heeschen C, Mata A, Loessner D. Bioengineered 3D models of human pancreatic cancer recapitulate in vivo tumour biology. Nat Commun. 2021 Dec;12(1):5623.

194. Moniri MR, Sun X-Y, Rayat J, Dai D, Ao Z, He Z, Verchere CB, Dai L-J, Warnock GL. TRAIL-engineered pancreas-derived mesenchymal stem cells: characterization and cytotoxic effects on pancreatic cancer cells. Cancer Gene Ther. 2012 Sep;19(9):652–8.

195. Griffith TS, Wiley SR, Kubin MZ, Sedger LM, Maliszewski CR, Fanger NA. Monocyte-mediated Tumoricidal Activity via the Tumor Necrosis Factor–related Cytokine, TRAIL. J Exp Med. 1999 Apr 19;189(8):1343–54.

196. Liguori M, Buracchi C, Pasqualini F, Bergomas F, Pesce S, Sironi M, Grizzi F, Mantovani A, Belgiovine C, Allavena P. Functional TRAIL receptors in monocytes and tumor-associated macrophages: A possible targeting pathway in the tumor microenvironment. Oncotarget. 2106 Jul 5;7(27):41662–76.

197. Lotfi N, Zhang G-X, Esmaeil N, Rostami A. Evaluation of the effect of GM-CSF blocking on the phenotype and function of human monocytes. Sci Rep. 2020 Dec;10(1):1567.

198. Joel MDM, Yuan J, Wang J, Yan Y, Qian H, Zhang X, Mao F. MSC: immunoregulatory effects, roles on neutrophils and evolving clinical potentials. Am J Transl Res. 2019 Jun 30;11(6):3890–904.

199. Martínez-Lorenzo MJ, Alava MA, Gamen S, Kim KJ, Chuntharapai A, Piñeiro A, Naval J, Anel A. Involvement of APO2 ligand/TRAIL in activation-induced death of Jurkat and human peripheral blood T cells. Eur J Immunol. 1998 Sep;28(9):2714–25.

200. Clancy L, Mruk K, Archer K, Woelfel M, Mongkolsapaya J, Screaton G, Lenardo MJ, Chan FK-M. Preligand assembly domain-mediated ligand-independent association between TRAIL receptor 4 (TR4) and TR2 regulates TRAIL-induced apoptosis. Proc Natl Acad Sci. 2005 Dec 13;102(50):18099–104.

201. Mirandola P. Activated human NK and CD8+ T cells express both TNF-related apoptosis-inducing ligand (TRAIL) and TRAIL receptors but are resistant to TRAIL-mediated cytotoxicity. Blood. 2004 Jun 29;104(8):2418–24.

202. Wendling U, Walczak H, Dörr J, Jaboci C, Weller M, Krammer PH, Zipp F. Expression of TRAIL receptors in human autoreactive and foreign antigen-specific T cells. Cell Death Differ. 2000 Jul;7(7):637–44.

203. Lünemann JD, Waiczies S, Ehrlich S, Wendling U, Seeger B, Kamradt T, Zipp F. Death Ligand TRAIL Induces No Apoptosis but Inhibits Activation of Human (Auto)antigen-Specific T Cells. J Immunol. 2002 May 15;168(10):4881–8.

204. Park S-Y, Billiar TR, Seol D-W. IFN-γ Inhibition of TRAIL-Induced IAP-2 Upregulation, a Possible Mechanism of IFN-γ-Enhanced TRAIL-Induced Apoptosis. Biochem Biophys Res Commun. 2002 Feb;291(2):233–6.

205. Park S-Y, Seol J-W, Lee Y-J, Cho J-H, Kang H-S, Kim I-S, Park S-H, Kim T-H, Yim JH, Kim M, Billiar TR, Seol D-W. IFN-γ enhances TRAIL-induced apoptosis through IRF-1: IFN-γ enhances TRAIL-induced apoptosis. Eur J Biochem. 2004 Oct 20;271(21):4222–8.

206. Liu F, Hu X, Zimmerman M, Waller JL, Wu P, Hayes-Jordan A, Lev D, Liu K. TNFα Cooperates with IFN-γ to Repress Bcl-xL Expression to Sensitize Metastatic Colon Carcinoma Cells to TRAIL-mediated Apoptosis. Wu GS, editor. PLoS ONE. 2011 Jan 17;6(1):e16241.

207. Kyurkchiev D. Secretion of immunoregulatory cytokines by mesenchymal stem cells. World J Stem Cells. 2014;6(5):552.

208. Marti LC, Pavon L, Severino P, Sibov T, Guilhen D, Moreira-Filho CA. Vascular endothelial growth factor-A enhances indoleamine 2,3-dioxygenase expression by dendritic cells and subsequently impacts lymphocyte proliferation. Mem Inst Oswaldo Cruz. 2014 Feb;109(1):70–9.

209. Nagineni CN, William A, Cherukuri A, Samuel W, Hooks JJ, Detrick B. Inflammatory cytokines regulate secretion of VEGF and chemokines by human conjunctival fibroblasts: Role in dysfunctional tear syndrome. Cytokine. 2016 Feb;78:16–9.

210. Herrmann JL, Weil BR, Abarbanell AM, Wang Y, Poynter JA, Manukyan MC, Meldrum DR. IL-6 and TGF-α Costimulate Mesenchymal Stem Cell Vascular Endothelial Growth Factor Production by ERK-, JNK-, and PI3K-Mediated Mechanisms. Shock. 2011 May;35(5):512–6.

9. ACKNOWLEDGEMENTS

This thesis has been possible thanks to the close collaboration and training between University of Modena and Reggio Emilia and Rigenerand Srl within an industrial PhD program, benefiting from High Apprenticeships grant funded by Rigenerand.

I would like to thank my academic tutor Prof. Massimo Dominici, head of the Laboratory of Cellular Therapies at University of Modena and Reggio Emilia, for his supervision and assistance at every stage of the PhD research project.

I also want to thank Dr. Giorgio Mari, CEO of Rigenerand Srl, for the opportunity to undertake my PhD program within Rigenerand.

I would like to express my gratitude to my company tutor Dr. Giulia Grisendi, researcher of the Laboratory of Cellular Therapies, for her constant support and precious advice throughout the course of my PhD.

I would like to thank colleagues and research team of both Cellular Therapy Laboratory and Rigenerand for a cherished time spent together in the laboratory.

Finally, I would like to express my gratitude to my parents, my sister, my grandmothers, Michele and all my friends for their invaluable understanding and encouragement.